SYNTHESIS, CHARACTERIZATION, AND AGRICULTURAL APPLICATION OF BIOPOLYMER-BASED ORGANIC HYDROGELS

A THESIS

Submitted to the Delhi Technological University

For the award of the degree of

DOCTOR OF PHILOSOPHY
IN
CHEMISTRY

By
RITU MALIK

(2K19/Ph.D./AC/07)
Under the Supervision and Co-supervision of

Prof. Sudhir. G. Warkar
Supervisor
Department of Applied Chemistry
Delhi Technological University
Delhi, India

Prof. Reena Saxena
Co-supervisor
Department of Chemistry
KMC, University of Delhi
Delhi, India

July-2023

DEPARTMENT OF APPLIED CHEMISTRY

DELHI TECHNOLOGICAL UNIVERSITY

Delhi-110042 (INDIA)

JULY 2023

DELHI TECHNOLOGICAL UNIVERSITY

(*Formerly Delhi College of Engineering*)

Department of Applied Chemistry

Shahbad Daulatpur, Bawana Road Delhi- 110042, India

DECLARATION

I declare that the research work reported in the thesis entitled "**Synthesis, Characterization and Agricultural Application of Biopolymer-Based Organic Hydrogels**" for the award of the degree of ***Doctoral of Philosophy*** in Chemistry has been carried out by me under the supervision of **Prof. Sudhir Gopalrao Warkar**, Department of Applied Chemistry, Delhi Technological University, India & and co-supervision of **Prof. Reena Saxena,** Department of Chemistry, Kirori Mal College, University of Delhi, India.

The research work embodied in this thesis, except where otherwise indicated, is my original research. This thesis has not been submitted by me in part or full to any other University for the award of any degree or diploma. This thesis does not contain other people's data, graphs, or other information unless specifically acknowledged.

Ritu Malik
Research Scholar
Roll No.: 2K19/Ph.D./AC/07
Date: 27th July 2023
Time: 5:00 p.m.

Department of Applied Chemistry

Shahbad Daulatpur, Bawana Road Delhi- 110042, India

CERTIFICATE

This is to certify that the thesis entitled **"Synthesis, Characterization and Agricultural Application of Biopolymer-Based Organic Hydrogels"** submitted to the Delhi Technological University, Delhi-110042, in fulfilment of the requirement for the award of the degree of **Doctor of Philosophy** by the candidate **Ms. RITU MALIK**, (Reg. No. 2K19/Ph.D./AC/07) under the supervision of **Prof. Sudhir Warkar**, Department of Applied Chemistry, Delhi Technological University, India and co-supervision of **Prof. Reena Saxena,** Department of Chemistry, Kirori Mal College, University of Delhi, India.

It is further certified that the work embodied in this thesis has been neither partially nor fully submitted to any other university or institution for the award of any degree or diploma.

Prof. Sudhir. G. Warkar
Supervisor
Department of Applied Chemistry
DTU

Prof. Reena Saxena
Co-supervisor
Department of Chemistry
KMC, University of Delhi

Prof. Anil Kumar
Head of Department
Applied Chemistry, DTU

DEDICATION

GOD, my guardian & everything,

Working out all my life's happening,

Blessing me with everything I needed,

Good people, love & knowledge, the most needed

Offer my heartful gratitude to that ALMIGHTY!

For being with me & enlightening me brightly.

My Parents

Mrs. and Mr. Kapoor

Mrs. & Mr. Malik

My Husband

Lt. Dr. Sanjay malik

My Kids

Chaitanya & Ritunjay

Tanushree & Heman

THANKS FOR YOUR ENDLESS SACRIFICES, SUPPORT, LOVE, AND PIOUS PRAYERS.

ACKNOWLEDGMENTS

Living a life with a goal of making yourself and your environment the best, aligns you with your true self & happiness. And for this, you need the main source: the GOD and HIS resources, especially the people who lighten up your path.

I feel grateful to express my sincere gratitude to my life lighteners who expanded my horizons and broadened my knowledge during the research for the successful accomplishment of my Ph.D. thesis.

First and foremost, I offer this endeavour to **"GOD"** as **HE** was the only super-catalyst who blessed me with the health, knowledge, determination, and positive environment; that was utmost required for the completion of this research.

It's my immense pleasure to acknowledge my supervisor Prof. Sudhir Gopalrao Warkar. an exemplary and visionary mentor, who not only motivated & guided me for the research but also extended cooperation and kindness during my work. He is a man of scientific attitude and at the same time, a man of values and principles, believing in simple living and high thinking. He always spared his time whensoever needed and patiently listened and solved my research queries. It's a blessing to work under his supervision. He always gave me the freedom to work and always appreciated my work, which further motivated me to give my best. I was able to explore the world of hydrogels because the insights he provided were simple and easy to comprehend and experiment with. I offer my sincere gratitude to him, without whom this research would not have been possible.

I feel grateful to express my deepest gratitude to my co-supervisor Prof. Reena Saxena, who motivated me to pursue the Ph.D. course. She always motivated me to give my best with her positive vibes and helped me out in every possible way. She always encouraged me to spread my wings and fly higher each day.

I express my heartfelt admiration for my lovely family, my husband Lt. Dr. Sanjay Malik who always wished that I should pursue my Ph. D., & my sons, Chaitanya & Ritunjay, who were always there to support me during my Ph. D. tenure. I thank them for their unconditional love which helped me to complete my research work.

For efficaciously accomplishing a project, a healthy environment is a must. I acknowledge the great personalities who helped me to accomplish my research.

- My colleagues and especially lab-mates (especially Khushbu) of Delhi Technological University for their support, inspiring discussions, and fun, we had during my Ph.D.
- I thank all the non-teaching (special mention to Mr. Raju) and official staff of the Department of Applied Chemistry, DTU, for their obligatory help whenever needed.
- I must also thank ICAR-NBSS and ICAR-SS&AC, Indian Agricultural Research Institute, Delhi, special mention to Mr. Kuldeep Singh for providing instrumentation facilities (AAS, UV-VIS spectrophotometer, Pressure Plate Apparatus), and the instrumentation facilities at DTU for SEM and at DU for FTIR and TGA analysis.
- I want to offer my gratitude to Dr. R.L. Ray, Head of R&D, Hindustan Gums Pvt. Ltd. for always providing me with CMTKG.
- I am grateful to Prof. Jai Prakash Saini, Vice Chancellor, Delhi Technological University, for giving me this opportunity to conduct my research work.
- I offer my sincere thanks to Prof. D. Kumar, Chairman, DRC., Prof. Anil Kumar, HOD, Ap. Chemistry, Prof. S. S. Umare, VNIT, Nagpur (External DRC member), Prof. Sreedevi Upadhayayula, IIT Delhi (External DRC member), Prof. Sanjay Dhakate, CSIR-NPL, Delhi (External SRC member), Dr. Deeksha Katyal, GGSIPU, Delhi (External SRC member), Prof. Ramesh Srivastava, Applied Mathematics, DTU (SRC member), Prof. R. K. Gupta, Applied Chemistry, DTU (SRC member), all SRC/DRC members and all faculty members, Department of Applied Chemistry, DTU.
- I also want to thank all those whom I have failed to mention specifically and personally, but they have helped me in various ways during this work.

Thank you so much!!!!!

RITU MALIK

ABSTRACT

The sustainable and increased agronomical production has headed the need for more conservative usage of water, which in turn necessitates research in the development of innovative soil-water conditioning alternatives with a lower rate of application and boosted water availability to the plants. Eyeing at the prospects of the necessity of a continuous reliant water supply for agronomy, that follows a greener approach; demands less money, time, and labour; requires low maintenance, and aids in enhanced growth rate and high crop yields. The aim of the research is the synthesis of an innovative biodegradable carboxymethyl tamarind Gum (CMTKG) based hydrogels, that can fulfil the above agricultural challenges and sustains the crops for a longer time with lesser frequent water supply, reinforcing the environmentally friendly methodology of water conservation. Further, it also targets the effect of hydrogel amendment on different physical and applicable attributes of different types of soil.

The first type of innovative biopolymer-based organic hydrogels was concocted by free radical polymerization of carboxymethyl tamarind kernel gum (CMTKG) and sodium-methacrylate (SMA) for application in agronomical procedures as a soil water conditioner/water harvester for sustainable agronomy. The second avant-garde organic agricultural hydrogel was formulated by free-radical polymerization of biopolymer carboxymethyl Tamarind Kernel Gum (CMTKG) and sodium acrylate (SA) and acrylamide (AA) monomers, to explore its application to different types of soils as a soil water conditioner. The structural morphologies of both the hydrogels were characterized by techniques viz. Fourier transform infrared spectroscopy, scanning electron microscopy, and thermogravimetric analysis. The hydrogels were evidenced as biodegradable hydrogel via the soil burial biodegradability test. The swelling behaviour of hydrogel was analysed as a function of temperature, pH, and salt solutions. Maximum water holding capacity, bulk density, porosity, and water retention capacity of soil were assessed to examine the effects on the soil by the hydrogel amendment. To maximize the utility, the implication of one of the hydrogel's agricultural dynamics has been researched on different types of soil for its precise application.

THESIS ORGANIZATION

The thesis constitutes six chapters. The contextual work inclusive of a relevant literature survey of the Biopolymers-based bio-matrices (especially hydrogels) and their application in agronomy as soil conditioners, nutrient/micronutrient carrier vehicles, and for purification of water to be used for irrigation purposes along with background work related to carboxymethyl tamarind kernel gum is summarized in ***Chapter 1***. ***Chapter 2*** deals with the synthesis, characterization, and swelling studies of organic CMTKG-PSMA hydrogel. ***Chapter 3*** entails the evaluation of the synthesized CMTKG-PSMA hydrogel for agricultural application as a potent soil water conditioner. ***Chapter 4*** incorporates the synthesis, characterization, and swelling studies of organic CMTKG-PSA-PAM hydrogel. ***Chapter 5*** comprises the evaluation of CMTKG-PSA-PAM hydrogel as a soil conditioner in different types of soils. The conclusions and the future scope of the work constitute ***Chapter 6*** of the thesis.

LIST OF PUBLICATIONS AND CONFERENCES

Journal Articles:

1. Malik, R., Saxena, R., & Warkar, S. G. (2022). Biopolymer-Based Biomatrices–Organic Strategies to Combat Micronutrient Deficit for Dynamic Agronomy. *ChemistrySelect*, *7*(16), e202200006.
2. Malik, R., Saxena, R., & Warkar, S. G. (2023). Organic Hybrid Hydrogels: A Sustenance Technique in Waste-Water Treatment. *ChemistrySelect*, *8*(5), e202203670.
3. Malik, R., Warkar, S. G., & Saxena, R. (2023). Carboxymethyl tamarind kernel gum based bio-hydrogel for sustainable agronomy. *Materials Today Communications*, *35*, 105473.

Publications in conference/workshop proceeding:

1) "Synthesis, Characterization and Agronomical Applications of Biopolymer-based Organic Hydrogel". International Conference on "Recent trends in drug discovery and development" organized by the Department of Chemistry, Maitreyi College, University of Delhi held on 08-09, October 2021. Secured first position in Poster Presentation.
2) Presented a Poster titled "Synthesis , Characterization and agronomical applications of Biopolymer based Organic Hydrogels" at an International Conference on "Rethinking science for Sustainable Development" organized by the Department of Chemistry, Rajdhani College, University of Delhi, India held on 20-21, April 2021.
3) Presented a Poster titled "Synthesis, characterization and applications of biopolymer based super absorbant hydrogel (SAH) for sustainable agronomy" at an International Conference on "Advanced materials for societal Applications (ICAMSA-2021), organized by the Department of Physics, J. C, Bose University of Science and Technology, YMCA, Faridabad held on 26 -28, October 2021.

INDEX

LIST OF FIGURES

LIST OF TABLES

LIST OF ABBREVIATIONS

AM	Acrylamide
AWC	Available Water Content
BD	Bulk Density
CMTKG	Carboxymethyl Tamarind Kernel Gum
FTIR	Fourier Transform Infrared
KPS	Potassium per sulphate
MBA	N,N'-methylenebis(acrylamide)
MWHC	Maximum Water Holding Capacity
PAM	Poly (Acrylamide)
PD	Particle Density
PSA	Poly (Sodium Acrylate)
PSMA	Poly (Sodium Methacrylate)
SA	Sodium Acrylate
SAH	Superabsorbent Hydrogel
SEM	Scanning Electron Microscopy
SMA	Sodium Methacrylate
TGA	Thermogravimetric Analysis
WC	Water Content
WRC	Water Retention Capacity

Chapter 1

INTRODUCTION AND LITERATURE REVIEW

1.1. Introduction

Crop-raising is solely contingent on water. Besides being a major domineering food resource, the agronomics role in imparting livelihood, growth of the industrial and commercial sector, and contribution to national income cannot be flouted, especially when the population is over-expanding globally. The advancement of technology to upgrade the agricultural practices and quality of the soil still necessitates research and development. The climatic upheavals, urbanization, and land degradation are the triggering factors for the multiplied droughts and floods, which imposes a dilemma in terms of water scarcity and water inundations, respectively, and water and nutrient depletion owing to topsoil erosion.

Usually, the major sources of water tapped for irrigation purposes are always either not available or inconsistent in use. In rainfed agriculture [1], which compromises almost 80% of global agronomy, the sustainability of agriculture and food production depends on rainfall, which is turning erratic day by day due to anthropogenic acts. Rainfed agronomy is responsible for most of the fulfillment of the food demand of the poor inhabitants of developing countries. It constitutes greater than 95% of agricultural land in sub-Saharan Africa, 90% in Latin America, 75% in near East and North America, 65% in East Asia, and 60 % in South Asia. Owing to increased weather

variability, rain-fed farmers become more susceptible to climate change [2]. A dropout in rainfall or untimely rainfall results in lesser Agri-production, poverty, hunger, and water scarcity and hence the economic meltdown of these countries. As rainfall is a natural irrigation process, there is a need for a paradigm shift that reduces farmers' dependency on rainfall.

Even drought-resistant plant species also necessitate water for their sustenance. Underground water may be very deep, contaminated, or scanty. Erection of dams is not propitious at all sites and is also high money demanding. These disruptions lead to a shortage of food, it's high pricing, and hence social disturbance. Irrigation, being an artificial process is accomplished using various methods: surface irrigation, localized irrigation, sprinkler irrigation, drip irrigation, center-pivot irrigation, Lateral move irrigation, sub-irrigation, and manual irrigation, in which most of the water is wasted [3]. With these practices, the available water content for the plants is not high as water is wasted, thereby raising the need for frequent irrigation. Henceforth, various practices are being explored so that moisture/water content in the soil is not lost due to evaporation or deep percolation, or erosion and is maintained for a prolonged duration of time. The major challenge the farmers face is to deal with the growing food needs and declining water resources i.e., water/nutrient stress conditions, that too in an economical way and such that no toxicity is introduced into the soil/crops and growth is also not affected.

Water’s critical role and excessive usage in agronomical practices viz. irrigation, nutrient and pesticide application, crop cooling, and frost control, has opened a new outlook in research to develop innovative technologies for water’s sustenance by effectual use with less wastage for global economic balance and food security. Henceforth, various practices are being explored that make the plants accessible to high available water content and lower the frequency of irrigation [4].

One of the solutions to the above-mentioned challenge is biopolymer-based organic hydrogels that act not only as a continuous, reliant water supply system but also as supplements of nutrients and micronutrients. Hydrogels have a high tendency for water absorption and retention and have high nutrient/micronutrient loading capacity, enhance the growth of plants, increase crop yields, and are also harmless to flora and fauna [4].

1.1.1. Hydrogels

Scientifically, hydrogels **(Figure. 1.1.)** constitute a group of three-dimensional cross-linked polymeric materials, which owing to the presence of hydrophilic functionalities in them, have the potential to entrap or release variable amounts of water/biological fluids reversibly (swell or shrink), in response to the external stimuli (physical/chemical/biochemical - temperature, solvent, pH, electric field, etc.), without altering the core matrix framework of the polymers.

Figure 1.1. Hydrogels

Witchterle and Lim prepared hydrogel for the first time in the 1960s [5]. Various methods of synthesis of hydrogels include graft polymerization, free radical polymerization, crosslinking, frontal polymerization, and ionic radiation technique [6-10]. Cross-linking in hydrogels is usually

achieved either through physical linkages viz. Vanderwaal forces or electrostatic interactions or hydrogen bonding [11]; or through chemical linkages via covalent bonds [12] formation during polymerization. Hydrogels formed owing to chemical linkages[13] are preferred in comparison to hydrogels involving physical linkages as the physical linkages disrupt easily due to weaker interactions. Chemically crosslinked Hydrogels[13,14] have been successfully applied in various areas

The hydrogels that can retain a large amount of water with a Swelling Ratio (SR) > 100 of water/biological fluids are termed Superabsorbent hydrogels (SAH) [15,16]. Crosslinking in the SAH is the reason behind the non-disintegration of the 3-dimensional structure of the SAH during swelling. The hydrophilicity of the SAH is due to the presence of hydrophilic functionalities (such as -COOH, $-NH_2$, $-CONH_2$, -CONH<, $-SO_3H$, -OH, etc.), capillary effect, and osmotic pressure [16]. Crosslinking can be attained either in vitro, i.e., during the preparation itself; or in vivo, i.e., after its administration, as in the case of biomedical application.

The swelling ratios of the hydrogels are interrelated to the nature of the polymer employed for its fabrication and the solvent in which swelling is done. Once the water is absorbed by a hydrogel, it is released gradually as a response to stimulus, (usually following diffusion gradient and polymer relaxation), which humidifies the soil and enables the plants to cope with the water paucity, thus averting their collapse.

The biopolymer-based hydrogels serve as water/nutrients supplementary capsules, that aid in their prolonged survival when the need arises due to droughts, or intensive crop practices. It mitigates a rain-water harvester, as when they are incorporated into the soil, absorbs rainwater, thereby preventing its loss due to seepage or evaporation, and avails the water to the crop for irrigation

when the rain stops. Biopolymer-based hydrogels may also be labelled as synthetic humus [17]. Humus keeps the soil fertile, pest-resistant, and disease-free and enables the plant to thrive well in drought and temperature extremes; so is a hydrogel. They have hydrophilic functionalities associated with them such as carboxylic acids, which have high electronegative oxygen atom, which forms a hydrogen bond with the electropositive hydrogen atom of a water molecule and thus encapsulates the water molecules inside them. The functioning of hydrogels has been shown in **Figure. 1.2.**

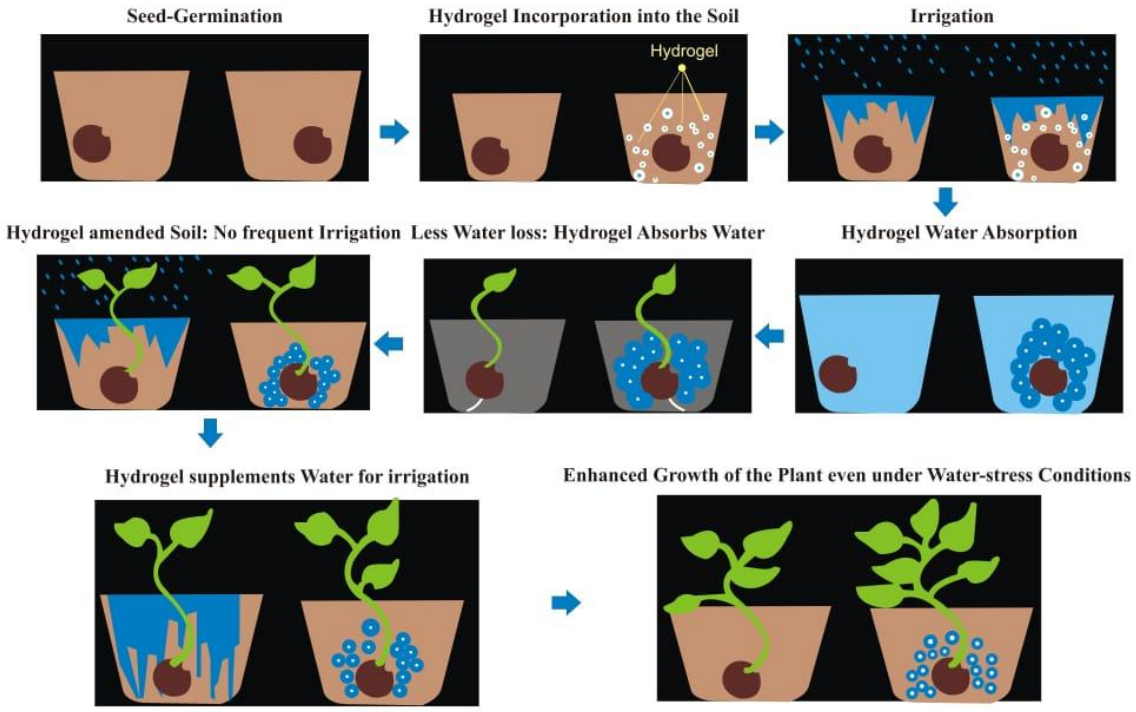

Figure 1.2. Functioning of Hydrogels

Thus, hydrogels [18] have multifunctional hydrophilic groups due to which water or any other fluid is entrapped in the spaces between them and are released back into the environment due to

diffusion or polymer relaxation or both or due to changes in temperature, solvent, and pH. Different types of classification of hydrogels based on their properties are depicted in **Figure.1.3.**

Water diffuses inside the hydrogel matrix [19] and adheres to the roots of the plants. And when water stress or drought conditions prevail, they release water due to diffusion and/or polymer relaxation, thus serving as a reservoir of water. If nutrients and/or micronutrients are also injected into the hydrogel, it also supplements the same to the plants. Thus, Hydrogels readily avail water to the plants, avoiding its wastage due to seepage down the earth, erosion, and evaporation.

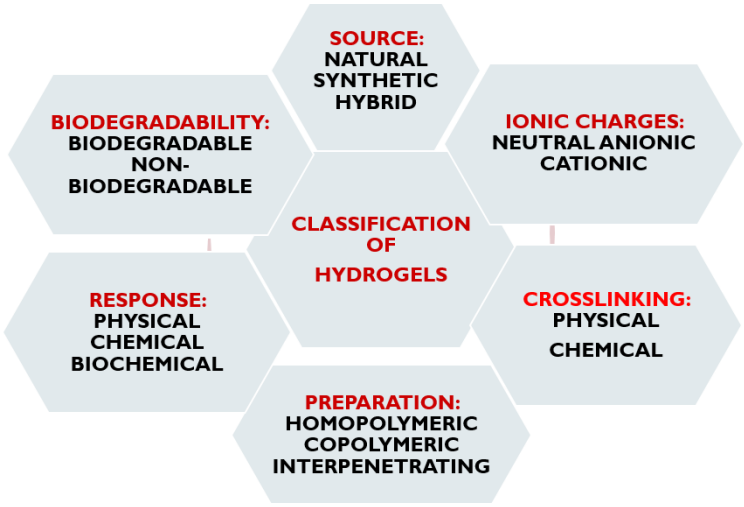

Fig 1.3. Different types of classifications of Hydrogels based on their properties.

The hydrogels may be pH sensitive[20] and thermo-sensitive[21]. They can be easily applied in agriculture as a soil conditioner and for the supplementation of nutrients and micronutrients. If the polymers employed are natural, extracted from plants and animals, their usage is a boon for the environment. Usually, the natural polymers are polymerized with synthetic monomers and cross-linked using a crosslinker for fabricating a hydrogel matrix.

Synthesis of Hydrogels

The method of synthesis of hydrogels is depicted in **Figure. 1.4**, implicates physical or chemical, or hybrid bonding. The bond formation is achieved via various ways viz. free radical polymerization, bulk polymerization, interpenetrating network, radiation method, solution mixing, and solution casting. The feedstock for the formation of hydrogels may be a natural biopolymer, synthetic polymer, or a hybrid (a mixture of natural and synthetic polymers). A hybrid polymer is usually preferred as the desired characteristics can be introduced into the hydrogel and the problem of non-biodegradability as in the case of the use of synthetic polymers and short lifespan in the case of natural polymers can be overwhelmed. Crosslinking agent and initiator (in the case of free radical polymerization) are also required.

The synthesis of hydrogels may involve physical crosslinking or chemical crosslinking. Physical cross-linking usually incorporates hydrogen bonding or electrostatic forces amongst polymer chains. The synthesis of physically crosslinked hydrogels usually involves the mixing of polymers under suitable circumstances or by just melding nonionic polymers. Chitosan forms physically crosslinked hydrogels through ionic interactions between the protonated amino group of cytosine and other small anionic molecules. Chemically cross-linked hydrogels usually incorporate the use of the following:

- Crosslinkers: mono or bi-functional such as formaldehyde, N,N'-methylene bisacrylamide, etc.
- Chemical reactions between reactive functional groups: Schiff's base reaction, disulfide bonding, Michael addition, etc.

- Ionizing radiation by employing light-sensitive groups e.g., Functional azides and functional acrylates.

- Free Radical polymerization involves the initiator such as potassium persulfate (KPS), ammonium persulfate (APS), 2-2'-azobisisobutyronitrile (AIBN), etc. to polymerize the monomers through crosslinker.

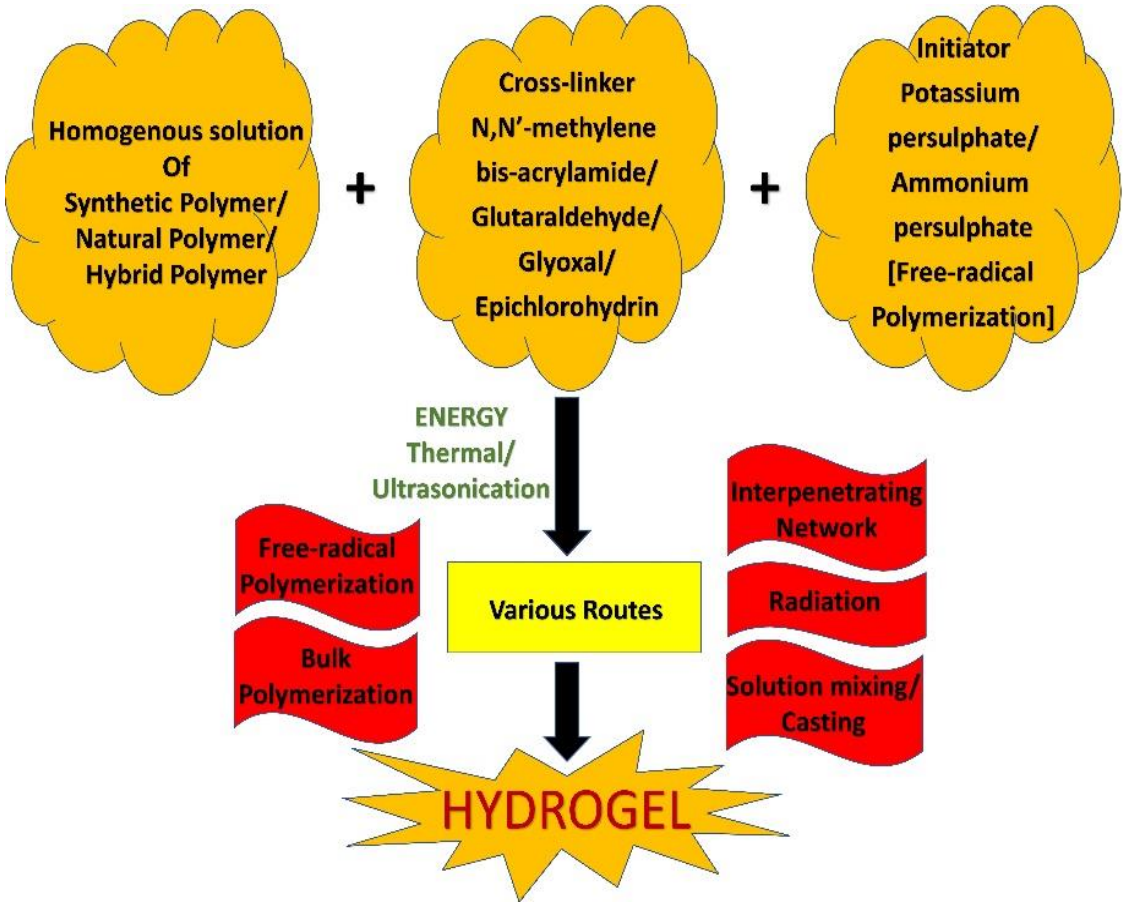

Figure 1.4. Synthesis of Hydrogel.

1.1.2. Biopolymers

The implication of the term “bio” in biopolymers is slated for the polymers that are engendered genetically from living components. Usually, made of monomers of nucleic acids or amino acids, or saccharides, these biopolymers have the capability of polymerization with various monomers (both synthetic and natural), to form tri-dimensional heteropolymers. The term “biodegradable” refers to the matter that can decompose microbiologically into recyclable carbon dioxide and water, and the term “bio-based” implies matter in which carbon originates from renewable sources via biological metabolism. Neither every biodegradable polymer is biobased, nor every biobased polymer is biodegradable. “Compostable” polymer epitomizes the polymers that are biodegradable in a composting environment[22].

Based on biodegradability, biopolymers are classified as biodegradable polymers and non-biodegradable polymers. Further, biodegradable polymers; predicated on origin, are grouped into biobased biodegradable polymers (starch, chitosan, carboxymethyl tamarind kernel gum - CMTKG) and fossil-based biodegradable biopolymers [Polyglycolic acid (PGA), Polycaprolactone (PCL), Polybutylene succinate (PBS)]. Bio-based polymers may occur naturally or are procured from renewable sources or microorganisms while fossil-based are obtained from natural gas or crude oil. Depending upon their response to heat, they may be classified into thermoplastics, thermosets, and elastomers. Thermoset biopolymers are a little trendier nowadays. The classification of polymers is shown in **Figure 1.5.**

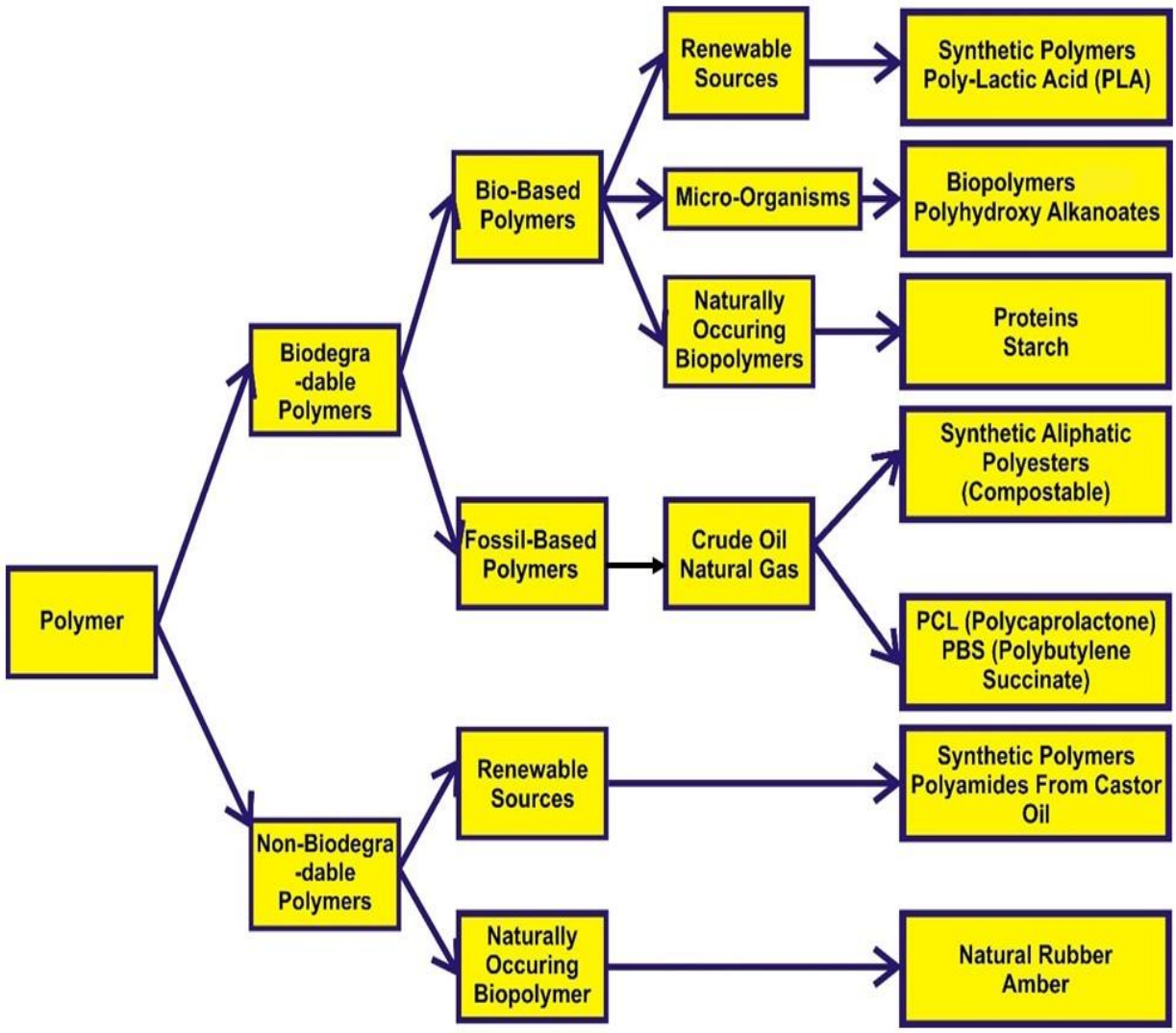

Figure 1.5. Classification of Polymers based on Biodegradation

Biopolymers play a significant role in agriculture. Soil enhancing characteristics such as retention of moisture/water, controlled release of fertilizers, and micronutrients, thwarting the growth of weeds, maintenance of soil temperature, and most conspicuously, the ability to degrade; eliminates the labor and cost required for its removal [22]. The dominant traits of biopolymers viz. non-toxicity, natural abundance, biodegradable, biocompatible economical, and ease of chemical modification enable the researchers to apply them in agriculture for the benefit of plants, humans,

and the environment. The positive aspects of biopolymers are shown in **Figure 1.6**. The biopolymers usually employed for applications in agronomy include chitosan [23], guar gum [24], alginate [25], cellulose [26], starch [27], tamarind kernel gum [28], and many more.

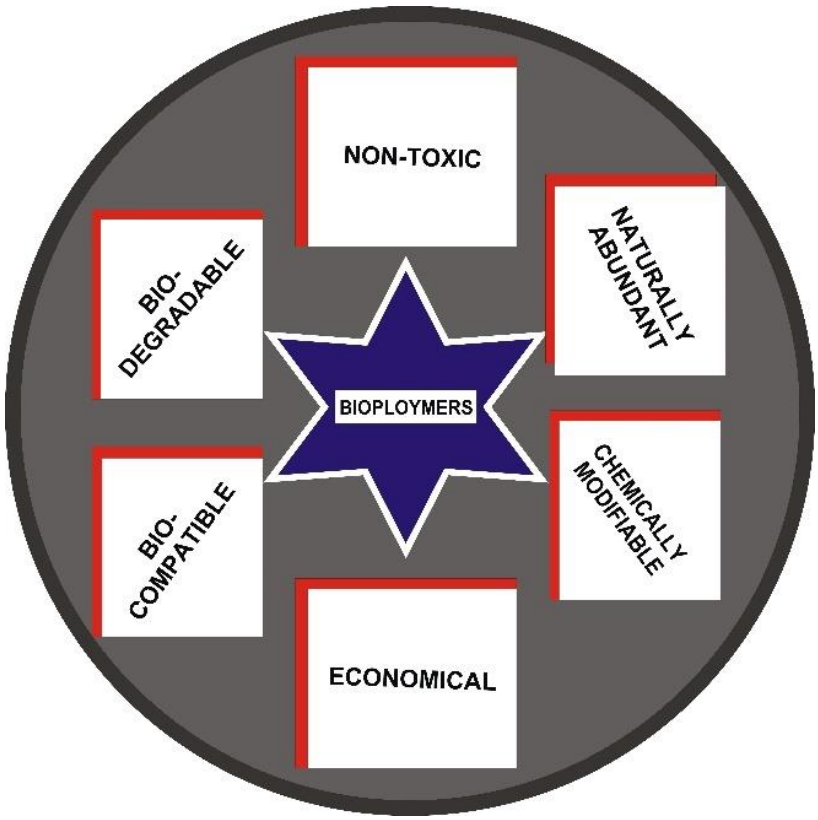

Figure 1.6 Positive aspects of Biopolymers

To deal with the agronomical problems faced, synthetic hydrogels have been introduced into the market. They solve the purpose but, being synthetic, are non-biodegradable, and generate permanent waste, a pitfall for our environment. To overcome this problem, biopolymers or natural polymers are being employed to fabricate biodegradable hydrogels, that are successfully applied as soil conditioners [29] and for nutrient/micronutrient supplementation [32, 33]. Chitosan [5],

starch [31], alginate [32], cellulose [33] and guar gum [34], carboxymethyl cellulose [38 -40] are some of the natural polymers that are continuously being explored for the synthesis of biopolymer-based hydrogels.

1.1.3. Carboxy Methyl Tamarind Kernel Gum (CMTKG)

The Greener approach to the utilization of renewable feed stocks is a step toward a sustainable future. Scientists and researchers are eyeing, the usage of natural polymers as raw materials as they possess distinctive characteristics viz. being environment-friendly, bio-degradable, bio-compatible, cost-effective, less toxic, easily accessible, and many more (**Figure 1.7**). Tamarind kernel Gum (TKG) is one such biopolymer. To introduce desired properties into it for its efficient application in various fields, it is chemically modified into carboxymethyl Tamarind Kernel Gum (CMTKG), through a simple derivatization method. CMTKG, owing to multifunctionality and other attributes, is being progressively exploited for different applications in different fields. The plant-derived Biopolymer TKG is a polysaccharide consisting of D-glucose, D-galactose, and D-xylose in the molar ratio of 3:2:1[36]. Derivatization of carboxymethylated form renders anionic nature to CMTKG and aids in the development of a network of hydration. The numerous enhanced attributes of CMTKG as compared to TKG include enhanced stability, boosted swelling power, high drug loading capacity, broad pH tolerance, mucoadhesion, hydrophilicity, and slow-release kinetics **(Figure. 1.7.)**. It also reveals enhanced life-shell, low degradation, and anti-bacterial properties. Due to these beneficial aspects, it is being applied in the field of oral drug delivery[37], medicine [38], tissue engineering[39], waste-water treatment[40], and agronomy[41].

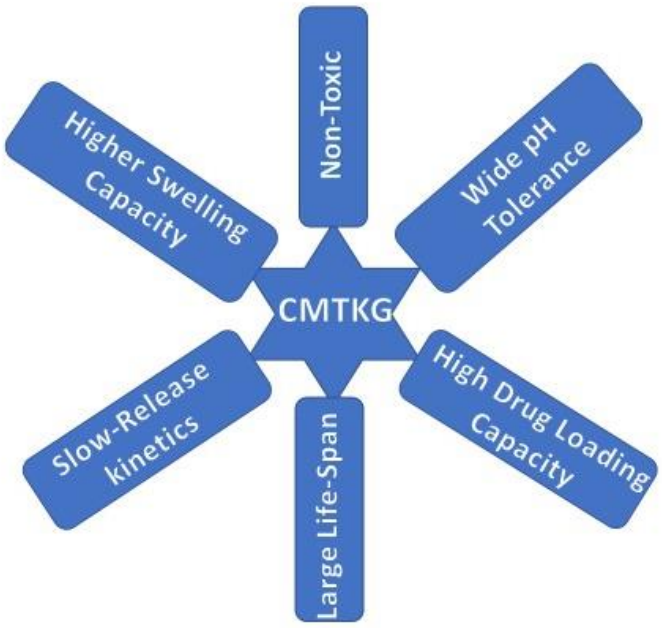

Fig 1. 7 Various Aspects of CMTKG

Synthesis of CMTKG

Tamarind Kernel Gum, extracted from the seeds of Tamarindus Indica L, composed of Xyloglucans is the green feedstock applied in the synthesis of CMTKG.

Derivatization is accomplished by the dissolution of TKG in an aqueous alkaline methanol solution (0.15 mol of NaOH), followed by a reaction with monochloroacetic acid (MCA) (0.15 mol). The reaction is completed by keeping it in a hot water bath with a temperature maintained at 70℃ for about an hour. The solution obtained is filtered on a G-3 sintered glass crucible.

The residue obtained is dissolved in water and neutralized with dilute HCl (1:1 v/v). CMTKG in the solution is precipitated out with ethanol and cleaned up of the impurities by washing it first with aqueous methanol (Methanol: water: 80:20), and then with pure methanol. The product is dried, initially at room temperature followed by vacuum dehydration in an oven at 40℃ for about

4 hours[42]. A titrimetric method is usually employed to find the degree of carboxymethylation of TKG. The derivatization is a two-step process, in which sodium hydroxide converts the hydroxyl groups of TKG into alkoxide groups first, followed by Williamson's etherification (S_N2 reaction) to introduce carboxymethyl groups between TKG-alkoxide and MCA. **(Figure.1.8)**

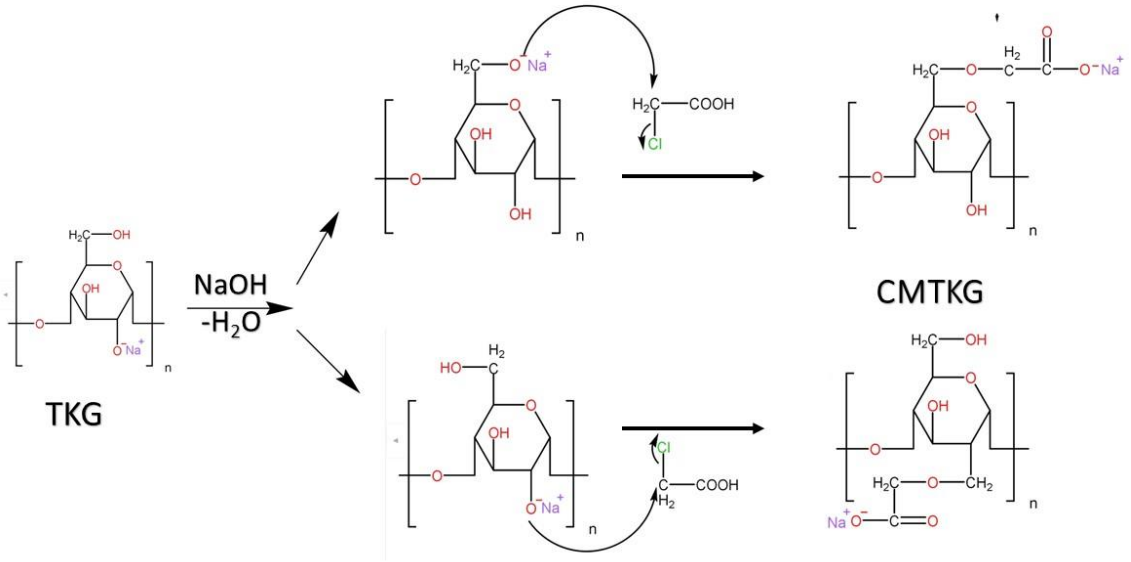

Fig 1.8. Mechanism of synthesis of CMTKG

$$TKG\text{-}OH + NaOH \rightarrow TKG\text{-}ONa + H_2O$$

$$TKG\text{-}ONa + ClCH_2COONa \rightarrow TKG\text{-}OCH_2COONa + NaCl$$

The optimization of derivatization is done by varying various parameters viz. duration of reaction, temperature, the concentration of MCA, and methanol-water ratio [42].

1.2. Review of Literature

Review of Literature was conducted for the different agronomical applications of hydrogels viz. micronutrient supplementation, purification of wastewater to be used for irrigation purposes and as a soil water conditioner.

1.2.1. Hydrogel Applications in Agronomy

Hydrogels can be applied in agronomy for various practices such as for fertilizer/micronutrient/pesticide supplementation [43], as purifiers of wastewater [44] to be used for the purpose of irrigation or as a soil-water conditioner [45](**Figure. 1.9.)**.

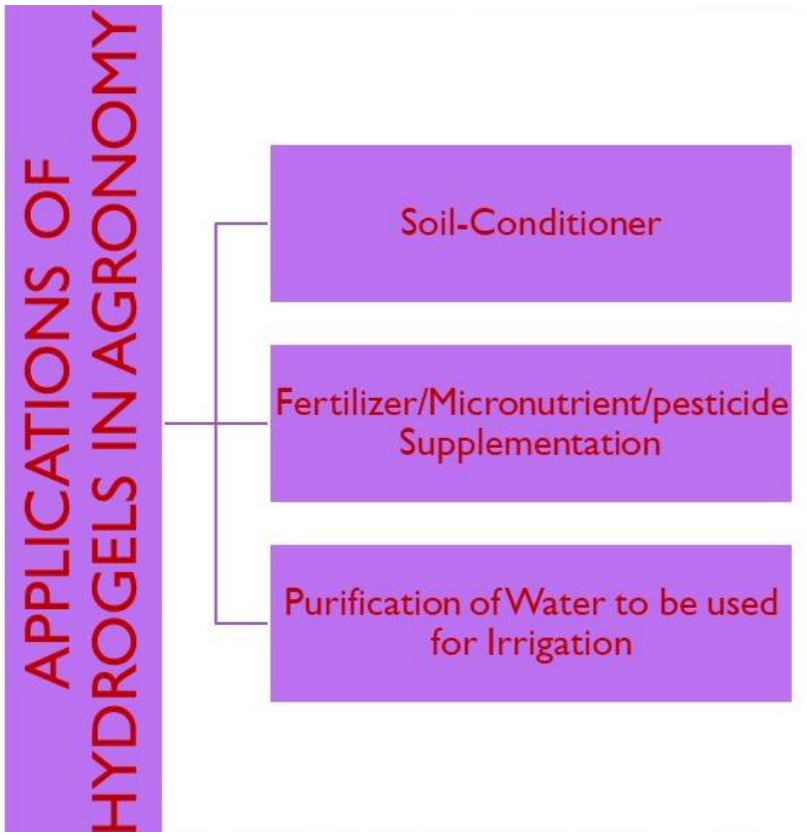

Fig 1.9. Applications of Hydrogels in Agronomy

1.2.1.1. Micronutrient Supplementation

Agronomy's prominent role in global expansion cannot be ignored. Agriculture accomplishes some of the major brass tacks – serves as a primary food resource, maintains a sustainable economy, relieves the dearth of capital, and supplies raw materials for other industrial sectors. Micronutrients are imperative in agriculture for the sustainable production of crops. Their inclusion into the crops not only aids in proper growth and good health of plants but of whole species on earth as micronutrients are naturally introduced into the food cycle through plants only. Healthy crops relate to a healthier life, therefore, the need for micronutrient supplementation arises owing to continuous recultivation for a longer period without any micronutrient application, intensive cropping practices, spray for high analysis fertilizers with little micronutrient level, reduced application of organic manures, leaching, liming of soils, and other anthropogenic and natural dynamics [46]. All the above-listed factors render the soil deficient in micronutrients. Henceforth, replenishment of micronutrients in a greener way to protect, sustain, and conserve the environment, by the utilization of natural renewable and biodegradable sources, are the priorities that require investigation for agricultural advancement. Polymers have made them marked by achieving recognition in every aspect of modern life, by being extremely versatile, having structural multifunctionality due to the presence of a varied number of polymerizable groups, and high relative molecular weights. The different functional groups affect the formation and degree of cross-linking. Biopolymers are the greatest eye-catchers for researchers as compared to synthetic polymers as they are economical, low in toxicity, bio-degradable, easily available, biocompatible, and easily modifiable. These traits not only safeguard our environment but also enhance their applicability in oral drug delivery, medicine, tissue engineering, wastewater treatment, and the agricultural sector. On the other hand, synthetic polymers usually employ non-

renewable feedstock, may release toxins, and lead to environmental degradation. Biopolymers of plant and animal origin serve as a structural organization, that permits the variations in the concentration gradient which affects the uptake of nutrients, micronutrients, and water by the cells, and this attribute of biopolymers can be exploited for various applications in different areas. Biopolymer-based matrices ensure a promising sustainable future for agriculture. Applications of these are one of the environment-friendly and greener techniques to achieve realistic objectives of controlled release of micronutrients. The optimistic attributes of such biopolymers-based matrices viz. wide pH tolerance, stability, higher bio adhesion (ready adherence to seeds), biocompatibility, and good kinetics release; render a challenge for researchers to be investigated and explore more and more in the future. Biopolymer-based biomatrices function as reservoirs of micronutrients by retaining micronutrients inside them. These matrices prevent the seepage of micronutrients deep into the ground and prevent their removal by soil or water or both. Further, their controlled release helps the plants to grow perfectly and healthy, prevents them from diseases, and results in a good yield of the crops. The application of such biomatrices saves time, money, and labour. This review of literature is innovative as it entails all the perspectives hitherto, i. e., the synthesis of bio-matrices (using eco-friendly biopolymers), loading them with micronutrients, and the kinetics and release mechanism of micronutrients. This will aid the researchers to fabricate different combinations of biopolymers to develop different types of bio-matrices to be used as a micro-nutrient carrier vehicle (**Figure.1.10.)** and thus, will contribute to sustainable agronomical practices.

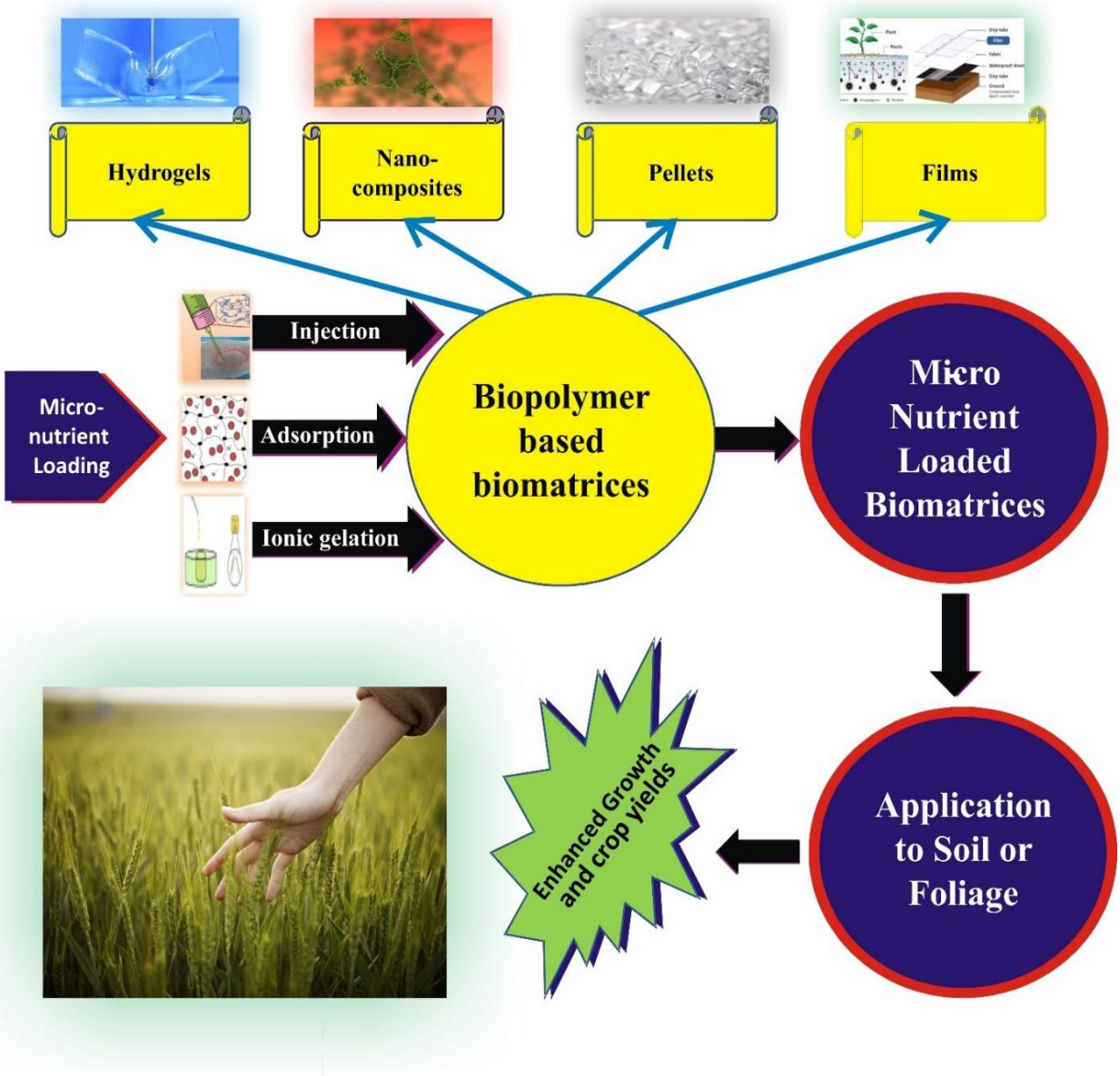

Figure 1.10. Hydrogel application as a supplement of micro-nutrient

Micronutrients and Agronomy

Mineral nutrients are a must for the completion of the prolific biological clock of plants. They are classified into macronutrients and micronutrients based on the concentrations in which they are required by the plants. Macronutrients are required in large concentrations >1–150 g per kg of plant dry matter while micronutrients are needed in trace amounts= 0.1–100 mg per kg of plant

dry matter. The categorized macronutrients are nitrogen (N), phosphorous (P), potassium (K), calcium (Ca), magnesium (Mg), and sulphur (S) and the micronutrients are iron (Fe), zinc (Zn), manganese (Mn), copper (Cu), boron (B), molybdenum (Mo) and chlorine (Cl). Micronutrients encompass less than 1% of the overall dry weight of the majority of the plants [47]. Micronutrients are essential not only for the proper growth of plants but also for the exhibition of their morphological and anatomical features. Besides being the building constituents of the metalloproteins and co-factors for the activation of various enzymes [48], they also account for energy storage, electron transport, and enzyme activity [49]. The transition metals act as micronutrients, e.g. copper, iron, manganese, and zinc, owing to their variable oxidation states and are vital for photosynthesis in addition to the maintenance of homeostasis within chloroplasts[31,32] . A critical concentration of micro-nutrients is required for the proper growth of the plants. The concentrations below lead to deficiency symptoms and the above results in toxicity and even death of the plant. **Table 1.1** lists micro-nutrients, their functions, physiological effects due to its deficiency and symptoms [52]. Generally, the micronutrient concentration in plant dry matter is boron (2–100 ppm, copper (5–20 ppm), iron (50– 150 ppm), molybdenum (0.1–2 ppm), zinc (20–100 ppm), chlorine (0.2–2%). And the critical levels of deficiency of various micronutrients in plants in India in mg Kg^{-1} dry matter are boron (20), copper (3–10), iron (25–30), molybdenum (0.1), zinc (10–20), manganese (10–30)).

Table 1. 1. Micronutrients, their functions, and deficiency Symptoms [52]**.**

Micronutrient	**Function**	**Physiological effects due to its deficiency**	**Symptoms**	**Ref.**
IRON (Fe)	Protein synthesis, lipid synthesis, Porphyrin synthesis Co-factor for oxygenases Iron is a part of mitochondrial and photosynthetic electron transport. Important for pollen-stigma interaction.	Affects the structure/ development of chloroplasts. Inhibited formation of chlorophyll and heme. Detoxification of oxygen free radicals is inhibited. Altered purine metabolism.	Chlorosis Growth inhibition due to inhibited photosynthetic electron transport. Necrosis Accumulation of riboflavin in apical root zones.	[53]
MANGANESE (Mn)	Enzymes- nicotinamide adenine dinucleotide (NAD) malic enzyme and phosphoenolpyruvate carboxykinase enzyme. Synthesis of lipids, gibberellic acid, and isoprenoids A constituent of OEC, oxygen-evolving complex (Photosystem II).	Affects redox processes - electron transport in photosynthesis. Inhibits the detoxification of oxygen-free radicals and superoxide-free radicals.	Decreased chlorophyll concentration. Reduced concentration of soluble carbohydrates in the roots Growth inhibition Interveinal chlorosis of the leaves. Necrosis	[54]
COPPER (Cu)	Cu is a constituent of plastocyanin, that links photosystem II to photosystem I.	Reduced plastocyanin leads to decreased photosynthetic electron transport. Reduced activity of enzymes.	Chlorosis Necrosis	[55]

	Respiration Detoxification of superoxide radicals Lignification Reproduction	Lipid composition altered in thylakoid membranes. Depressed nodulation and reduced nitrogen fixation in legumes. Depressed reproductive growth	Leaf distortion Wilting Shoot bending. Reduced disease resistance. Reduced seed or fruit yields.	
MOLYBDENUM (Mo)	Electron transfer from Mo to NO_3 A constituent of nitrogenase enzyme, xanthine dehydrogenase, and haemoprotein. A Significant role in pollen formation.	Accumulation of soluble nitrogen compounds – amides and High NO_3 concentration in tissues Lower chlorophyll concentration. Increase in the number of root nodules in legumes; nitrogen-fixing power is reduced. Affects the reproductive system.	Whip tailing Interveinal mottling, marginal chlorosis, and premature sprouting. Inhibition of tasselling, anthesis and growth of anthers Impoverished and late flowering, and lessened fruit formation.	[56]
ZINC (Zn)	Acts as a co-factor of many enzymes. Protein synthesis, Carbohydrate metabolism Photosynthetic electron transfer reaction (Hill reaction) Synthesis of IAA (indole acetic acid) Phosphorous retranslocation from shoots to roots. Anaerobic root respiration.	Disturbed chloroplast structure. Destruction of fatty acids and phospholipids, lipid oxidation. leakage of K^+, sugars, and amino acids. Inhibition of protein synthesis. Disorientation of membrane proteins exposes them to fungal infection.	Stunted growth Chlorosis Phosphorous toxicity results in interveinal chlorosis and necrosis.	[57]

BORON (B)	Formation and stabilization of cell walls. Lignification and phenol metabolism. Xylem differentiation An important role in reproduction. Stomatal opening (K transport inside the guard cells)	Alterations in structure and composition of cell walls. Affects the synthesis of lignin Impaired plasma membrane functions. Cessation of cell division, affecting the growth of roots. Inhibition of growth of pollen tube and sustainability of pollens	Stunted growth Necrosis The pronounced dropping of buds, flowers, and growing fruits. Seizure of seed and fruit formation.	[58]
CHLORINE (Cl)	Osmoregulation controls stomatal opening-closing. Charge neutralization. Enzyme activity is affected. Mn-containing water splitting enzymes catalytically deprotonates water and export H^+ from the active Mn site.	The evolution of photosynthetic O_2 is reduced. Lesser osmotic movement of active solutes inside the vacuoles inhibits roots elongation. Stomatal opening is affected leading to inhibited growth.	Inhibited growth. Wilting of leaves Curling of leaflets Chlorosis Hindered growth of roots	[59]

Biopolymer-based biomatrices and Micronutrient release

The worth of utilization of bio-based products to save our environment and earth can be judged by the framework of laws and orders relating to it by different countries. For instance, the biomass research and development act of 2000, US public law 106224, presidential executive orders 13134 (triplicating America's usage of bio-based products by 2010) and 13101; and greening the environment through recycling and waste prevention and the farm security and rural investment act of 2002 public law 10717 (2002 farm bill. These laws directly or indirectly encourage the employment of biobased products for a sustainable tomorrow. Henceforth, the implication of biopolymer-based biomatrices for the controlled release of micronutrients is a global necessity to be envisaged for. "All India Coordinated Research Project on Micronutrients" has been contouring the various soils of India relating to the type and extent of micronutrient deficiency. It has been acknowledged that in India, most of the soils lack zinc, subsequently followed by iron, copper, and manganese. Besides these micronutrients, boron and molybdenum deficiencies have been specified in some regions. About 48.1% of Indian soils are reported to be deficient in zinc, 11.2% in iron, 7% in copper, and 5.1% in manganese. Calcareous soils are usually short of iron micronutrients owing to less solubility of oxidized ferric state in the oxygen-rich environment. Neutral, alkaline, and calcium-rich soils usually reveal zinc and manganese deficiency [60]. The application of biopolymer matrices for micronutrient release is due to the ease of chemical modification of biopolymers, which paves a way to produce different types of biomatrices with explicit properties required for its application in the related field. The term "bio-matrices" implies the matrices derived from bio-based polymers. The micronutrient deficit, as well as surplus, is hazardous for the plants. While formulating biomatrices, the requirement of the crops, the soil nutrient level (to know the micronutrients it is short off), must be known properly for crop's proper

growth and environmental protection. Depending on the type and extent of deficiency, appropriate biomatrix treatment can be fabricated, that nourishes the soil with the lacked nutrient effectively without much maintenance practices at a low cost. It also overcomes the problem of the application again and again over short periods. As per the literature, micronutrient supplementation has been achieved either by foliar application or through soil treatment or hydroponic solution. The fabrication of matrices from biopolymers is not only economical, environment friendly, and easy, but it also enhances their mechanical properties (impact and tensile strength, heat deformation temperature, moduli properties) and degradation capability as against the conventional methods used such as complexes involving chelation, which after releasing the micronutrient; generate permanent waste, that is harmful to the environment [38]. Henceforth, biopolymer-based biomatrices are being explored at a large scale for applications in various fields.

Biomatrices and their efficacy on agronomy

The various forms of biomatrices synthesized are hydrogels[61], nanocomposites [62], pellets/microspheres [63], and films/membranes [64], which have been successfully applied in soil conditioning, nutrient, and micronutrient release in agricultural practices. The various aspects of biopolymer-based biomatrices used till date for micronutrient release in agronomy are enlisted in **Table. 1.2**

Table 1.2. Biopolymer-based biomatrices for micronutrient release in agronomy

Micro-nutrient	Matrix	Biopolymer and other constituents	Formulation Methods	Outcomes	Ref
IRON (Fe)	Calcium alginate matrix	Sodium alginate/Iron chloride and calcium chloride (dihydrate)	Crosslinking, Micro-emulsion technique	Rate of release of Iron increased: i) up to 1.5 g of sodium alginate, followed by a further decrease. ii) till pH 7.4, with a subsequent decrease at higher pH The concentration of the crosslinker and temperature had an inverse effect on the rate of release of iron. Non-Fickian transport mechanism.	[65]
	Microfibers	Sodium carboxyl cellulose (CC), sodium periodate, and sodium chlorite	Chelation of Fe (II) on CC	Great adhesivity to the leaf surface increased utilization efficiency of micronutrient iron.	[66]
	Micro-capsules	Ethyl cellulose, Glycerol monostearate, and Compritol 888 ATO	Extrusion or spheronization method.	Microcapsules containing compritol released iron at the slowest rate.	[67]
COPPER (Cu)	Hydrogel Matrix	Sodium alginate (ALG) and carboxymethyl cellulose (CMC)	Response Surface Methodology (RSM) (Box-Behnken design (BBD))	Slow and controlled release of Cu^{2+} ions (9wt% / 14 days). Rate constants and maximum sorption capacities for dry and wet capsules: 0.358, 0.259, 49mg g^{-1}, and 281mg g^{-1}respectively.	[68]
	Nanofibers	Cellulose acetate, gelatin from porcine skin, acetic	Electrospinning	Nanofibers with no surfactant and less gelatin revealed a slower release of Cu^{2+} (20% release in first three hours followed by 50% gradual release for 28 days), as	[69]

		acid, copper (II) oxide-nano-powder.		compared to faster release (80% release within first three hours) by the nanofibers with surfactant added.	
	Carbon nanofibers	Bovine serum albumin (BSA), Copper nitrate, sodium dodecyl sulfate (SDS), phenolic resin-based activated carbon microfibers (ACFs)	Calcination, reduction. chemical vapor deposition (CVD).	Increased water absorption Enhanced rate of germination Increase in root and shoot length. High chlorophyll and protein contents.	[70]
	Pellets	Keratin fiber, ethylene acrylate, cuprous oxide	Extrusion followed by granulation into pellets	An increase in Cu^{2+} ions was noticed (40 ppm- 115 ppm). No further increase was observed beyond 115 ppm. The biodegradable pots supplements localized the micronutrients, avoiding the application of external fertilizer.	[71]
	Bio-composite	Chitosan, epoxidized rubber latex, stearic acid, and sulfur. $Cu(NO_3)_2$.	Adsorption-Desorption.	Rate of adsorption increased with an increase in the concentration of chitosan. Desorption of Cu^{2+} ions follows zero-order kinetics. Degrade easily.	[72]
	Micro-capsules	Sodium Alginate, Chitosan, Copper sulfate pentahydrate, T. viride	Ionic gelation technique	One application is enough to provide micronutrients/protection for one complete vegetation period. The copper ions exhibited earlier bursts followed by their slow release.	[73]
	Hydrogel	NaCMC, $FeCl_3$	Ionic crosslinking reaction	Release of copper ions into the soil: 80% on the 16^{th} day.	[74]

				Release in water as compared to soil was about 15 times rapid.	
ZINC (Zn)	Nanofibrils	Poly (butylene adipate-co-terephthalate) (PBAT), zinc nitrate	Solution blow spinning (SBS)	Enhanced rate of growth and high yields in maize plants.	[75]
	Zn-based engineered nanomaterials (ENMs)	Microcrystalline cellulose (MCC), chitosan and alginate (ALG), Calcium chloride, zinc chloride, and zinc acetate dihydrate, ZnO NP's	Cross-linking	Controlled rate of release. Proper growth of maize plants Reduced loss of zinc.	[76]
	Protein-based bioplastics	Soy protein isolate (SPI), Glycerol as a plasticizer, $ZnSO_4.H_2O$	Minijet Piston Injection Moulding System	Supplementation of micronutrient zinc in horticultural crop applications.	[77]
	Hydrogels	NaCMC, $FeCl_3.6H_2O$ $ZnSO_4.7H_2O$. Glutaraldehyde	Chemical crosslinking method.	Water absorbance has an inverse relationship with the concentration of both polymer and crosslinker. Rate of micronutrient zinc release in water and soil decreased with high gel composition and crosslinking density. Enhanced growth of wheatgrass	[78]
	Superabsorbent Hydrogel composites	Carboxymethylcellulose (CMC), acrylamide (AM), ($ZnSO_4.7H_2O$), Natural zeolite.	*in situ* graftings, free-radical polymerization	Less water absorbance for zincate hydrogels as compared to non-zincate hydrogels. Fickian diffusion Hydrogels enhanced the water-holding capacity of the sandy loam soil along with the controlled release of zinc.	[79]

BORON (B)	Super absorbent nanocomposites	Sodium alginate, montmorillonite (MMT) and boric acid	In-situ method	An increased concentration of MMT enhanced water swelling capacities. Optimized nanocomposite had 426.337 g/g, having MMT-20.0 % wt. and boric acid- 0.1 g. Rate of release of boron followed pseudo-first-order kinetics and its release was 25.561 % for 8000 min (about 6 days).	[80]
	Nano-composite hydrogels	PAAm, CMC, calcium montmorillonite (MMt)	Free radical polymerization	Increased MMT concentration enhanced the macronutrient-nitrogen and micronutrient -boron; loading capacity and slowed down their rate of release.	[81]
Copper (Cu) and Zinc (Zn)	Membranes	Chitosan, Dodecanoyl chloride, and suberoyl chloride	Crosslinking	Permeability of the membranes was reduced leading to the controlled release of micronutrients.	[64]
Copper (Cu) and Zinc (Zn)	Starch film Nanoparticle Nanofiber	Polyvinyl acetate (PVAc), starch**,** copper nitrate $Cu(NO_3)_2..3H2O$, zinc nitrate $Zn(NO_3)_2..6H2O$	Esterification, Chemical linkage	Superoxide radicals and hydrogen peroxide concentrations are less in PBMC-grown plants as compared to the control plants indicating the role of Zn nanoparticles in scavenging these species. Micronutrient release rates were found to be slower for PBMC as against Cu-Zn/CNF.	[82]
Zinc (Zn) and Boron (B)	Nano-particle emulsion, Nano fertilizer	Chitosan, Sodium tripolyphosphate (TPP), $ZnSO_4$, H_3BO_3	Ionic gelation	Higher intake of zinc and boron by coffee leaves led to increased chlorophyll content, enhanced photosynthesis, increased leaf area, increased plant height, increased stem diameter,	[83]
Copper (Cu) and Manganese (Mn)	Hydrogel	K-CG, $CuSO_4.5H_2O$, $MgSO_4.H_2O$	Crosslinking	Swelling ratios decreased with the increased concentration of GA. Hydrogels were pH sensitive. Controlled release of micronutrients.	[84]

Synthesis of Biomatrices:

This section investigates the various methods of synthesis of different bio-matrices for micronutrient supplementation hitherto.

Hydrogels

Hydrogels for micronutrient release, are usually formulated through free radical polymerization of two or more polymers using a crosslinker and initiator[76,, 83]. Lay-out of the design process for the application of Biopolymers in Agronomy is shown in **Figure. 1.11**.

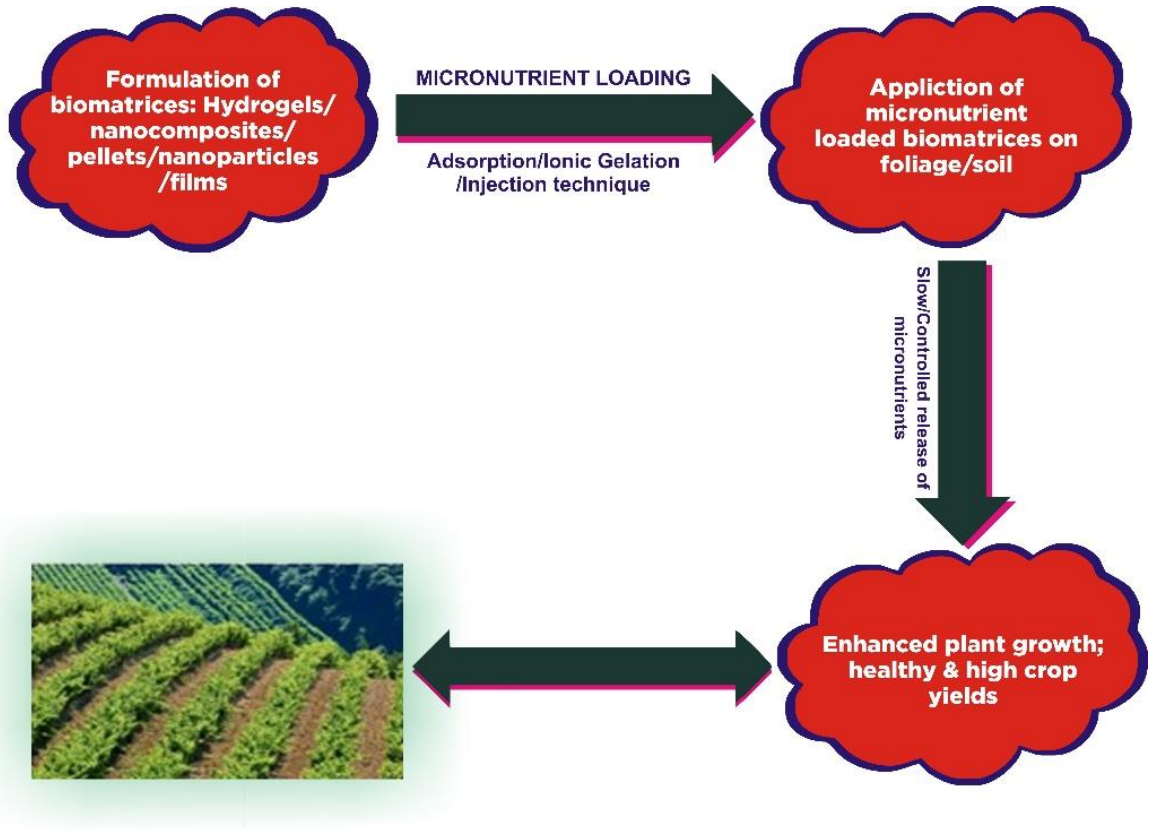

Figure. 1.11 Lay-out of the design process for the application of Biopolymers in Agronomy

D. Skrzypczak, et al.[86], fabricated alginate-carboxymethyl cellulose eggshell bio-composites (sodium alginate – 5.0wt%, carboxymethyl cellulose (CMC)- 12wt%, eggshells- 10.0wt%), employing $CaCl_2$ as a crosslinker, via external ionic gelation technology, using response surface methodology, and studied the slow and controlled release of Cu^{2+} ions (9wt% / 14 days). Similarly, Gulen Oytun Akalin, et.al.,[85], prepared nano-porous sodium carboxymethyl cellulose (NaCMC) hydrogels by their dropwise addition into iron chloride (crosslinker)and observed the release of copper ions into the soil (80% on the 16^{th} day). It was also stated that release in water as compared to soil was about 15 times more rapid. Further, Gulen Oytun Akalin; et al.,[78] extended the research and studied the effect of controlled release of zinc (Zn) by fabricating carboxymethyl cellulose (CMC), and carrageenan (CG) hydrogels, using an ionic crosslinking technique, on the growth of wheatgrass, where iron chloride [III], and glutaraldehyde (GA) were used as crosslinkers. It was observed that water absorbance has an inverse relationship with the concentration of both polymer and crosslinker. The rate of micronutrient zinc release in water and soil decreased with high gel composition and crosslinking density. Exploring more, Gulen Oytun Akalin et al.,[84] synthesized pH-sensitive κ-carrageenan (κ-CG) hydrogels for the controlled release of copper (Cu) and manganese (Mn) micronutrients, by crosslinking with glutaraldehyde (GA). The swelling ratios decreased with the increased concentration of GA. Comparably, Dhruba Jyoti Sarkar, et al.,[79] also researched the release of zinc by synthesizing superabsorbent hydrogels (using carboxymethylcellulose (CMC), acrylamide (AM), N, N-methylene bisacrylamide (MBA) (crosslinker), persulphate (initiator), zinc sulfate heptahydrate ($ZnSO4.\ 7H_2O$)); via in situ graft free radical polymerization. Two samples were prepared. i) zeolite-free hydrogels; ii) zeolite-containing hydrogels. Less water absorbance was reported for zincate hydrogels as compared to non-zincate hydrogels. Adriel Bortolin et al.,[81] synthesized

nanocomposite hydrogels via a free radical mechanism using CMC, PAM, clay montmorillonite (MMT), MBA as a crosslinker, aqueous N,N,N′,N′- tetramethylethylenediamine (TEMED) as a catalyst and sodium persulfate as initiator. An increase in the concentration of MMT enhanced the macronutrient-nitrogen and micronutrient -boron; loading capacity and slowed down their rate of release.

Nanocomposites

Nanocomposites are typically synthesized using three approaches:

- suspension of nanoparticles in a fluidic monomer, forming particle reinforced composites.
- sandwich/structural/interpenetrating polymer networks (IPN/semi-IPN), synthesized by a layering of two or more materials, joined through bonds.
- fibres of two or more materials entrenched into each other, forming fibre-reinforced composites. Nano-particle biomatrices are generally prepared by mixing nanoparticles with biopolymer solution, employing a crosslinker [87].

Nanocomposites when applied for micronutrient release, cause enhanced plant growth, which is supported by the research by Minha Naseer et al., [88]. The outcomes of the studies revealed that the administration of iron particles (10mg L^{-1}) along with Glomus intradices augmented the growth-promoting and drought-tolerant effects of Glomus intradices in wheat.

Sunita Patel et al. [89], fabricated nanocarriers of iron, employing biopolymer alginate and crosslinker calcium chloride dihydrate. A stabilized emulsion of alginate using paraffin wax was prepared followed by the addition of crosslinker-calcium chloride and subsequent loading of micronutrient-iron, using iron chloride. The rate of release of Iron increased up to 1.5 g of sodium

alginate, followed by a further decrease in increasing the concentration of alginate. The concentration of the crosslinker and temperature had an inverse effect on the rate of release of iron. The rate of release of iron also increased till pH 7.4, with a subsequent decrease at higher pH. Non-Fickian transport mechanism was obeyed during the release of iron.

Opting for the same biopolymer, H Helmiyati et al. [80], fabricated superabsorbent nanocomposites, employing sodium alginate, acrylic acid and acrylamide, potassium persulfate (initiator), N,N′-Methylenebisacrylamide (crosslinker), montmorillonite as clay, and boric acid (micronutrient source); via a free radical mechanism to study the release of micronutrient – Boron. It was observed that the increased concentration of montmorillonite enhanced water swelling capacities. The best and optimized nanocomposite had 426.337 g/g, having montmorillonite -20.0 % wt. and boric acid- 0.1 g. The rate of release of boron was 25.561 % for 8000 min (about 6 days).

San-Lang Wang et al., [83], further for releasing zinc simultaneously with boron, prepared Zn/B nano fertilizer by adding chitosan solution in acetic acid to sodium tripolyphosphate (TPP) solution (prepared in de-ionic water), magnetically stirring it at 900 rpm for 1 hour at room temperature. The chitosan nanoparticles obtained were saturated with zinc sulfate ($ZnSO_4$) and boric acid (H_3BO_3), to form Zn/B nano fertilizer. The application of this nano fertilizer on the coffee leaves led to increased chlorophyll content, enhanced photosynthesis, increased leaf area, increased plant height, and increased stem diameter, indicating a higher intake of zinc and boron.

Further exploration of chitosan includes the works of GunaSunderi Raju, et.al., [72], who along with his team, synthesized chitosan epoxidized natural rubber bio-composites, by homogenizing chitosan slurry (chitosan mixed with acetic acid) and epoxidized natural rubber (with 50% epoxy

composition) and casting of compounding materials (zinc oxide, stearic acid, N cyclohexyl-2-benzothiazole sulfonamide (CBS), zinc oxide, stearic acid, and sulphur), on a glass mold. Bio-composites were obtained on drying. Copper was made to adsorb by keeping these bio-composites in-stock solutions of copper nitrate, Cu $(NO_3)_2$. It was found that the rate of adsorption increased with an increase in the concentration of chitosan. These bio-composites degrade easily and exhibit a controlled release of copper.

The synthesis of biomatrices for the release of copper was extended beyond by Mohammad Ashfaq, et.al., [70], by employing an aqueous colloidal suspension of copper nanoparticle-grown carbon nanofibers (CNFs) as a carrier of copper nanoparticles, prepared by chemical vaporization deposition. For application in agriculture, it needs to be encapsulated inside a biodegradable polymer, polyvinyl alcohol (PVA), which releases copper by its dispersal in water. The application of these nanofibers led to increased water absorption, enhanced rate of germination, increase in root and shoot length, and high chlorophyll and protein contents.

Zinc (Zn) performs a key role in a plant's lifespan. Caio V. L Natarelli, et.al., [75], developed biodegradable poly (butylene adipate-co-terephthalate (PBAT)) nanofibers for the release of zinc micronutrient, employing solution blow spinning. Zinc nitrate was dissolved in the PBAT solution (homogenized PBAT and chloroform), through an ultrasonic bath. Solution blow spinning was carried out at constant air pressure (0.14MPa). The polymer solution was fed at a rate of about 7.2 ml h^{-1}. Temperature and relative humidity were retained at about 27℃ and 55% respectively. The effect of these nanofibers was observed on maize plants (enhanced rate of growth and high yields).

Broadening the studies for the release of zinc, Martins. N. C. T., et.al., [76], synthesized various types of composites employing biopolymers and zinc oxide nanoparticles (ZnO NPs). i) composite

procured by mixing microcrystalline cellulose and water suspension of ZnO NPs for 20 minutes, ii) in situ syntheses of composite by refluxing the suspension of microcrystalline cellulose or (chitosan) and methanolic zinc acetate solution, followed by dropwise addition of NaOH, iii) treatment of composites obtained via in situ synthesis, with alginate solution, iv) the suspension of ZnO NPs in water (prepared in an ultrasonic bath) was added to the solution of CH in acetic acid. The gel procured was dried and grounded to get the powder. v) ZnO NPs were added to the homogenous solution of sodium alginate and water and this solution was added dropwise to $CaCl_2$ or $ZnCl_2$ (crosslinker), leading to the formation of alginate beads. The different composites released Zn at a controlled rate. It aids in the proper growth of maize plants and at the same time, reduces the loss of zinc.

Beholding the benefits of MCC, Wang. M. et.al., [66], prepared pH-responsive ferrous foliar fertilizer by carboxylation of microcrystalline cellulose to carboxyl cellulose, which contains many -COOH groups, having an affinity for chelation with Fe^{2+}. Further, these CC-Fe (II) microfibers were coated with Attapulgite (ATP). In an acidic medium, Fe^{2+} becomes secluded and ATP coating gets loosened, facilitating the release of iron. Application of this ferrous foliar fertilizer was possible as it exhibited great adhesivity to the leaf surface, thus increasing the utilization efficiency of micronutrient iron and enhancing the growth of the crops.

Pellets

Pellets are synthesized using the ionic gelation technique. Marko Vincekovic, et.al. [73], prepared chitosan/alginate microcapsules (loaded simultaneously with Cu^{2+} ion and Trichoderma viride), by ionic gelation technique and examined the effect of copper ions and mycelial growth. It was

examined that one application is enough to provide micronutrient/protection for one complete vegetation period. The copper ions exhibited earlier bursts followed by their slow release.

Jahangir Abedi-Koupai et al. [67], further fabricated three types of microcapsules for iron release, applying three polymers ethyl cellulose, glycerol monostearate, and compritol 888 ATO, mixing each of them with avicel, ferrous sulphate, and lactose in distilled water. The mass obtained was sieved, spheronized, and dried. For control release of iron, the microcapsules were coated with ethylene-vinyl acetate.

Pots for release of Copper

Eton. E. codling, et.al. [90], framed Feather Fiber biopolymer with copper (FFBP-Cu) nursery pots. The duck feathers, ethylene acrylate, and cuprous oxide were extruded and granularized to yield pellets (length-11 mm), and further, molded (via injection molding technique) into the pots. The seed was grown after removal of the seed coat and immersing in 10% bleach for 5 min., followed by rinsing with distilled water, in a greenhouse (18℃ - 29℃). An increase in Cu^{2+} ions was noticed (40 ppm- 115 ppm). No further increase was observed beyond 115 ppm, indicating its maximum solubility in the pots. These biodegradable pots supplemented copper locally, avoiding the application of external fertilizer.

Films/Membranes

Films/membranes are also fabricated by crosslinking the polymers and then molding them in the form of membranes.

M. Jiménez-Rosado., et al. [77], fabricated protein-based bioplastic matrices involving three steps. 1) Homogenous mixture of Soy protein isolate (SPI), glycerol (Gly), and zinc sulphate

($ZnSO_4.H_2O$); were obtained under adiabatic conditions and at room temperature (50 rpm for 10 mins.). ii) The mixture obtained was processed by injection moulding, under optimized conditions. The biomatrices obtained were heated to about 50 ℃, for a duration of 24 hrs. (Dehydro-thermal treatment); to obtain dried bio-plastic matrices. iii) The dried biomatrices were left in 300ml of distilled water, for an absorption process, in which glycerol, soy protein, and micronutrient are released into the water, which is finally frozen and dried to obtain a dry protein matrix. This dry protein matrix has been employed to supplement micronutrient zinc in horticultural crop applications.

Rahul Kumar et al. [91], synthesized biofilms using polyvinyl acetate, starch, methyl acetate, methanol, sodium hydroxide, zinc nitrate ($Zn(NO_3)_2.6H_2O$), copper ($Cu(NO_3)_2.3H_2O$), sodium dodecyl sulphate, trichloroacetic acid, potassium sodium tartrate, α-naphthylamine, and sulphanilamide. It involves three steps. i) The activated carbon nanofibers were removed from impurities (by treating them with 0.03 M nitric acid) and neutralized (washing with Milli-Q water), vacuum dried (to escape moisture and entrapped gases, if any), and saturated with zinc nitrate ($Zn(NO_3)_2.6H_2O$), copper ($Cu(NO_3)_2.3H_2O$); with the addition of surfactant-SDS. After drying overnight, the sample was calcined at 400℃, followed by a reduction to generate Cu-Zn/ACFs. ii) Homogenous solution of PVA in methanol was prepared and methanol, methyl acetate, and Milli-Q water were added to it and stirred to obtain a clear solution. Methanolic NaOH solution was added to form PVA gel. iii) The Cu-Zn/ACFs, prepared in the first step were added to the solution prepared in the second step. The resulting solution was heated to obtain a clear solution. The black slurry-like material formed, was cast to thick(0.5mm) film on a Teflon sheet. The concentration of superoxide radicals and hydrogen peroxide was reported to be less in PBMC grown plants as

compared to the control plants, indicating the role of Zn nanoparticles in scavenging these species. The micronutrient release rates were found to be slower for PBMC as against Cu-Zn/CNF.

Analogously to study the simultaneous release of copper and zinc, Chao Chen. et al. [64], prepared chitosan membranes by crosslinking N-phthaloyl acylated chitosan using crosslinker- suberoyl chloride. Chitosan and phthalic anhydride were reacted in the mixture of solvents- DMF and distilled water under optimized conditions. (125 °C under nitrogen for 8 hrs.), followed by washing with methanol and filtration thrice. The N-phthaloylated chitosan formed, was added to dodecanoyl chloride (in a mixture of DMF, pyridine (2:1) at room temperature for 6 hrs.). The precipitates of N-phthaloyl acylated chitosan were collected (by cooling in a mixture of iced water and methanol (2:1)) and dissolved in solvents (DMF and pyridine) with continuous stirring at room temperature under nitrogen. Dropwise addition of Suberoyl chloride was done after cooling it in a bath of iced water and methanol when a yellowish flocculent precipitate out. These precipitates were filtered and suspended in methanol with continuous stirring for 4 hrs. and filtered again. After dissolving the product in ethyl acetate, it was poured onto a plate of tetrafluoroethylene. N-phthaloyl acylated chitosan membrane is obtained after drying it at 40℃ under vacuum for 12 hrs. The permeability of the membranes was reduced leading to the controlled release of micronutrients.

Thus, a researcher can opt for a greener approach that is energy and time-efficient, exploring the non-hazardous synthesis method. An agriculturist can explore the ways to supplement two or more micronutrients together through the application of a single biomatrix.

Loading of micronutrients.

This section includes the different ways of administering the micronutrients into the bio-matrices for their supplementation into the soil for effective absorption by the roots of the plants.

The biomatrices synthesized are uploaded with the micronutrients using adsorption [78, 84], , ionic gelation [84], or injection technique [91], in-situ addition of micronutrient containing compound during crosslinking step [73, 81, 86] and applied either to the soil or leaves or hydroponic solution, from where the roots/leaves of the plants absorb these micronutrients. Micronutrient utilization by the plants is reflected by their enhanced growth performance as well as healthy and high crop productivity.

Kinetics and Mechanism of micronutrient release

Once the micronutrient is absorbed by a biomatrix, it is released gradually, (usually as per the diffusion gradient or polymer relaxation), which nourishes the soil and enables the plants to cope with the micronutrient paucity, thus averting their collapse. These biomatrices serve as micronutrient supplementary capsules, that aid in their enhanced growth and performance, whensoever the need arises due to intensive crop practices. These biomatrices prevent micronutrient loss due to percolation into the ground or leaching or surface run-off and avail the micronutrients to the crop. They let the micronutrients bio-available in the soil layer, where roots usually grow and adhere to the roots of the plants making them accessible for absorption to be used up by the plants. The effective concentration of the micronutrients that a plant can absorb is dependent on various factors such as pH and fertility of the soil and the concentration of other existing ions in the soil [92].

Foliar application of different matrices has also been accomplished by applying sprays. But, owing to less penetration through thick waxy cuticle coatings of the leaves, loss due to evaporation, and run-off due to rainfall or hydrophobic surfaces, the use of sprays is avoided[93]. Direct application of micronutrients into the soil does not make them available to the plants as they may undergo oxidation or precipitation in reaction with oxygen and other constituents of the soil, respectively [94].

The kinetics and mechanism of release of micronutrients are usually diffusion-based or due to polymer relaxation.

Semi-empirical Korsmeyer-Peppas equation [95] is applied to understand the mechanism of micronutrient release [Eq. 1]:

$$f(M) = \frac{Mt}{M\infty} = kt^n \qquad \text{[Eq. 1]}$$

where, f(M), is the fraction of metal ions released; M_t is the amount of metal ions released in time t, and M_∞ is the total amount of metal ions loaded in the bio-matrix; k is the kinetic constant and n is the diffusional exponent that is dependent on the geometry of the matrix and on the physical mechanism of release. In cylindrical-shaped matrices, three cases may be observed:

- If $n < 0.5$, the transport mechanism is Quasi-Fickian (polymer relaxation time is greater than solvent diffusion time); the Release mechanism is non-swellable matrix diffusion.
- If $n = 0.5$, the transport mechanism is Fickian diffusion and the release mechanism is non-swellable diffusion.
- If $0.5 < n < 0.1$, the transport mechanism is anomalous, i.e., the combination of classical Fickian and Type II transport; and the release mechanism is both diffusion and relaxation.

- If n = 1.0, the transport mechanism is Case II transport, and the release mechanism is independent of the concentration of metal ions but is time-dependent.
- If n > 1.0, the transport mechanism is Super case II transport (involving swelling and relaxation of polymer matrix) and the release mechanism is both diffusion and relaxation.

Higuchi Equation [Eq. 2] [67]**:**

$$Q = \frac{Mt}{M\infty} = k_H t^{1/2} \qquad \text{[Eq. 2]}$$

Where k_H is the rate constant; Q is the fraction of metal ions released in time t. This equation describes the micronutrient release as a square root of a time-dependent process based on the Fickian diffusion equation.

Weber and Morris Diffusion model[86]**:**

Weber and Morris derived an equation [Eq. 3]:

$$q_t = k_i t^{1/2} + C \qquad \text{[Eq. 3]}$$

where q_t = uptake of absorbent, k_i = intraparticle diffusion rate constant (mg/g $min^{1/2}$), t is the time (in mins.), C is the intercept. This equation is utilized to determine the rate of intraparticle diffusion by linearizing it. If intraparticle diffusion is involved, we get a linear graph of uptake (q_t) versus the square root of time ($t^{1/2}$). Further, the line passing through the origin implies the intraparticle diffusion to be the rate-determining step whereas if some intercept is present, it indicates the involvement of other kinetic models in adsorption.

Marko Vincekovic, [73] et.al. applied the above equation to study the mechanism of release of copper ions from chitosan/alginate microcapsules and reported the mechanism to be classical

Fickian for larger microcapsules and non-Fickian type for small-sized microcapsules. Gulen Oytun Akalin, et.al.[85], prepared nano-porous sodium carboxymethyl cellulose (NaCMC) hydrogels and reported zero-order kinetics for the release of copper ions in water. Dhruba Jyoti Sarkar, et al.,[79] synthesized superabsorbent hydrogels (using carboxymethylcellulose (CMC) and acrylamide (AM) and reported the release of zinc ions to be non-Fickian/anomalous type. H Helmiyati et al.,[80] fabricated superabsorbent nanocomposites, employing sodium alginate, acrylic acid, and acrylamide, and found the release of Boron to follow pseudo-first-order kinetics. Gulen Oytun Akalin et al.,[84] synthesized κ-carrageenan (κ-CG) hydrogels for their application in the release of copper (Cu) and manganese (Mn) micronutrients and found the release of both the micronutrients to be of Case type II. GunaSunderi Raju, et.al.[72], observed that the release of copper ions from chitosan (CTS)/epoxidized natural rubber (ENR) bio-composite followed zero-order kinetics, i.e., the release due to diffusion is independent of the concentration of copper ions. The statistics observed corresponded well with the Higuchi square-root equation (amount of micronutrient ions released vs. function of the square root of time), with a high value of correlation coefficient, indicating the micronutrient release to be diffusion controlled. Jahangir Abedi-Koupai et al [67]., applied Higuchi's equation to reveal the release of iron via microcapsules fabricated by them, employing different types of polymers. D. Skrzypczak, et al .[86], fabricated alginate-carboxymethyl cellulose eggshell bio-composites for the release of zinc. The Weber-Morris diffusion model was used to explain the sorption kinetics. The rate constants and maximum sorption capacities for dry and wet capsules were found to be 0.358, 0.259, and 49mg g^{-1}, 281mg g^{-1} respectively.

1.2.1.2. Waste-water Treatment for Irrigation

Water, being a major natural resource, must be reused for its conservation and sustenance, thus paving the way for innovations in waste-water treatment for researchers. Progress and extreme industrialization are the key factors in rendering water pollution. The polluted water usually has inorganic impurities: due to the presence of heavy metals, inorganic anions, and radionuclides) and organic impurities due to the presence of dyes and persistent organic pollutants such as polychlorinated biphenyls, organochlorine pesticides, Hexa-chloro benzene, dichloro-diphenyl-trichloroethane, dioxins, and furan [96]. Though, present in trace quantities, these pollutants are life-threatening to the existent species. Polluted water if used for irrigation will lead to the pollutant's entry into the food chain and will be toxic for the environment and all living species existent on earth. Therefore, water to be applied for irrigation needs to be purified. Though many methods are being used such as reverse osmosis, chromatography, electrodialysis, and many others, hydrogels can also be applied as a cleaner technique to clean wastewater as it is cheaper and requires less labour and a greener way.

The swelling and deswelling tendency of the hydrogels allow them to be applied in waste-water treatment. As the adsorption and desorption of water pollutants by the hydrogels is a complex phenomenon, the hydrogel synthesis must be worked upon considering the various parameters for boosting and amending the attributes of the hydrogels. Based on the functional groups present in the polymers employed in the hydrogel synthesis, chemical properties of the contaminants to be removed from wastewater, and experimental conditions viz. temperature, pH, and concentration of salts; the various contaminants to be removed from the wastewater may involve chelation/ion-exchange/electrostatic interaction/hydrogen bonding/acid-base interactions/hydrophobic

interactions or a combination of all these processes. The adsorption process may involve multiple enlisted processes to varying degrees, including both physisorption and chemisorption.

Hydrogel adsorption properties are regulated by the hydrophilicity of the polymer employed and the cross-linking density [97]. Due to the high swelling capacity of the biopolymer-based hydrogels and the presence of hydrophilic cross-linking units, these hydrogels can entrap organic contaminants such as dyes involving diffusion and/or polymer relaxation [98].

Hydrogel application in the removal of inorganic impurities, mainly heavy metal removal owes to the process of diffusion and electrostatic attractions. The heavy metals either penetrate inside the hydrogel due to the concentration gradient or sets up the electrostatic attraction between the metal ions and functional group active sites of the polymer applied. Further, in some cases, there is an ion exchange [99] i.e., the exchange of heavy metal ions with the metal of the hydrogel network ($-COO^-Na^+$).

Organic hybrid hydrogels are significant for their application as adsorbent materials as they have a large surface area, highly porous structure, low interfacial tension, modifiable attributes, and relevant surface functions. Hydrogels can easily interact with organic and inorganic atoms/ions/molecules and therefore, are of great interest in their effective separation from a mixture [100]. Further, the existence of variable functional groups (-OH, -COOH, $-NH_2$, $-SO_3H$, etc.) serves as active sites for the separation process and aid in selective adsorption and percentage separation (adsorption capacity) [101]. High adsorption, the easy penetrability of small molecules, quick responsiveness, simple methods of fabrication, and economical and ease of practicability; are some of the positive attributes of hydrogels to be used as adsorbents for the removal of organic

and inorganic impurities from wastewater. Another key characteristic of these hydrogels is their reusability as they can be recovered and recycled.

Hydrogel's role in various agronomical applications, pharmaceutical applications, in drug delivery has been explored widely, with minor research on its application in the removal of organic and inorganic impurities from wastewater. This literature review surveys the hybrid hydrogels synthesized for effective use in waste-water treatment to date, opening a gateway for the usage of lesser applied polymers having positive and desired attributes, for the fabrication of hydrogels to serve as green techniques for waste-water treatment. Further, as Carboxymethyl tamarind kernel gum has been explored a little in this research area, it can be a good option for hydrogel fabrication and its usage in wastewater treatment **(Figure. 1.12.)**.

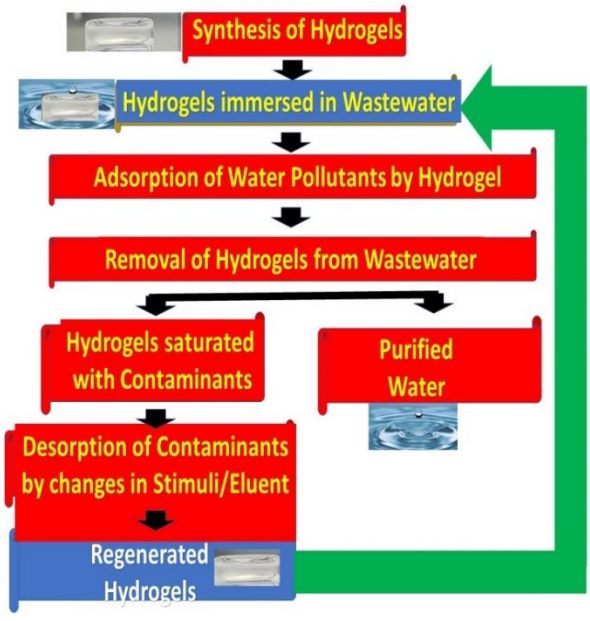

Figure 1.12. Hydrogels as sustenance Technique in Waste-Water Treatment for irrigation

The design for the application of Hydrogels in wastewater purification

The methodology adopted for the application of Hydrogels in the removal of impurities from wastewater includes synthesis of hydrogel, putting them in wastewater for adsorption of impurities, removal of hydrogels after adsorption, and recovery of hydrogels by desorption of impurities by altering external stimuli or solvent extraction and finally reusing them.

An increase in organic and inorganic contaminants load in water and further slow or negligible biodegradation and susceptibility to biomagnification of these contaminants; poses a challenge to the researchers to design and develop novel hydrogels for water purification. Hydrogels, being porous (to favour adsorption) and sensitive to different stimuli (for easy recovery and reuse), can easily be employed for the removal of organic as well as inorganic impurities as displayed in **Figure.1.13**.

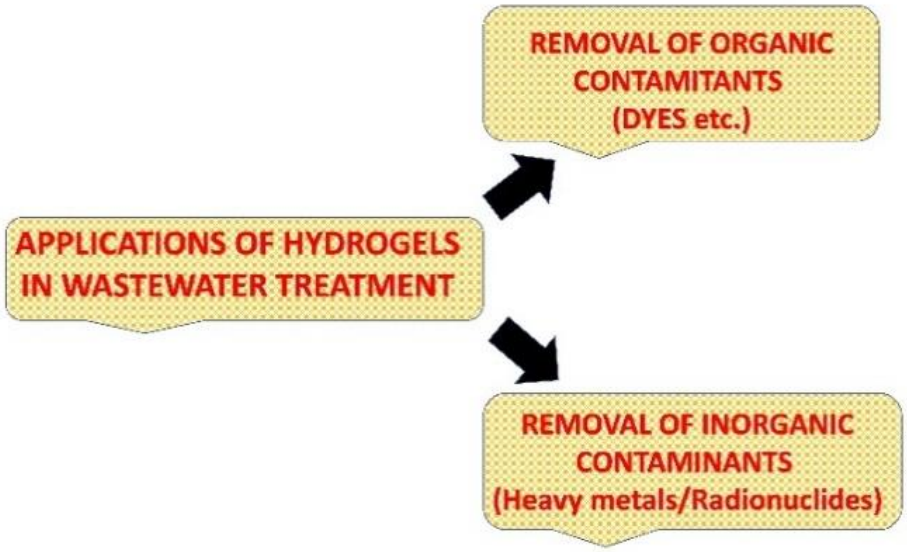

Figure 1.13. Applications of Hydrogels in Wastewater Treatment.

The properties of the hydrogels facilitate them to adsorb organic and inorganic impurities in the presence of ionic charges in them. The electrostatic forces of attraction between these charges and the charges present on cationic and anionic impurities help in efficient adsorption and hence easy separation. Hydrogen bonding between hydrogel and impurities also boosts adsorption. Further, covalent, and non-covalent interactions as observed between the carboxylic group of hydrogels and the amino group of dyes also favour adsorption. Aromatic moieties present either in dyes or hydrogel also impart strong $\pi - \pi$ interactions. The hydrogels removing the impurities, should have specific elimination attributes, pollutant retention capacity, higher stability, and regeneration ability. For organic impurities such as dyes, the functional groups (-COOH, -OH) interact with the sorbents and dyes via electrostatic attraction, hydrogen bonds, and $\pi - \pi$ interactions while for inorganic impurities as heavy metal ions or radionuclides, the interactions involved are electrostatic attractions, surface complexes, ion exchange, exposure to more active sites (oxygen-containing groups), more of negative charges leading to $\pi - \pi$ stacking interactions, ion-exchange, hydrogen bonds, strong $\pi - p$ stacking interactions.

Hydrogels for Removal of Inorganic Impurities

Air pollution, agricultural fertilizers and pesticides, sewage sludge, industrial waste, and other anthropogenic activities release heavy metals into the environment [102]. Metals having a mass greater than 5 cm^{-3} are regarded as heavy metals [103]. They are about 40 in number. These heavy metals are toxic and harmful to the biotic and abiotic components of the environment, even in trace amounts. On the other hand, water is also polluted due to the radioactive waste produced due to the nuclear processes and needs its removal to avoid serious ill effects on human health and the environment [104].

As already discussed previously, hydrogels can be effectively applied in the removal of heavy metals as well as radionuclides in an environmentally friendly way. **Table 1.3** and **Table 1.4**. enlist some of the bio-hydrogels that have been successfully applied in the removal of major heavy metals and radionuclides found in wastewater respectively. This will aid scientists to research new natural-based hydrogels having better and desired properties that can be used efficiently for the removal of heavy metals and radionuclides.

Table 1.3. Hydrogels for removal of Heavy Metal

Hydrogel Constituents	Heavy Metals removed	Recovery Method	Reference
Ulvan dialdehyde and Gelatin	Cu^{2+} (14 mg/g), Co^{2+} (7 mg/g), Ni^{2+} (6 mg/g) and Zn^{2+} (6 mg/g).	Precipitation with Ethanol	[105]
Chitosan and Poly (Acrylamide-Acrylic Acid)	Cr (III) and Cd (II)	-	[106]
F127-Diacrylated and Polyacrylic acid	Cu^{2+} (283.4mg/g) and Hg^{2+} (222.1 mg/g). In Bovine Serum Albumin-containing water, the reported removal ratio of Cu^{2+} and Hg^{2+} was 94% and 70.2% respectively, and in humic acid-containing water, it was reported to be 89.5% and 72.1%.	Immersion into HNO_3 at 25℃ for 24 hours. Sorbents were regenerated with 0.1 M NaOH solution followed by washing with deionized water.	[107]
Microcrystalline Cellulose and ε-polylysine	Pb^{2+} and Cu^{2+} showed maximum adsorption capacities of 259.64 mg/g and 161.59 mg/g at pH 5-6.	Changes in temperature and pH	[108]
DNA and Chitosan	Adsorption of Hg^{2+}, Pb^{2+}, Cd^{2+} and Cu^{+2}.	-	[109]
α-ketoglutaric acid grafted Chitosan and Acrylamide	Adsorption capacities recorded were Cu^{2+}(72.39 mg/g), Pb^{2+} (61.41 mg/g) and Zn^{2+} (51.89 mg/g)	Elution with 0.1 M HCl solution followed by regeneration with 0.1 mol/L NaOH solution and washing with deionized water.	[110]

Polyaniline-polypyrrole modified graphene oxide and alginate matrix.	Adsorption capacities recorded were Cr^{4+}(133.7 mg/g), and Cu^{2+} (87.2 mg/g) at pH 3.0.	Cr^{4+}adsorbed hydrogels: Immersion in 0.01 M NaOH solution for 10 mins: Cu^{2+}adsorbed hydrogels: immersion in 0.2 M HCl for 15 mins.	[111]
Sulphomethylated lignin and polyacrylic acid.	The adsorption capacities recorded were Co^{2+} (145.14 mg/g), Cu^{2+} (117.65 mg/g), Ni^{2+} (166.67 mg/g), Cd^{2+} (277.78 mg/g), and Pb^{2+} (344.85 mg/g).	-	[112]

N. Wahlström et al. fabricated a hydrogel using Ulvan dialdehyde and Gelatin for removal of Cu^{2}, Co^{2+}, $Ni^{2+}$and Zn^{2+} and found the maximum adsorption capacities to be 14 mg/g, 7 mg/g, 6 mg/g and 6 mg/g respectively. The studies were done at pH 6.5 and 3. The concentration of heavy metals was analyzed using induced coupled plasma optical emission spectroscopy [105]. L. S. Jasim et al. developed a hydrogel employing Chitosan and Poly (Acrylamide-Acrylic Acid) for eliminating the pollutants Cr (III) and Cd (II) and found the kinetics of adsorption [106]. Q. Meng et al. synthesized a hydrogel from F127-Diacrylated and Polyacrylic acid and found the maximum adsorption capacities for heavy metal ions to be Cu^{2+}: 283.4mg/g and Hg^{2+}: 222.1 mg/g. In Bovine Serum Albumin-containing water, the percentage removal of Cu^{2+} and Hg^{2+} was 94% and 70.2% respectively and in humic acid-containing water, it was 89.5% and 72.1% respectively. The concentrations of heavy metals were measured using an atomic absorption spectrometer [107]. X. Huang et al. formulated a hydrogel using Microcrystalline Cellulose and ε-polylysine and recorded showed maximum adsorption capacities of Pb^{2+} and Cu^{2+} to be 259.64 mg/g and 161.59 mg/g respectively at pH 5-6. The rate of adsorption of heavy metals was investigated by employing inductively coupled plasma mass spectrometry [108]. K. Chan et al. constituted DNA and Chitosan-based hydrogel and studied the adsorption of Hg^{2+}, Pb^{2+}, $Cd^{2+,}$ and Cu^{+2}. Owing to the presence of both cationic and anionic sites in the hydrogel, both cationic (methylene blue) and anionic (Congo red) dyes could be removed. The hydrogel revealed a higher adsorption capacity for Hg^{2+} ions [109].

Table 1.4. Hydrogels for removal of Radionuclides

Hydrogel Constituents	Radionuclides removed	Recovery method	Reference
Polyacrylamide, Sodium Alginate	Radioactive Strontium and Cerium.	-	[113]
Sodium Alginate, PVA	Radioactive ^{137}Cs were removed.	Ion -exchange	[114]
Graphene oxide and ascorbic acid	Uranium [VI]	Treating with HCl (pH 0.2) on a rotary shaker (100 rpm) for 24 hours followed by washing with deionized water.	[115]
Graphene oxide and polyethyleneimine	Simultaneous removal of cationic U (VI) and anionic Re (VII) with the highest adsorption capacities of 629.5 mg/g (at pH 5.0) and 262.6 mg/g (at pH 3.5) respectively.	Elution with 0.1 M HNO_3 or NaOH solution at pH 5 for uranium and at pH 3.5 for rhenium.	[116]
Graphene oxide and Bayberry tannin sponge	^{90}Sr was removed with a maximum adsorption capacity of 67.98 mg/g.	-	[117].
Graphene oxide and Phytic acid	The maximum adsorption capacity of U(VI) reported is 545.7 mg/g at 1.2 V and pH 5.0.	Immersion in HNO_3 solution followed by washing with deionized water	[118]
Graphene oxide, chitosan, and guanamine-deuterated polyacrylonitrile	The maximum adsorption capacity of U (VI) observed was 247 mg/g.	Treatment with 0.1 mol/L $NaHCO_3$.	[119]
Chitosan, Graphene oxide and poly ethyleneimine	The maximum adsorption capacity of Selenium reported is 1.62mg/g at 25 ℃.	-	[120]

F. M. Cui et al. fabricated a Polyacrylamide and Sodium Alginate hydrogel for the removal of Radioactive Strontium and Cerium from skin wounds [113]. S. K. Pathak et al. developed potassium nickel hexacyanoferrate (NNiHCF) beads using PVA and Sodium Alginate (as a binding agent) for the removal of Radioactive ^{137}Cs. The sorption studies were completed following an ion-exchange mechanism where the potassium ions were exchanged with the caesium ions. The adsorption followed the intra-particle diffusion model and pseudo-second-order kinetics [114]. Y. He et al. fabricated Graphene oxide and ascorbic acid hydrogel for the removal of Uranium [VI]. The Uranium concentration was measured using induced coupled plasma optical emission spectroscopy (at 652 nm) [115]. Z. W. .Huang et al. formulated a graphene oxide and polyethyleneimine matrix for simultaneous removal of cationic U (VI) and anionic Re (VII) with maximum adsorption capacities of 629.5 mg/g (at pH 5.0) and 262.6 mg/g (at pH 3.5) respectively. The radionuclide concentration was measured using induced coupled plasma optical emission spectroscopy. The hydrolysis precipitation along with the affinity of uranium for the free amines present in the hydrogel are accountable for the removal of radioactive uranium while electrostatic attraction and hydrogen bonding between rhenium and free/protonated amines in the hydrogel are responsible for the removal of radioactive nuclide [116]. Rhenium.X. Deng et al. synthesize a hydrogel using graphene oxide and Bayberry tannin sponge. ^{90}Sr was removed with a maximum adsorption capacity of 67.98 mg/g. The concentration of strontium ions for the determination of adsorption capacity was measured using atomic absorption spectrometry [117].

Hydrogels for Removal of Organic Impurities

Organic impurities predominantly, dyes are one of the major constituents of wastewater. Dyes, usual effluents from the textile industry and chemical industry affect human and aquatic life extremely. As dyes are generally stable and have a complex structure, their degradability rate is very slow and difficult and may accumulate with time [121]. Therefore, dyes need to be removed from wastewater to prevent them from entering the food chain. Hydrogels play a significant role in the removal of dyes from wastewater commendably. **Table 1.5**. enlists some of the hydrogels applied well in the removal of dyes from wastewater, including their synthesis.

Table 1.5. Hydrogels for removal of Dyes

Hydrogel Constituents	Dyes removed	Recovery Method	Reference
Magnetite-functionalized cellulose nanocrystals, starch, acrylamido-2-methylpropanesulphonic acid, and acrylic acid	The maximum adsorption capacities recorded, for Crystal violet were 2500.00mg/g, and for methylene blue was 1428.6 mg/g.	Treatment with HCl solution (pH 4) followed by drying at 50℃.	[122]
Ulvan dialdehyde and Gelatin	The maximum adsorption capacity recorded, for Methylene blue was 465 mg/g.	Precipitation with Ethanol	[105]
Gelatin and glutaraldehyde	The maximum adsorption capacities recorded of crystalline violet was 138.89 mg/g, methyl orange: 72.63 mg/g, acid fuchsin: 66.29 mg/g, Congo red: 64.84 mg/g, malachite green: 64.64 mg/g, and methylene blue: 60.32 mg/g.	Treatment with a mixture of NaCl and methanol.	[123]
Locust bean gum and N, N-dimethyl acrylamide	The maximum adsorption capacity of Brilliant green dye was observed to be 142.85 mg/g at pH 5.8.	Elution with 0.1 M HCl solution.	[124]
Carboxymethyl cellulose, polyvinyl alcohol	The maximum adsorption capacity observed was 46.79 mg/g for methylene blue and 44.89 for Rhoda-amine B	Treatment with ethanol/water, 0.1 N NaCl medium via ultrasonication for 4 hours.	[125]
Chitosan and graphene oxide	An increase in graphene oxide concentration leads to higher cationic dye removal while an increase in chitosan concentration increased the anionic dye removal.	Treatment with 0.5M NaOH solution	[126]
The composite Hydrogels: Graphene oxide, L-ascorbic acid, hydrazine hydrate, P25 TiO_2 nanopowder, and MWCNT-Graphene hydrogels:	The maximum adsorption capacity of methylene Blue was reported to be 87.63 mg/g.	Photodegradation by UV or visible light irradiation.	[127]

Graphene oxide, L-ascorbic acid, hydrazine hydrate, and P25-MWCNT'S.			
1) Chitosan (CS) beads: Chitosan 2) Epichlorohydrin (ECH)-Chitosan beads: Chitosan and ECH 3) CS/CNT (Carbon nanotubes): Chitosan, CNT 4) ECH-CS/CNT beads: CS, CNT, and ECH	The maximum adsorption capacity of Congo Red dye was reported to be: 1)CS Beads:178.32 ± 1.32 2)ECH-CS Beads: 181.01 ± 1.67 CS/CNT Beads: 423.34 ± 2.86 ECH-CS/CNT Beads: 422.06 ± 2.23	-	[128]
Lignin and polyvinyl methyl ether (PVME) and maleic acid (MA).	Methylene Blue (MB) removal was studied. SKL-NH_4OH Hydrogel showed maximum removal of 95.78% of MB. SSL (Wheat straw soda lignin)-NaOH revealed 80% of MB. SKL-NaOH and OSL-NaOH showed 78.09% and 62.72% respectively. The lowest adsorption (below 46.57%) was observed for control Hydrogels.	-	[129]

Hydrogel Recovery: Reusability and regeneration of hydrogels after saturation with impurities

Hydrogels once saturated with water contaminants after adsorption are either subjected to a reversed stimulus or treated with a suitable eluent for the desorption of contaminants from the hydrogel so that they can be reused again for the same. For the successful application of hydrogels in wastewater treatment, the chemical attribute of hydrogels to be recovered and reused is of utmost significance. Besides exhibiting a higher rate of adsorption and higher adsorption capacity, the hydrogel's regeneration should be economically viable and sustainable too. The solutions generally employed for the recovery of hydrogels are centred on acids and alkalis, thus altering the pH. The various other parameters under consideration include concentration, volume, and time for which a contaminant-saturated hydrogel is to be kept in contact with enlisted solutions for a proficient recovery. Further, the changes in temperature, regeneration of ion-exchange chambers, and photodegradation also lead to the desorption of impurities. The different recovery methods for the referred hydrogels employed for the removal of metal ions, radionuclides, and dyes have been discussed in **Table.1.3, Table. 1.4 and Table. 1.5.** Thus, we can conclude that hydrogels are recovered by altering pH by the addition of any acid or base (HCl/HNO_3 or $NaOH/NaHCO_3$), by altering the temperature, or by regeneration of ion-exchange chambers, or by use of an appropriate desorbing agent.

The studies related to the recovery and reusability of hydrogels once they adsorb to their maximum capacity reveal that altering the external stimuli leads to the regeneration of hydrogels for usage. The recoverable capability of a hydrogel is the most critical factor for its wide and practical applicability of it. Hydrogel is effective if it can be reused multiple times sustaining almost the

same adsorption capacity every usage, as demonstrated in its first-time application. Gao et al. recovered polydopamine-functionalized graphene (PDA-GH) hydrogel after applying it for the removal of heavy metal ions and dyes (rhodamine B and ρ-nitrophenol), by using low-cost 0.1 M HCl solution and ethanol respectively. The recovered hydrogel retained an adsorption capacity of more than 80% even after ten adsorption and desorption cycles [130]. Swami et al. fabricated superabsorbent polyelectrolytic hydrogels and applied them for adsorption of Cr^{6+}, Ni^{2+}, Cu^{2+}, and Pb^{2+} and found that the hydrogels were 97% recoverable with 1N HCl eluting agent. Moreover, the hydrogel can be used repeatedly for about 10 cycles [131]. Xiao-Jie Ju et al. [132] (p9NIPAM-co-BCAm) hydrogels for removal of Pb^{2+} ions and found that the hydrogels can be recovered by altering the temperature as Pb^{2+} ions are adsorbed at a temperature lower than LCST and get desorbed at a temperature higher than LCST.

Mohammadi et al. recovered chelator-mimetic multi-functionalized hydrogel post-removal of metal ions (Cd, Pb, and As), by using HCl as an eluent, maintaining 60% removal post five adsorption-desorption cycles [133]. Pourjavadi et al. also applied 1 M HCl as a solvent for the effective removal of Pb from Pb-adsorbed hydrogel based on Chitosan, acrylamide, and amine-functionalized nano-silica, maintaining almost the same adsorption capacity post three cycles of reusage [134].

Tang et al. effectively recovered Cr (IV) loaded magnetic hydrogel by using NaCl solution and efficiently reused the hydrogel for 20 cycles with 97-98% removal capacity [135].

For successful application in procedures and praxes of waste-water treatment, the reusability of the hydrogel is one of the most vital attributes to be considered. But, following swelling in water, the hydrogel loses its mechanical toughness and strength that is utmost required for its reusage.

So, this is a foremost challenge that needs to be focused on. Keeping this point of view, Gong et al. fabricated double network hydrogels possessing high mechanical strength [136].

Adsorption Isotherms of adsorption by the Hydrogels

For the applications of hydrogels in wastewater treatment, quantitative analysis of the rate of adsorption by the hydrogels is critical. The fabricated hydrogel is kept in contact with the wastewater having the specific contaminant whose removal is proposed. The original concentration of the contaminant in wastewater and after hydrogel treatment is found by instrumental spectrophotometric analysis. To know the rate of adsorption and adsorption isotherm the hydrogel fits into, the amount of adsorption is determined after specified intervals of time and the data is fitted into the different adsorption models. Further, the maximum rate of adsorption is also found by varying various parameters viz. temperature, pH, soil concentration, etc.

Adsorption kinetics are of significance for the evaluation of adsorption efficiency. Usually, three models are employed to express the kinetics of adsorption :

1) Pseudo-first order Model: It is described by Equation:

$$\frac{dqt}{dt} = k_1(q_e - q_t)$$

For linearized data plotting, the above formula on integration becomes:

$$\text{Log}(q_e - q_t) = \log(q_e) - \frac{k1}{2.303}\ t$$

Where q_t = amount of pollutants adsorbed at time t (mg g^{-1})

q_e = amount of pollutants adsorbed at equilibrium (mg g^{-1})

t = contact time (min)

k_1 = rate constant of pseudo-first-order adsorption (min^{-1})

2) Pseudo-second order Model

It is expressed by:

$$\frac{dqt}{dt} = k_2(q_e - q_t)^2$$

Integrating, we get:

$$\frac{1}{dqe-qt} = \frac{1}{qe} + k_2t$$

Where k_2 = second-order rate constant of adsorption (g/ (mg min))

3) Intra-particle diffusion Model:

Following Weber and Morris, adsorption capacity is calculated by:

$$q_t = K_{id}\, t^{0.5} + I$$

Where q_t = adsorption capacity at time t

$T^{0.5}$ = half-life time (sec)

K_{id} = rate constant of intra-particle diffusion (mg g^{-1} $min^{0.5}$)

I = Intercept (mg/g)

Adsorption Isotherm

Adsorption isotherm predicts the feasibility of the adsorption. Two parameter isotherm models

which are generally used are:

1) Langmuir Adsorption Isotherm Model:

It is based on assumptions of monolayer adsorption and the adsorbent surface being homogenous having a single type of binding site It is expressed by:

$$\frac{Ce}{qe} = \frac{1}{qm\,b} + \frac{Ce}{qm}$$

Where C_e = Adsorbate concentration at equilibrium (mg/L)

q_e = amount of adsorbates adsorbed at equilibrium

b = Langmuir constant (L/mg)

q_m = maximum adsorption capacity of the adsorbent (mg/g)

The separation Factor or the equilibrium parameter is given by the:

$$R_L = \frac{1}{1+b\,Co}$$

Where C_O = initial concentration of adsorbates in solution (mg/L)

If $R_L > 1$, the Langmuir process is unfavorable

If $R_L = 1$, the Langmuir process is linear

If $0 < R_L < 1$, the Langmuir process is favorable

If $R_L = 0$, the Langmuir process is irreversible

2) Freundlich Adsoroption Isotherm

It is based on the assumption of multilayer adsorption on a heterogenous surface [48]. It is calculated by employing Equation:

$$\text{Log } q_e = \log K_F = \frac{1}{n} \log C_e$$

Where K_F = Freundlich isotherm constant

n = Adsorption Intensity

Though most of the metal ions adsorptions follow either Langmuir or Freundlich model, the adsorption of some metal ions apt well to both models. Kumari et al. [137] revealed that the adsorption of Pb^{2+} ions by the Calcium alginate matrix followed both the isotherms, indicating multilayer sorption. Similarly, nano-hydroxyapatite-alginate composite synthesized by Jiali Guo et al. [138] adsorbed Cu^{2+}ions fitting into both models. Magnetite nanoparticle embedded pectin-graft-poly(N-hydroxyethyl acrylamide) hydrogel fabricated by P. Kulal et al. [139] revealed that the adsorption of Rhodamine 6G dye and metal ions [Cu(II), Hg (II)] fit well to both the Langmuir and Freundlich models. W. Zhang et al. [140] fabricated alginate-based nanocomposite hydrogels for removing Cr (VI) and Cu (II) and revealed Freundlich isotherm following pseudo-second-order kinetics .

Niklas Washington et al. [141] revealed that the Ulvan dialdehyde-gelatin hydrogels adsorbed methylene blue dye by Langmuir adsorption isotherm, following pseudo-second-order kinetics. Q. Meng et al. [142] fabricated F127/Polyacrylic acid hydrogels that followed the pseudo-1st order model during the adsorption of Cu^{2+} and Hg^{2+} ions by the Langmuir model of kinetics. Z. Zhao et al. [143] synthesized α-ketoglutaric acid-modified chitosan/polyacrylamide semi-interpenetrating polymer network hydrogel for Cu (II), Pb (II), and Zn (II) for adsorption following pseudo-second

order fitting into Langmuir isotherm model. Gao-Jie Jiao et al. [144] fabricated lignin-based composite hydrogels for the adsorption of Co^{2+}, Cu^{2+}, Ni^{2+}, Cd^{2+}, and Pb^{2+} fitting into the Langmuir model, following pseudo-second-order kinetics.

Layth S. Jasim et al. [145] synthesized Chitosan and Poly (Acrylamide-Acrylic Acid hydrogels and revealed that these hydrogels followed Freundlich isotherms during the adsorption of Cr (III) and Cd (II) ions . Xin Huang et al. [146] synthesized ε-polylysine-modified microcrystalline cellulose-based hydrogels and found the Freundlich model suitable following pseudo-second-order kinetics.

Kayee Chan et al. [147] fabricated DNA-Chitosan hydrogels that fit using the pseudo-second-order kinetic model for methylene blue adsorption and inter-particle diffusion kinetics model.

Application of Carboxymethyl Tamarind Kernel Gum based Hydrogels in Wastewater treatment:

Carboxymethyl tamarind kernel gum (CMTKG) has been applied a little in wastewater treatment. Due to scarcer exploration, and worthy potential aspects of CMTKG (natural polymer, non-toxic, abundant availability, cheap, biodegradability, ease of its derivatization from tamarind kernel gum), CMTKG is a good option for researchers to explore and fabricate innovative hydrogels for its application in wastewater treatment. G. Sen et al.,[148] fabricated a hydrogel by employing carboxymethyl tamarind kernel gum and polyacrylamide and applied it as a flocculant. Another nano-composite synthesized using Carboxymethyl tamarind kernel gum and silicon dioxide as nano-filler was used as a flocculant and in the removal of methylene blue dye with a maximum adsorption capacity of 43.859 mg/g [149]. Further, tamarind kernel gum-based hydrogel developed by a free radical mechanism was applied for the removal of Cu^{2+} with a maximum adsorption

capacity of 68.03 mg/g Adsorption of Cu2+ from Aqueous Solution [150]. As the present research on carboxymethyl tamarind kernel gum is rare, this polymer is an eye-catcher for scientists and can be efficiently applied in wastewater management.

1.2.1.3. Soil water-Conditioner

Hydrogel's role in agronomy is significant as they are addressing the major agricultural challenges viz. water scarcity, boosted food productivity, water conservation, enhanced soil quality thus promoting sustainable green practices for environmental resilience. The worthy potentials of hydrogels such as higher swelling capacity, water retention, adhesion, biocompatibility and biodegradability, open new outlook for researchers for them to be explored more and more. The major boon is that the properties of the hydrogels can be tailored and customized by employing specific polymers, crosslinkers and incorporating hydrophilic functional groups. Moreover, hydrogels are versatile as they can be applied to all the types of soils viz. clay, silty, loamy, and sandy with positive outputs of enhanced plant performance, high crop yields and better soil attributes. Hydrogels help to overcome the limitations of different types of soils, making them fit for agriculture.

Hydrogels have been successfully applied as a soil water conditioner in agronomical practices as depicted in **Table.1.6.**

Table.1.6. Hydrogels Applications as Soil water Conditioner

Matrices	Outcomes	References
Polymers: starch polyacrylonitrile graft copolymers, vinyl alcohol-acrylic acid copolymers and acrylamide sodium acrylate copolymers	Adding the polymers to the soil had beneficial effects on the plant performance, especially tomato	[151]
Polymerization of acrylic acid-co-acrylamide onto a cellulose backbone employing ammonium persulfate as an initiator and MBA as a crosslinker.	Superabsorbent hydrogel revealed water absorbance of 875 g/g distilled water, 490g/g natural rainwater and 90 g/g in aqueous NaCl solution.	[152]
Graft copolymerization of monomers acrylic acid onto the surface of east by employing ammonium persulfate as a free radical initiator and MB as a crosslinker	The superabsorbent hydrogels revealed excellent water absorption and retention for its application in agricultural sector	[153]
Poly acrylic acid- iron rich smectite (IRS) superabsorbent composites were prepared by polymerization of acrylic acid in the presence of MBA as a crosslinker.	The swelling capacity of IRS free superabsorbent was revealed to be 23,000 % of water and therefore can be employed in the agricultural sector as a water-conditioner.	[154]
Photopolymerization of acrylic acid with acrylamide in the presence of kaolinite powder under 30 minutes of ultraviolet irradiation at room temperature.	The Super absorbent revealed water absorbency of 433 g/g and salt solution absorbency of 108 g/g, therefore can be employed for soil water retention in agriculture.	[155]
Polymerization of acrylamide, acrylic acid, sodium vinyl sulfonate, sodium styrene sulphonates and bentonite clay employing potassium persulfate as an initiator and MBA as a crosslinker.	The superabsorbent has excellent water absorption capacity of up to 1000 grams of water.	[156]
Copolymerization of acrylic acid on attapulgite micro powder using MBA as a crosslinker and ammonium persulfate as an initiator.	The Super absorbent exhibited 1017 g water/g sample (distilled water) and 77 g water/gram sample (NaCl solution).	[157]
polymerization of acrylic acid or acrylamide with sodium silicate without the use of any other cross-linking agent.	The hybrid superabsorbent revealed high absorbancy in both distilled water and normal saline solution.	[158]

Polymerization of chitosan and poly (acrylic acid-co-acrylamide) three layer hydrogel using MBS crosslinker	It revealed water absorption of 70 gram per gram.	[159]
Polymerization of chitosan with polyvinyl alcohol and Poly (acrylic acid-co-acrylamide) 3 layered hydrogel, in the presence of crosslinker glutaraldehyde and MBA.	It revealed water absorption of 233 g/g.	[160]
Polymerization of chitosan and poly (acrylic acid-co-acrylamide) and basalt hydrogel in the presence of MBA as a crosslinker.	It increased the maximum water absorbency to 650 g/g versus 450 g/g for the hydrogel without basalt.	[161]
Polymerization of sodium carboxymethylcellulose with acrylic acid and 2-acrylamido-2-methylpropane sulfonic acid.	the hydrogel showed water absorbance of 604 and 119 percentage in distilled water and saline water respectively.	[162]
Polymerization of carboxymethyl tamarind kernel gum with sodium acrylate.	The hydrogel revealed high water retention.	[163]
Polymerization of sodium methacrylate and carboxymethyl tamarind kernel gum.	The hydrogel absorbed 248ml/g of the water and can be applied as a soil conditioner in the agriculture.	[164]

H. Agaba et al.[165] revealed that the hydrogel treatment to the sandy soil lowered the frequent irrigation and also enhanced the bio-mass of Agrostis stolonifera. C. Demitrri et al.[166] developed a superabsorbent hydrogel employing cellulose derivatives and applied it for water consumption by varying ionic strength and pH. P. C. Parvathy et al.[167] fabricated super absorbent hydrogels using cassava starch-g-poly(acrylamide) with varied absorbances. Khushbu et al.[168] synthesized hydrogels employing carboxymethyl tamarind kernel gum and sodium acrylate and applied it as a soil conditioner in agriculture.

1.2.2. Applications of CMTKG

Different Bio-matrices of CMTKG have been fabricated viz. hydrogels, nano-particles, pellets, films, composites, etc., and have been applied in several fields: tissue engineering (medicine, drug-delivery), wastewater treatment[40] agronomy, and thickener (Table 1.1).

Tissue Engineering

The novel bio-matrices of CMTKG have been applied in Tissue Engineering. Sanyasi et al.[169] synthesized a hydrogel from CMTKG and hydroxyethyl methacrylate and applied it in the field of bone tissue engineering. The films of CMTKG loaded with the drug (ciprofloxacin) revealed high microbial properties against E. coli. Choudhary et al.[170] fabricated bio-compatible CMTKG scaffolds and applied them for skin tissue engineering. Shaw et al.[171] synthesized drug (ciprofloxacin) loaded CMTKG-based films and applied them in skin tissue engineering.

Waste-Water Treatment

Sen et al.[172] synthesized novel flocculant for recycling wastewater by grafting polyacrylamide on the CMTKG skeleton. S. Pal et al.[149] synthesized CMTKG-based nanocomposite which

revealed high dye-absorption as well as flocculation. C. Niu et al.[173] showed that CMTKG-based bio-matrix can be effectively applied for the removal of Cu^{+2} ions from the water**.**

Agronomy

CMTKG has rarely been applied in agronomy. Khushbu et al. fabricated CMTKG hydrogel with sodium acrylate and applied it as a soil conditioner in the fields. Further, the same hydrogel was applied for the slow micronutrient (Zinc) release [3].

Thickener

The property as a thickener in CMTKG is exhibited due to the TKG skeleton[174]. N.R. Gupta et al.[175] grafted amino terminated poly(ethylene oxide-co-propylene oxide) onto the CMTKG skeleton and applied them as thickeners in pharmaceuticals and cosmetics. Wang et al. [176] synthesized mixtures of CMTKG and carboxymethyl Starch (CMS) of varied concentrations and observed the mixture having higher concentrations of CMTKG, exhibited better double-sided printing effects on georgette with higher penetration and better colors.

Table 1.7. Applications of CMTKG-based hydrogels

BIOPOLYMER	CO-POLYMER	APPLICATION	REFERENCES
CMTKG	Polyacrylamide	Removal of dye	[149]
CMTKG	Hydroxyethyl methacrylate	Skin Tissue Engineering	[169]
CMTKG/Gelatin	___	Skin tissue Engineering	[170]
CMTKG	Hydroxyethyl methacrylate	Skin wound healing/tissue engineering	[171]
CMTKG	___	Waste-water treatment (Adsorption of Cu^{2+})	[172]
CMTKG/Starch	___	Dye printing	[173]
CMTKG/Carboxymethyl Guar Gum	Poly (ethylene oxide-co-propylene oxide)	Thickener in cosmetics	[175]
CMTKG/ CM Starch	___	Printing of fabrics	[176]
CMTKG/Chitosan	___	Colon Drug Delivery	[177]
CMTKG	Acrylic acid	Agricultural applications	[30]

Eyeing the prospects of the necessity of a continuous reliant water supply system, that follows a greener approach, low maintenance, and favours enhanced growth even under drought conditions; this research implicates the usage of Carboxymethyl Tamarind Kernel Gum (CMTKG), a bio-based biopolymer to synthesize an organic hydrogel for dynamic agronomics.

1.3. Conclusions

Reviewing the literature on different applications of hydrogels in agronomy, it was found that many hydrogels have been applied for micronutrient supplementation and waste-water treatment but hydrogel's application as a soil water conditioner needs more research as water conservation is the most critical challenge that the world is facing today. Further literature survey of different applications of CMTKG led us to following conclusions:

- CMTKG has been scarcely explored in agronomical practices.
- Biopolymer based hydrogels has not ever been evaluated as a soil water conditioner in all the four types of the soil.

Application of Carboxy methyl Tamarind Kernel Gum-based Hydrogels as Soil-Conditioner in Agronomy

Carboxymethyl tamarind kernel gum (CMTKG) has been applied a little in agronomy. Due to scarcer exploration, and worthy potential aspects of CMTKG (natural polymer, non-toxic, abundant availability, cheap, biodegradability, ease of its derivatization from tamarind kernel gum), CMTKG is a good option for researchers to explore and fabricate innovative hydrogels for its application as a soil water conditioner in agronomy.

Biopolymer-based biomatrices own a potent position in agronomy but are yet to be exploited more for future applications as soil moisteners.

Owing to the high swelling ratios of the CMTKG-based organic hydrogels, these hydrogels may be applied as a continuous reliant water supply system, that follows a greener approach, low maintenance, and favours enhanced growth even under drought conditions; this research implicates the usage of Carboxymethyl Tamarind Kernel Gum (CMTKG), a bio-based biopolymer to synthesize an organic hydrogel for dynamic agronomics. This research demonstrates pragmatical synthesis, optimization, and characterization of two organic superabsorbent CMTKG-based hydrogels for their application as soil water conditioners.

1.4. Aims & Objectives

1) Multiple series of the CMTKG-based hydrogels were projected for synthesis, employing a chemical cross-linker and other apt monomers:
    - PSMA (Poly Sodium Methacrylate)
    - PSA (Poly Sodium acrylate) and PAM (Poly Acrylamide)
2) Systematic optimization was accomplished to target the most viable and best hydrogel of both types with the highest swelling capacity that may execute and confirm the other objectives of the purposed research.
3) The synthesized hydrogels were characterized utilizing various instrumental methods of analysis:
    - FTIR spectroscopy

- SEM studies
- TGA

4) Equilibrium swelling studies were piloted for both hydrogels. The effect of the cross-linker, initiator, and biopolymer concentrations used was monitored. Percent swelling as a function of pH, and the variance of equilibrium swelling in distilled water & salt solutions was also examined.

5) Bio-degradation experiments of the optimized hydrogels were conducted via the soil burial method.

6) The synthesized hydrogel was assessed for its application in the agricultural field for soil conditioning by monitoring and computing its effects on various below listed physical attributes of soil:

- Particle density
- Bulk density
- Porosity
- Maximum water holding capacity.
- Water retention capacity by Plantation method.
- Available Water Content by Pressure Plate Apparatus.

7) Furthermore, one of the synthesized hydrogels was valued as water conditioner in different types of soils. To the best of our knowledge, this type of study has not been reported in the literature.

References

[1] S.P. Wani, T.K. Sreedevi, J. Rockström, Y.S. Ramakrishna, Rainfed agriculture - past trends and future prospects, Rainfed Agric. Unlocking Potential. (2009) 1–35. https://doi.org/10.1079/9781845933890.0001.

[2] J. Vanschoenwinkel, S. Van Passel, Climate response of rainfed versus irrigated farms: the bias of farm heterogeneity in irrigation, Clim. Change. 147 (2018) 225–234. https://doi.org/10.1007/S10584-018-2141-2.

[3] A. Gupta, R. kumar Singh, M. Kumar, C.P. Sawant, B.B. Gaikwad, On-farm irrigation water management in India: Challenges and research gaps*, Irrig. Drain. 71 (2022) 3–22. https://doi.org/10.1002/IRD.2637.

[4] Khushbu, S.G. Warkar, N. Thombare, Zinc micronutrient-loaded carboxymethyl tamarind kernel gum-based superabsorbent hydrogels: controlled release and kinetics studies for agricultural applications, Colloid Polym. Sci. 2021 2997. 299 (2021) 1103–1111. https://doi.org/10.1007/S00396-021-04831-8.

[5] S. Nangia, S. Warkar, D. Katyal, A review on environmental applications of chitosan biopolymeric hydrogel based composites, J. Macromol. Sci. Part A Pure Appl. Chem. 55 (2018) 747–763. https://doi.org/10.1080/10601325.2018.1526041.

[6] A. Pourjavadi, G.R. Mahdavinia, M.J. Zohuriaan-Mehr, Modified chitosan. II. H-chitoPAN, a novel pH-responsive superabsorbent hydrogel, J. Appl. Polym. Sci. 90 (2003) 3115–3121. https://doi.org/10.1002/app.13054.

[7] Y. Yue, X. Sheng, P. Wang, Fabrication and characterization of microstructured and pH sensitive interpenetrating networks hydrogel films and application in drug delivery field, Eur. Polym. J. 45 (2009) 309–315. https://doi.org/10.1016/j.eurpolymj.2008.10.038.

[8] G.B. Marandi, K. Esfandiari, F. Biranvand, M. Babapour, S. Sadeh, G.R. Mahdavinia, pH sensitivity and swelling behavior of partially hydrolyzed formaldehyde-crosslinked poly (acrylamide) superabsorbent hydrogels, Wiley Online Libr. 109 (2008) 1083–1092. https://doi.org/10.1002/app.28205.

[9] Q.-Z. Yan, W.-F. Zhang, G.-D. Lu, X.-T. Su, C.-C. Ge, Frontal Copolymerization Synthesis and Property Characterization of Starch-graft-poly(acrylic acid) Hydrogels, Chem. - A Eur. J. 11 (2005) 6609–6615. https://doi.org/10.1002/chem.200500554.

[10] H.A. Abd El-Rehim, E.-S.A. Hegazy, H.L. Abd El-Mohdy, Effect of various environmental conditions on the swelling property of PAAm/PAAcK superabsorbent hydrogel prepared by ionizing radiation, J. Appl. Polym. Sci. 101 (2006) 3955–3962. https://doi.org/10.1002/app.22904.

[11] A.R. Fajardo, M.B. Silva, L.C. Lopes, J.F. Piai, A.F. Rubira, E.C. Muniz, Hydrogel based on an alginate-Ca2+/chondroitin sulfate matrix as a potential colon-specific drug delivery system, RSC Adv. 2 (2012) 11095–11103. https://doi.org/10.1039/c2ra20785k.

[12] W.E. Hennink, C.F. van Nostrum, Novel crosslinking methods to design hydrogels, Adv. Drug Deliv. Rev. 64 (2012) 223–236. https://doi.org/10.1016/j.addr.2012.09.009.

[13] Y. Yue, X. Wang, J. Han, L. Yu, J. Chen, Q. Wu, J. Jiang, Effects of nanocellulose on sodium alginate/polyacrylamide hydrogel: Mechanical properties and adsorption-desorption capacities, Carbohydr. Polym. 206 (2019) 289–301. https://doi.org/10.1016/J.CARBPOL.2018.10.105.

[14] Y. Yue, S. Shen, W. Cheng, G. Han, Q. Wu, J. Jiang, Construction of mechanically robust and recyclable photocatalytic hydrogel based on nanocellulose-supported CdS/MoS2/Montmorillonite hybrid for antibiotic degradation, Colloids Surfaces A Physicochem. Eng. Asp. 636 (2022) 128035. https://doi.org/10.1016/J.COLSURFA.2021.128035.

[15] M.R. Guilherme, F.A. Aouada, A.R. Fajardo, A.F. Martins, A.T. Paulino, M.F.T. Davi, A.F. Rubira, E.C. Muniz, Superabsorbent hydrogels based on polysaccharides for application in agriculture as soil conditioner and nutrient carrier: A review, Eur. Polym. J. 72 (2015) 365–385. https://doi.org/10.1016/j.eurpolymj.2015.04.017.

[16] J.M. Rosiak, F. Yoshii, Hydrogels and their medical applications, Nucl. Instruments Methods Phys. Res. Sect. B Beam Interact. with Mater. Atoms. 151 (1999) 56–64. https://doi.org/10.1016/S0168-583X(99)00118-4.

[17] A. Hüttermann, L.J.B. Orikiriza, H. Agaba, Application of Superabsorbent Polymers for Improving the Ecological Chemistry of Degraded or Polluted Lands, CLEAN - Soil, Air, Water. 37 (2009) 517–526. https://doi.org/10.1002/clen.200900048.

[18] N. Peppas, A.H.-B. science, undefined 2020, Hydrogels, Elsevier. (n.d.). https://www.sciencedirect.com/science/article/pii/B9780128161371000143 (accessed April 29, 2022).

[19] F. Ganji, S. Vasheghani-Farahani, E. Vasheghani-Farahani, Theoretical description of hydrogel swelling: a review, Polym. J. 19 (2010) 375–398. https://www.sid.ir/en/Journal/ViewPaper.aspx?ID=171784 (accessed April 29, 2022).

[20] V. Balamuralidhara, … T.P.-A.J.D.D., undefined 2011, pH sensitive drug delivery systems: a review, Researchgate.Net. (n.d.). https://doi.org/10.3923/ajdd.2011.24.48.

[21] Z. Li, J. Guan, Thermosensitive hydrogels for drug delivery, Expert Opin. Drug Deliv. 8 (2011) 991–1007. https://doi.org/10.1517/17425247.2011.581656.

[22] K. Van De Velde, P. Kiekens, Biopolymers: Overview of several properties and consequences on their applications, Polym. Test. 21 (2002) 433–442. https://doi.org/10.1016/S0142-9418(01)00107-6.

[23] S. Nangia, S. Warkar, D. Katyal, A review on environmental applications of chitosan biopolymeric hydrogel based composites, J. Macromol. Sci. Part A. 55 (2018) 747–763. https://doi.org/10.1080/10601325.2018.1526041.

[24] N. Thombare, U. Jha, S. Mishra, M.S.-I. journal of, undefined 2016, Guar gum as a promising starting material for diverse applications: A review, Elsevier. (n.d.). https://www.sciencedirect.com/science/article/pii/S0141813016303099?casa_token=lLSb8BS8ZaUAAAAA:qs8zSqccfEsNGTrlZ6jrnEAQzp19Tt3aGUN48HB_CdF_RMVCqa-NaPcIILTuf1NWt_crGuwRNA (accessed February 7, 2021).

[25] H.A. Abd El-Rehim, Characterization and possible agricultural application of polyacrylamide/sodium alginate crosslinked hydrogels prepared by ionizing radiation, J. Appl. Polym. Sci. 101 (2006) 3572–3580. https://doi.org/10.1002/app.22487.

[26] C. Chang, L.Z.-C. polymers, undefined 2011, Cellulose-based hydrogels: Present status and application prospects, Elsevier. (n.d.). https://www.sciencedirect.com/science/article/pii/S0144861710010003?casa_token=yPKry542trsAAAAA:FhStZG7WL8mBSBIprKROVZ6LuclwcqYn-pQh7Tkn91CFYCveXPpfCe0Q5i9uf1k0on8hzgBVVw (accessed February 7, 2021).

[27] N. Dispat, S. Poompradub, S. Kiatkamjornwong, Synthesis of ZnO/SiO2-modified starch-graft-polyacrylate superabsorbent polymer for agricultural application, Carbohydr. Polym. 249 (2020) 116862. https://doi.org/10.1016/j.carbpol.2020.116862.

[28] Khushbu, S.G. Warkar, A. Kumar, Synthesis and assessment of carboxymethyl tamarind kernel gum based novel superabsorbent hydrogels for agricultural applications, Polymer (Guildf). 182 (2019) 121823. https://doi.org/10.1016/j.polymer.2019.121823.

[29] L.Z. Linan, A.C.M. Cidreira, C.Q. da Rocha, F.F. de Menezes, G.J. d. M. Rocha, A.E.M. Paiva, Utilization of Acai Berry Residual Biomass for Extraction of Lignocellulosic Byproducts, J. Bioresour. Bioprod. 6 (2021) 323–337. https://doi.org/10.1016/J.JOBAB.2021.04.007.

[30] R. Malik, R. Saxena, S.G. Warkar, Biopolymer-Based Biomatrices – Organic Strategies to Combat Micronutrient Deficit for Dynamic Agronomy, ChemistrySelect. 7 (2022) e202200006. https://doi.org/10.1002/SLCT.202200006.

[31] H. Ismail, M. Irani, Z. Ahmad, Starch-Based Hydrogels: Present Status and Applications, Int. J. Polym. Mater. 62 (2013) 411–420. https://doi.org/10.1080/00914037.2012.719141.

[32] B. Song, H. Liang, R. Sun, P. Peng, Y. Jiang, D. She, Hydrogel synthesis based on lignin/sodium alginate and application in agriculture, Int. J. Biol. Macromol. 144 (2020) 219–230. https://doi.org/10.1016/j.ijbiomac.2019.12.082.

[33] C. Demitri, F. Scalera, M. Madaghiele, A. Sannino, A. Maffezzoli, Potential of cellulose-based superabsorbent hydrogels as water reservoir in agriculture, Int. J. Polym. Sci. 2013 (2013). https://doi.org/10.1155/2013/435073.

[34] N. Thombare, S. Mishra, M.Z. Siddiqui, U. Jha, D. Singh, G.R. Mahajan, Design and development of guar gum based novel, superabsorbent and moisture retaining hydrogels for agricultural applications, Carbohydr. Polym. 185 (2018) 169–178. https://doi.org/10.1016/j.carbpol.2018.01.018.

[35] W.B. Wang, A.Q. Wang, Preparation, Swelling and Water-Retention Properties of Crosslinked Superabsorbent Hydrogels Based on Guar Gum, Adv. Mater. Res. 96 (2010)

177–182. https://doi.org/10.4028/www.scientific.net/AMR.96.177.

[36] J. Joseph, … S.K.-… journal of green, undefined 2012, Tamarind seed polysaccharide: a promising natural excipient for pharmaceuticals, Search.Proquest.Com. (n.d.). https://search.proquest.com/openview/9f04a88abe221dd1bd4393707cc6a894/1?pq-origsite=gscholar&cbl=226497&casa_token=CVKN9zJ4_XgAAAAA:OrufZWf1NmRDbUJUFGJlAGBJ7ZnUdMhHgX3Vq0kn6mVnbOjLXCZBn3p6TsdFrRLSgUCUGgA60uMm (accessed April 28, 2022).

[37] A.D. Kulkarni, A.A. Joshi, C.L. Patil, P.D. Amale, H.M. Patel, S.J. Surana, V.S. Belgamwar, K.S. Chaudhari, C. V. Pardeshi, Xyloglucan: A functional biomacromolecule for drug delivery applications, Int. J. Biol. Macromol. 104 (2017) 799–812. https://doi.org/10.1016/j.ijbiomac.2017.06.088.

[38] A. Chilkoti, T. Christensen, J.A. MacKay, Stimulus responsive elastin biopolymers: applications in medicine and biotechnology, Curr. Opin. Chem. Biol. 10 (2006) 652–657. https://doi.org/10.1016/j.cbpa.2006.10.010.

[39] A. Di Martino, M. Sittinger, M. V. Risbud, Chitosan: A versatile biopolymer for orthopaedic tissue-engineering, Biomaterials. 26 (2005) 5983–5990. https://doi.org/10.1016/j.biomaterials.2005.03.016.

[40] D. Gomez-Maldonado, I.B.V. Erramuspe, M.S. Peresin, Natural Polymers as Alternative Adsorbents and Treatment Agents for Water Remediation, BioResources. 14 (2019) 10093–10160. https://ojs.cnr.ncsu.edu/index.php/BioRes/article/view/BioRes_14_4_Review_Gomez_Maldonado_Natural_Polymers_Alternative_Adsorbents (accessed December 9, 2021).

[41] A.P. Gupta, Micronutrient status and fertilizer use scenario in India, in: J. Trace Elem. Med. Biol., Elsevier GmbH, 2005: pp. 325–331. https://doi.org/10.1016/j.jtemb.2005.04.003.

[42] P. Goyal, V. Kumar, P.S.-C. Polymers, undefined 2007, Carboxymethylation of tamarind kernel powder, Elsevier. (n.d.). https://www.sciencedirect.com/science/article/pii/S0144861706004772?casa_token=z7dkRBPebO0AAAAA:XkWEBM_02rDTmy4_qCw-AHhcIYWyvPhqEQNMnN8RHnjN2fBIQlNLWl1FzKVeVv0MhK_cR5NvpCw (accessed April 28, 2022).

[43] R. Malik, R. Saxena, S.G. Warkar, Biopolymer-Based Biomatrices – Organic Strategies to Combat Micronutrient Deficit for Dynamic Agronomy, ChemistrySelect. 7 (2022). https://doi.org/10.1002/SLCT.202200006.

[44] R. Malik, R. Saxena, S.G. Warkar, Organic Hybrid Hydrogels: A Sustenance Technique in Waste-Water Treatment, ChemistrySelect. 8 (2023). https://doi.org/10.1002/SLCT.202203670.

[45] R. Malik, S. Warkar, R.S.-M.T. Communications, undefined 2023, Carboxy-methyl tamarind kernel gum based bio-hydrogel for sustainable agronomy, Elsevier. (n.d.). https://www.sciencedirect.com/science/article/pii/S2352492823001630 (accessed May 29, 2023).

[46] R. Hajiboland, Effect of Micronutrient Deficiencies on Plants Stress Responses, Abiotic Stress Responses Plants. (2012) 283–329. https://doi.org/10.1007/978-1-4614-0634-1_16.

[47] N. Pandey, Role of plant nutrients in plant growth and physiology, in: Plant Nutr. Abiotic Stress Toler., Springer Singapore, 2018: pp. 51–93. https://doi.org/10.1007/978-981-10-9044-8_2.

[48] S. Bhatia, S. Bhatia, Introduction to enzymes and their applications, Introd. to Pharm. Biotechnol. Vol. 2. (2018). https://doi.org/10.1088/978-0-7503-1302-5ch1.

[49] Plant Micronutrients - C P Sharma - Google Books, (n.d.). https://books.google.co.in/books?hl=en&lr=&id=JWO1DwAAQBAJ&oi=fnd&pg=PP1&dq=micronutrients+as+energy+storage+in+plants&ots=JQ-5ngTCvF&sig=bRJxrpwNURu2MXxpu2HLMmRatoY&redir_esc=y#v=onepage&q=micronutrients as energy storage in plants&f=false (accessed February 6, 2021).

[50] I. Yruela, Transition metals in plant photosynthesis, Metallomics. 5 (2013) 1090–1109. https://doi.org/10.1039/c3mt00086a.

[51] K. Mikula, G. Izydorczyk, D. Skrzypczak, M. Mironiuk, K. Moustakas, A. Witek-Krowiak, K. Chojnacka, Controlled release micronutrient fertilizers for precision agriculture – A review, Sci. Total Environ. 712 (2020) 136365. https://doi.org/10.1016/j.scitotenv.2019.136365.

[52] V. Romheld, H. Marschner, Function of Micronutrients in Plants, Micronutr. Agric. (2018) 297–328. https://doi.org/10.2136/SSSABOOKSER4.2ED.C9.

[53] G. Rout, S.S.-R. in A. Science, undefined 2015, Role of iron in plant growth and metabolism, Jstage.Jst.Go.Jp. 3 (2015) 1–24. https://doi.org/10.7831/ras.3.1.

[54] R. Millaleo, M. Reyes-Díaz, … A.I.-J. of soil science, undefined 2010, Manganese as essential and toxic element for plants: transport, accumulation and resistance mechanisms, SciELO Chile. (n.d.). https://www.scielo.cl/scielo.php?pid=S0718-95162010000200008&script=sci_arttext&tlng=pt (accessed May 28, 2023).

[55] N. Pandey, C.S.-I. journal of experimental biology, undefined 1996, Copper effect on photosynthesis and transpiration in safflower., Europepmc.Org. (n.d.). https://europepmc.org/article/med/8979495 (accessed May 28, 2023).

[56] B. Kaiser, K. Gridley, … J.N.B.-A. of, undefined 2005, The role of molybdenum in agricultural plant production, Academic.Oup.Com. (n.d.). https://doi.org/10.1093/aob/mci226.

[57] P.H. Brown, I. Cakmak, Q. Zhang, Form and Function of Zinc Plants, Zinc Soils Plants. (1993) 93–106. https://doi.org/10.1007/978-94-011-0878-2_7.

[58] J.J. Camacho-Cristóbal, C. Cristóbal, J. Jes´, J. Rexach, A. Gonzálezgonz´gonzález-Fontes, Boron in plants: deficiency and toxicity, Wiley Online Libr. 50 (2008) 1247–1255. https://doi.org/10.1111/j.1744-7909.2008.00742.x.

[59] S. Hanstein, H.F.-P. Physiology, undefined 2002, CO2-Triggered Chloride Release from Guard Cells in Intact Fava Bean Leaves. Kinetics of the Onset of Stomatal Closure,

Academic.Oup.Com. (n.d.). https://academic.oup.com/plphys/article-abstract/130/2/940/6102941 (accessed May 28, 2023).

[60] Z. Rengel, Availability of Mn, Zn and Fe in the rhizosphere, J. Soil Sci. Plant Nutr. 15 (2015) 397–409. https://doi.org/10.4067/s0718-95162015005000036.

[61] Khushbu, S.G. Warkar, Potential applications and various aspects of polyfunctional macromolecule- carboxymethyl tamarind kernel gum, Eur. Polym. J. 140 (2020) 110042. https://doi.org/10.1016/j.eurpolymj.2020.110042.

[62] H. Gupta, Role of Nanocomposites in Agriculture, Nano Hybrids Compos. 20 (2018) 81–89. https://doi.org/10.4028/www.scientific.net/nhc.20.81.

[63] D. Feng, B. Bai, H. Wang, Y. Suo, Novel Fabrication of Biodegradable Superabsorbent Microspheres with Diffusion Barrier through Thermo-Chemical Modification and Their Potential Agriculture Applications for Water Holding and Sustained Release of Fertilizer, J. Agric. Food Chem. 65 (2017) 5896–5907. https://doi.org/10.1021/acs.jafc.7b01849.

[64] C. Chen, Z. Gao, X. Qiu, S. Hu, Enhancement of the Controlled-Release Properties of Chitosan Membranes by Crosslinking with Suberoyl Chloride, Molecules. 18 (2013) 7239–7252. https://doi.org/10.3390/molecules18067239.

[65] S. Patel, A.K. Bajpai, J. Bajpai, R.K. Saini, S. Acharya, Facile preparation of iron loaded calcium alginate nanocarriers and study of controlled release of iron, J. Environ. Chem. Eng. 5 (2017) 5337–5346. https://doi.org/10.1016/J.JECE.2017.10.019.

[66] M. Wang, G. Zhang, L. Zhou, D. Wang, N. Zhong, D. Cai, Z. Wu, Fabrication of pH-Controlled-Release Ferrous Foliar Fertilizer with High Adhesion Capacity Based on Nanobiomaterial, ACS Sustain. Chem. Eng. 4 (2016) 6800–6808. https://doi.org/10.1021/acssuschemeng.6b01761.

[67] J. Abedi-Koupai, J. Varshosaz, M. Mesforoosh, A.H. Khoshgoftarmanesh, CONTROLLED RELEASE OF FERTILIZER MICROCAPSULES USING ETHYLENE VINYL ACETATE POLYMER TO ENHANCE MICRONUTRIENT AND WATER USE EFFICIENCY, J. Plant Nutr. 35 (2012) 1130–1138. https://doi.org/10.1080/01904167.2012.676126.

[68] D. Skrzypczak, A. Witek-Krowiak, A. Dawiec-Liśniewska, D. Podstawczyk, K. Mikula, K. Chojnacka, Immobilization of biosorbent in hydrogel as a new environmentally friendly fertilizer for micronutrients delivery, J. Clean. Prod. 241 (2019) 118387. https://doi.org/10.1016/J.JCLEPRO.2019.118387.

[69] T. Xu, C. Ma, Z. Aytac, X. Hu, K.W. Ng, J.C. White, P. Demokritou, Enhancing Agrichemical Delivery and Seedling Development with Biodegradable, Tunable, Biopolymer-Based Nanofiber Seed Coatings, ACS Sustain. Chem. Eng. 8 (2020) 9537–9548. https://doi.org/10.1021/acssuschemeng.0c02696.

[70] M. Ashfaq, N. Verma, S. Khan, Carbon nanofibers as a micronutrient carrier in plants: efficient translocation and controlled release of Cu nanoparticles, Environ. Sci. Nano. 4 (2017) 138–148. https://doi.org/10.1039/c6en00385k.

[71] W. Schmidt, M. Huda, E.E. Codling, M.E. Schmidt, W.F. Schmidt, M.S. Huda, Keratin

Nursery Pots as Potential Medium for Controlled Release of Copper Ions in Root Growth Control in Theobroma cacao L Morphology and Spectral Imaging View project New Plasticizer for Bioplastics View project Keratin Nursery Pots as Potential Medium for Controlled Release of Copper Ions in Root Growth Control in Theobroma cacao L, J Hortic. 6 (2019) 256. https://doi.org/10.4172/2376-0354.1000256.

[72] G. Raju, M.R.H. Mas Haris, A.R. Azura, A.M. Ahmed Mohamed Eid, Chitosan Epoxidized Natural Rubber Biocomposites for Sorption and Biodegradability Studies, ACS Omega. 5 (2020) 28760–28766. https://doi.org/10.1021/acsomega.0c04081.

[73] M. Vinceković, N. Jalšenjak, S. Topolovec-Pintarić, E. Dermić, M. Bujan, S. Jurić, Encapsulation of Biological and Chemical Agents for Plant Nutrition and Protection: Chitosan/Alginate Microcapsules Loaded with Copper Cations and Trichoderma viride, J. Agric. Food Chem. 64 (2016) 8073–8083. https://doi.org/10.1021/acs.jafc.6b02879.

[74] M. PULAT, G.O. AKALİN, Preparation of Sodium Carboxymethly Cellulose Hydrogels for Controlled Release of Copper Micronutrient, Eurasia Proc. Sci. Technol. Eng. Math. 2 (2018) 25–34. https://dergipark.org.tr/en/pub/epstem/454578 (accessed December 9, 2021).

[75] C.V.L. Natarelli, C.M.S. Lopes, J.S.S. Carneiro, L.C.A. Melo, J.E. Oliveira, E.S. Medeiros, Zinc slow-release systems for maize using biodegradable PBAT nanofibers obtained by solution blow spinning, J. Mater. Sci. 56 (2021) 4896–4908. https://doi.org/10.1007/s10853-020-05545-y.

[76] N.C.T. Martins, A. Avellan, S. Rodrigues, D. Salvador, S.M. Rodrigues, T. Trindade, Composites of Biopolymers and ZnO NPs for Controlled Release of Zinc in Agricultural Soils and Timed Delivery for Maize, ACS Appl. Nano Mater. 3 (2020) 2134–2148. https://doi.org/10.1021/acsanm.9b01492.

[77] M. Jiménez-Rosado, V. Pérez-Puyana, F. Cordobés, A. Romero, A. Guerrero, Development of soy protein-based matrices containing zinc as micronutrient for horticulture, Ind. Crops Prod. 121 (2018) 345–351. https://doi.org/10.1016/j.indcrop.2018.05.039.

[78] G.O. Akalin, M. Pulat, Controlled release behavior of zinc-loaded carboxymethyl cellulose and carrageenan hydrogels and their effects on wheatgrass growth, J. Polym. Res. 27 (2019) 1–11. https://doi.org/10.1007/s10965-019-1950-y.

[79] D.J. Sarkar, A. Singh, P. Mandal, A. Kumar, B.S. Parmar, Synthesis and Characterization of Poly (CMC-g-cl-PAam/Zeolite) Superabsorbent Composites for Controlled Delivery of Zinc Micronutrient: Swelling and Release Behavior, Polym. - Plast. Technol. Eng. 54 (2015) 357–367. https://doi.org/10.1080/03602559.2014.958773.

[80] H. Helmiyati, D. Nugraha, Superabsorbent nanocomposite as micronutrient slow-release fertilizer, in: IOP Conf. Ser. Mater. Sci. Eng., Institute of Physics Publishing, 2020: p. 012050. https://doi.org/10.1088/1757-899X/763/1/012050.

[81] A. Bortolin, A.R. Serafim, F.A. Aouada, L.H.C. Mattoso, C. Ribeiro, Macro- and Micronutrient Simultaneous Slow Release from Highly Swellable Nanocomposite Hydrogels, J. Agric. Food Chem. 64 (2016) 3133–3140. https://doi.org/10.1021/acs.jafc.6b00190.

[82] R. Kumar, M. Ashfaq, N. Verma, Synthesis of novel PVA–starch formulation-supported Cu–Zn nanoparticle carrying carbon nanofibers as a nanofertilizer: controlled release of micronutrients, J. Mater. Sci. 53 (2018) 7150–7164. https://doi.org/10.1007/S10853-018-2107-9.

[83] S.L. Wang, A.D. Nguyen, Effects of Zn/B nanofertilizer on biophysical characteristics and growth of coffee seedlings in a greenhouse, Res. Chem. Intermed. 44 (2018) 4889–4901. https://doi.org/10.1007/s11164-018-3342-z.

[84] G.O. Akalin, M. Pulat, Preparation and characterization of κ-carrageenan hydrogel for controlled release of copper and manganese micronutrients, Polym. Bull. 77 (2020) 1359–1375. https://doi.org/10.1007/s00289-019-02800-4.

[85] G.O. Akalin, M. Pulat, Preparation of Sodium Carboxymethly Cellulose Hydrogels for Controlled Release of Copper Micronutrient, Technol. Eng. Math. 2 (2018) 25–34. www.isres.org (accessed February 7, 2021).

[86] D. Skrzypczak, A. Witek-Krowiak, A. Dawiec-Liśniewska, D. Podstawczyk, K. Mikula, K. Chojnacka, Immobilization of biosorbent in hydrogel as a new environmentally friendly fertilizer for micronutrients delivery, J. Clean. Prod. 241 (2019) 118387. https://doi.org/10.1016/j.jclepro.2019.118387.

[87] Immobilization of biosorbent in hydrogel as a new environmentally friendly fertilizer for micronutrients delivery, Elsevier. (n.d.). https://www.sciencedirect.com/science/article/pii/S0959652619332573 (accessed July 20, 2023).

[88] M. Naseer, Y. Zhu, F. Li, Y. Yang, … S.W.-E., undefined 2022, Nano-enabled improvements of growth and colonization rate in wheat inoculated with arbuscular mycorrhizal fungi, Elsevier. (n.d.). https://www.sciencedirect.com/science/article/pii/S026974912102306X (accessed May 31, 2023).

[89] S. Patel, A.K. Bajpai, J. Bajpai, R.K. Saini, S. Acharya, Facile preparation of iron loaded calcium alginate nanocarriers and study of controlled release of iron, J. Environ. Chem. Eng. 5 (2017) 5337–5346. https://doi.org/10.1016/j.jece.2017.10.019.

[90] E.E. Codling, M.E. Schmidt, W.F. Schmidt, M.S. Huda, Keratin Nursery Pots as Potential Medium for Controlled Release of Copper Ions in Root Growth Control in Theobroma cacao L ., (2019) 1–7. https://doi.org/10.4172/2376-0354.1000256.

[91] R. Kumar, M. Ashfaq, N. Verma, Synthesis of novel PVA–starch formulation-supported Cu–Zn nanoparticle carrying carbon nanofibers as a nanofertilizer: controlled release of micronutrients, J. Mater. Sci. 53 (2018) 7150–7164. https://doi.org/10.1007/s10853-018-2107-9.

[92] Handbook of Plant Nutrition - Google Books, (n.d.). https://books.google.co.in/books?hl=en&lr=&id=Ttw_CQAAQBAJ&oi=fnd&pg=PP1&dq=Barker+and+Pilbeam,+2015&ots=VqV0-ttHVO&sig=9YrFa_Ah__Muq_4dyPllDwBZi8E&redir_esc=y#v=onepage&q=Barker and Pilbeam%2C 2015&f=false (accessed February 18, 2021).

[93] T. Eichert, V. Fernández, Uptake and Release of Elements by Leaves and Other Aerial Plant Parts, in: Marschner's Miner. Nutr. High. Plants Third Ed., Elsevier Inc., 2011: pp. 71–84. https://doi.org/10.1016/B978-0-12-384905-2.00004-2.

[94] J.W. Morse, Interactions of trace metals with authigenic sulfide minerals: implications for their bioavailability, Mar. Chem. 46 (1994) 1–6. https://doi.org/10.1016/0304-4203(94)90040-X.

[95] A. Imran, S. López-Rayo, J. Magid, H.C.B. Hansen, Dissolution kinetics of pyroaurite-type layered double hydroxide doped with Zn: Perspectives for pH controlled micronutrient release, Appl. Clay Sci. 123 (2016) 56–63. https://doi.org/10.1016/j.clay.2015.12.016.

[96] T. Clive, Persistent Organic Pollutants: are we... - Google Scholar, (n.d.). https://scholar.google.com/scholar?hl=en&as_sdt=0%2C5&q=+T.+Clive%2C+Persistent+Organic+Pollutants%3A+are+we+close+to+a+solution%3F+Arctic+Resources+Committee%2C+vol.+26%2C+Number+1%2C+Fall%2FWinter+%282000%29&btnG= (accessed May 17, 2022).

[97] O. Güven, M. Şen, E. Karadağ, D.S.-R.P. and Chemistry, undefined 1999, A review on the radiation synthesis of copolymeric hydrogels for adsorption and separation purposes, Elsevier. (n.d.). https://www.sciencedirect.com/science/article/pii/S0969806X99003266 (accessed February 8, 2023).

[98] N. Oladoja, E. Unuabonah, O. Amuda, O. Kolawole, Polysaccharides as a green and sustainable resources for water and wastewater treatment, 2017. https://books.google.com/books?hl=en&lr=&id=7AIkDwAAQBAJ&oi=fnd&pg=PR5&dq=N.+A.+Oladoja,+E.+Unuabonah,+O.+S.,+O.+M.+Kolawole,+Springer,+Polysaccharides+as+a+Green+and+Sustainable+Resources+for+Water+and+Wastewater+Treatment,+2017,+65-90.&ots=4ipdIyPAab&sig=R2nBVTYmB7WWmgzWb4_BD26gT68 (accessed February 8, 2023).

[99] M. Arrascue, H. Garcia, O. Horna, E.G.- Hydrometallurgy, undefined 2003, Gold sorption on chitosan derivatives, Elsevier. (n.d.). https://www.sciencedirect.com/science/article/pii/S0304386X03001567 (accessed February 8, 2023).

[100] A. Paulino, L. Belfiore, L. Kubota, … E.M.-C.E., undefined 2011, Efficiency of hydrogels based on natural polysaccharides in the removal of Cd2+ ions from aqueous solutions, Elsevier. (n.d.). https://www.sciencedirect.com/science/article/pii/S1385894710012714 (accessed February 8, 2023).

[101] M. Khan, I.L.-W. research, undefined 2016, A holistic review of hydrogel applications in the adsorptive removal of aqueous pollutants: recent progress, challenges, and perspectives, Elsevier. (n.d.). https://doi.org/10.1016/j.watres.2016.10.008.

[102] S. Chen, Q. Yue, B. Gao, X.X.-J. of colloid and interface science, undefined 2010, Equilibrium and kinetic adsorption study of the adsorptive removal of Cr (VI) using modified wheat residue, Elsevier. (n.d.). https://www.sciencedirect.com/science/article/pii/S0021979710005849 (accessed February 8, 2023).

[103] M.Z.- Gene, undefined 1996, Heavy metal detoxification in higher plants-a review, Elsevier. 179 (1996) 21–30. https://www.sciencedirect.com/science/article/pii/S0378111996004222 (accessed February 8, 2023).

[104] G. Jing, L. Wang, H. Yu, W. Amer, … L.Z.-S.A.P., undefined 2013, Recent progress on study of hybrid hydrogels for water treatment, Elsevier. (n.d.). https://www.sciencedirect.com/science/article/pii/S0927775712006644 (accessed February 8, 2023).

[105] N. Wahlström, S. Steinhagen, G. Toth, … H.P.-C., undefined 2020, Ulvan dialdehyde-gelatin hydrogels for removal of heavy metals and methylene blue from aqueous solution, Elsevier. (n.d.). https://www.sciencedirect.com/science/article/pii/S0144861720310146 (accessed February 8, 2023).

[106] L. Jasim, A.A.- NeuroQuantology, undefined 2021, Removal of Heavy Metals by Using Chitosan/Poly (Acryl Amide-Acrylic Acid) Hydrogels: Characterization and Kinetic Study., Go.Gale.Com. (n.d.). https://go.gale.com/ps/i.do?id=GALE%7CA676650064&sid=googleScholar&v=2.1&it=r&linkaccess=abs&issn=13035150&p=AONE&sw=w (accessed February 8, 2023).

[107] Q. Meng, B. Peng, C.S.-C. and S.B. Biointerfaces, undefined 2018, Synthesis of F127/PAA hydrogels for removal of heavy metal ions from organic wastewater, Elsevier. (n.d.). https://www.sciencedirect.com/science/article/pii/S0927776518302285 (accessed February 8, 2023).

[108] X. Huang, L. Wang, J. Zhang, X. Du, S. Wu, … H.W.-I.J. of, undefined 2020, A novel ε-polylysine-modified microcrystalline cellulose based antibacterial hydrogel for removal of heavy metal, Elsevier. (n.d.). https://www.sciencedirect.com/science/article/pii/S0141813020343981 (accessed February 8, 2023).

[109] K. Chan, K. Morikawa, N. Shibata, A. Zinchenko, K. Thakur, M.V. Dinu, Adsorptive removal of heavy metal ions, organic dyes, and pharmaceuticals by dna–chitosan hydrogels, Mdpi.Com. (2021). https://doi.org/10.3390/gels7030112.

[110] Z. Zhao, Y. Huang, Y. Wu, S. Li, H. Yin, J.W.-C. and S. A, undefined 2021, α-ketoglutaric acid modified chitosan/polyacrylamide semi-interpenetrating polymer network hydrogel for removal of heavy metal ions, Elsevier. (n.d.). https://www.sciencedirect.com/science/article/pii/S0927775721011316 (accessed February 8, 2023).

[111] W. Zhang, J. Ou, B. Wang, H. Wang, Q. He, J.S.-… of H. Materials, undefined 2021, Efficient heavy metal removal from water by alginate-based porous nanocomposite hydrogels: The enhanced removal mechanism and influencing factor insight, Elsevier. (n.d.). https://www.sciencedirect.com/science/article/pii/S0304389421013224 (accessed February 8, 2023).

[112] G. Jiao, J. Ma, Y. Li, D. Jin, J. Zhou, R.S.-J. of H. Materials, undefined 2022, Removed heavy metal ions from wastewater reuse for chemiluminescence: Successive application of

lignin-based composite hydrogels, Elsevier. (n.d.). https://www.sciencedirect.com/science/article/pii/S0304389421016873 (accessed February 8, 2023).

[113] F.M. Cui, Z.J. Wu, R. Zhao, Q. Chen, Z.Y. Liu, Y. Zhao, H.B. Yan, G.L. Shen, Y. Tu, D.H. Zhou, J. Diwu, J. Hou, L. Hu, G.J. Wang, Development and Characterization of a Novel Hydrogel for the Decontaminating of Radionuclide-Contaminated Skin Wounds, Macromol. Biosci. 21 (2021). https://doi.org/10.1002/MABI.202000399.

[114] T. Vincent, C. Vincent, E.G.- Molecules, undefined 2015, Immobilization of metal hexacyanoferrate ion-exchangers for the synthesis of metal ion sorbents—a mini-review, Mdpi.Com. (2015). https://doi.org/10.3390/molecules201119718.

[115] Y. He, S. Li, X. Li, Y. Yang, A. Tang, … L.D.-C.E., undefined 2018, Graphene (rGO) hydrogel: A promising material for facile removal of uranium from aqueous solution, Elsevier. (n.d.). https://www.sciencedirect.com/science/article/pii/S1385894718300378 (accessed February 8, 2023).

[116] Z. Huang, Z. Li, Q. Wu, L. Zheng, … L.Z.-E., undefined 2018, Simultaneous elimination of cationic uranium (VI) and anionic rhenium (VII) by graphene oxide–poly (ethyleneimine) macrostructures: a batch, XPS, EXAFS, and DFT, Pubs.Rsc.Org. (n.d.). https://pubs.rsc.org/en/content/articlelanding/2018/en/c8en00677f (accessed February 8, 2023).

[117] X. Deng, X. Liu, T. Duan, W. Zhu, … Z.Y.-M.R., undefined 2016, Fabricating a graphene oxide—bayberry tannin sponge for effective radionuclide removal, Iopscience.Iop.Org. (n.d.). https://iopscience.iop.org/article/10.1088/2053-1591/3/5/055002/meta (accessed February 8, 2023).

[118] Y. Liao, M. Wang, D.C.-A.S. Science, undefined 2019, Electrosorption of uranium (VI) by highly porous phosphate-functionalized graphene hydrogel, Elsevier. (n.d.). https://www.sciencedirect.com/science/article/pii/S0169433219310955 (accessed May 24, 2023).

[119] W. Lu, Z. Dai, L. Li, J. Liu, S. Wang, H. Yang, … C.C.-J. of M., undefined 2020, Preparation of composite hydrogel (PCG) and its adsorption performance for uranium (VI), Elsevier. (n.d.). https://www.sciencedirect.com/science/article/pii/S0167732219358490 (accessed May 24, 2023).

[120] P.C. Bandara, J.V.D. Perez, E.T. Nadres, R.G. Nannapaneni, K.J. Krakowiak, D.F. Rodrigues, Graphene Oxide Nanocomposite Hydrogel Beads for Removal of Selenium in Contaminated Water, ACS Appl. Polym. Mater. 1 (2019) 2668–2679. https://doi.org/10.1021/ACSAPM.9B00612.

[121] L. Wang, Y. Zhao, K. Zheng, J. She, S. Deng, N.X.-… S. Science, undefined 2019, Fabrication of large-area ZnO nanowire field emitter arrays by thermal oxidation for high-current application, Elsevier. (n.d.). https://www.sciencedirect.com/science/article/pii/S0169433219311699 (accessed February 8, 2023).

[122] W. Lu, Z. Dai, L. Li, J. Liu, S. Wang, H. Yang, … C.C.-J. of M., undefined 2020,

Preparation of composite hydrogel (PCG) and its adsorption performance for uranium (VI), Elsevier. (n.d.). https://www.sciencedirect.com/science/article/pii/S0167732219358490 (accessed February 8, 2023).

[123] J. Ren, X. Wang, L. Zhao, M. Li, W. Yang, Effective Removal of Dyes from Aqueous Solutions by a Gelatin Hydrogel, J. Polym. Environ. 29 (2021) 3497–3508. https://doi.org/10.1007/S10924-021-02136-Z.

[124] S. Pandey, J. Do, J. Kim, M.K.-J. of B. Macromolecules, undefined 2020, Fast and highly efficient removal of dye from aqueous solution using natural locust bean gum based hydrogels as adsorbent, Elsevier. (n.d.). https://www.sciencedirect.com/science/article/pii/S014181301936386X (accessed February 8, 2023).

[125] N. Sarkar, G. Sahoo, S.S.-J. of M. Liquids, undefined 2020, Graphene quantum dot decorated magnetic graphene oxide filled polyvinyl alcohol hybrid hydrogel for removal of dye pollutants, Elsevier. (n.d.). https://www.sciencedirect.com/science/article/pii/S0167732219350676 (accessed February 8, 2023).

[126] K. Lee, J.H. Kang, H.M. Kim, J. Ahn, H. Lim, J.J. Lee, W.J. Jeon, J.H. Lee, K.B. Kim, Direct electrophoretic microRNA preparation from clinical samples using nanofilter membrane, Nano Converg. 7 (2020). https://doi.org/10.1186/S40580-019-0212-3.

[127] C. Hou, Q. Zhang, Y. Li, H.W.-J. of hazardous materials, undefined 2012, P25–graphene hydrogels: Room-temperature synthesis and application for removal of methylene blue from aqueous solution, Elsevier. (n.d.). https://www.sciencedirect.com/science/article/pii/S0304389412000088 (accessed February 8, 2023).

[128] S. Chatterjee, M. Lee, S.W.- Carbon, undefined 2009, Enhanced mechanical strength of chitosan hydrogel beads by impregnation with carbon nanotubes, Elsevier. (n.d.). https://www.sciencedirect.com/science/article/pii/S0008622309003947 (accessed February 8, 2023).

[129] J. Domínguez-Robles, M. Peresin, … T.T.-I. journal of, undefined 2018, Lignin-based hydrogels with "super-swelling" capacities for dye removal, Elsevier. 115 (2018) 1249–1259. https://doi.org/10.1016/j.ijbiomac.2018.04.044.

[130] H. Gao, Y. Sun, J. Zhou, R. Xu, H. Duan, Mussel-inspired synthesis of polydopamine-functionalized graphene hydrogel as reusable adsorbents for water purification, ACS Appl. Mater. Interfaces. 5 (2013) 425–432. https://doi.org/10.1021/AM302500V.

[131] D. Kumar, P.K. Roy, V. Swami, D. Kumar, C. Rajagopal, Removal of toxic metals using superabsorbent polyelectrolytic hydrogels, Wiley Online Libr. 000 (2011) 0–000. https://doi.org/10.1002/app.34384.

[132] X. Ju, S. Zhang, M. Zhou, R. Xie, … L.Y.-J. of hazardous, undefined 2009, Novel heavy-metal adsorption material: ion-recognition P (NIPAM-co-BCAm) hydrogels for removal of lead (II) ions, Elsevier. (n.d.). https://www.sciencedirect.com/science/article/pii/S0304389408019407 (accessed

February 8, 2023).

[133] Z. Mohammadi, S. Shangbin, … C.B.-C.E., undefined 2017, Chelator-mimetic multi-functionalized hydrogel: Highly efficient and reusable sorbent for Cd, Pb, and As removal from waste water, Elsevier. (n.d.). https://www.sciencedirect.com/science/article/pii/S1385894716312128 (accessed February 8, 2023).

[134] A. Pourjavadi, Z.M. Tehrani, H. Salimi, A. Banazadeh, N. Abedini, Hydrogel nanocomposite based on chitosan-g-acrylic acid and modified nanosilica with high adsorption capacity for heavy metal ion removal, Iran. Polym. J. (English Ed. 24 (2015) 725–734. https://doi.org/10.1007/S13726-015-0360-1.

[135] S.C.N. Tang, D.Y.S. Yan, I.M.C. Lo, Sustainable wastewater treatment using microsized magnetic hydrogel with magnetic separation technology, Ind. Eng. Chem. Res. 53 (2014) 15718–15724. https://doi.org/10.1021/IE502512H.

[136] Z. Gong, G. Zhang, X. Zeng, J. Li, G. Li, W. Huang, R. Sun, C. Wong, High-Strength, Tough, Fatigue Resistant, and Self-Healing Hydrogel Based on Dual Physically Cross-Linked Network, ACS Appl. Mater. Interfaces. 8 (2016) 24030–24037. https://doi.org/10.1021/ACSAMI.6B05627.

[137] S. Kumari, S. Mahapatra, S.D.-C.E. Journal, undefined 2017, Ca-alginate as a support matrix for Pb (II) biosorption with immobilized biofilm associated extracellular polymeric substances of Pseudomonas aeruginosa N6P6, Elsevier. (n.d.). https://www.sciencedirect.com/science/article/pii/S1385894717312512 (accessed May 31, 2023).

[138] J. Guo, Y. Han, Y. Mao, M.W.-C. and S. A, undefined 2017, Influence of alginate fixation on the adsorption capacity of hydroxyapatite nanocrystals to Cu2+ ions, Elsevier. (n.d.). https://www.sciencedirect.com/science/article/pii/S0927775717306374 (accessed May 31, 2023).

[139] P. Kulal, V.B.-I. journal of biological, undefined 2020, Magnetite nanoparticle embedded Pectin-graft-poly (N-hydroxyethylacrylamide) hydrogel: Evaluation as adsorbent for dyes and heavy metal ions from waste water, Elsevier. (n.d.). https://www.sciencedirect.com/science/article/pii/S0141813019365626 (accessed May 31, 2023).

[140] W. Zhang, J. Ou, B. Wang, H. Wang, Q. He, … J.S.-J. of H., undefined 2021, Efficient heavy metal removal from water by alginate-based porous nanocomposite hydrogels: The enhanced removal mechanism and influencing factor insight, Elsevier. (n.d.). https://www.sciencedirect.com/science/article/pii/S0304389421013224 (accessed May 31, 2023).

[141] N. Wahlström, S. Steinhagen, G. Toth, … H.P.-C., undefined 2020, Ulvan dialdehyde-gelatin hydrogels for removal of heavy metals and methylene blue from aqueous solution, Elsevier. (n.d.). https://www.sciencedirect.com/science/article/pii/S0144861720310146 (accessed May 31, 2023).

[142] Q. Meng, B. Peng, C.S.-C. and S.B. Biointerfaces, undefined 2018, Synthesis of F127/PAA

hydrogels for removal of heavy metal ions from organic wastewater, Elsevier. (n.d.). https://www.sciencedirect.com/science/article/pii/S0927776518302285 (accessed May 31, 2023).

[143] Z. Zhao, Y. Huang, Y. Wu, S. Li, H. Yin, J.W.-C. and S. A, undefined 2021, α-ketoglutaric acid modified chitosan/polyacrylamide semi-interpenetrating polymer network hydrogel for removal of heavy metal ions, Elsevier. (n.d.). https://www.sciencedirect.com/science/article/pii/S0927775721011316 (accessed May 31, 2023).

[144] G. Jiao, J. Ma, Y. Li, D. Jin, J. Zhou, R.S.-J. of H. Materials, undefined 2022, Removed heavy metal ions from wastewater reuse for chemiluminescence: Successive application of lignin-based composite hydrogels, Elsevier. (n.d.). https://www.sciencedirect.com/science/article/pii/S0304389421016873 (accessed May 31, 2023).

[145] L. Jasim, A.A.- NeuroQuantology, undefined 2021, Removal of Heavy Metals by Using Chitosan/Poly (Acryl Amide-Acrylic Acid) Hydrogels: Characterization and Kinetic Study., Go.Gale.Com. (n.d.). https://go.gale.com/ps/i.do?id=GALE%7CA676650064&sid=googleScholar&v=2.1&it=r&linkaccess=abs&issn=13035150&p=AONE&sw=w (accessed May 31, 2023).

[146] X. Huang, L. Wang, J. Zhang, X. Du, S. Wu, … H.W.-I.J. of, undefined 2020, A novel ε-polylysine-modified microcrystalline cellulose based antibacterial hydrogel for removal of heavy metal, Elsevier. (n.d.). https://www.sciencedirect.com/science/article/pii/S0141813020343981 (accessed May 31, 2023).

[147] K. Chan, K. Morikawa, N. Shibata, A. Zinchenko, K. Thakur, M.V. Dinu, Adsorptive Removal of Heavy Metal Ions, Organic Dyes, and Pharmaceuticals by DNA-Chitosan Hydrogels, (2021). https://doi.org/10.3390/gels7030112.

[148] G. Sen, S. Pat, Polyacrylamide grafted carboxymethyl tamarind (CMT-g-PAM): Development and application of a novel polymeric flocculant, Macromol. Symp. 277 (2009) 100–111. https://doi.org/10.1002/MASY.200950313.

[149] S. Pal, S. Ghorai, C. Das, S. Samrat, A. Ghosh, A.B. Panda, Carboxymethyl tamarind-g-poly(acrylamide)/silica: A high performance hybrid nanocomposite for adsorption of methylene blue dye, Ind. Eng. Chem. Res. 51 (2012) 15546–15556. https://doi.org/10.1021/IE301134A.

[150] C. Niu, S. Li, F.L.-A.M. Research, undefined 2013, Adsorption of Cu2+ from Aqueous Solution by Crosslinked Carboxymethyl Tamarind, Trans Tech Publ. (n.d.). https://www.scientific.net/AMR.781-784.2100 (accessed August 20, 2022).

[151] M.S. Johnson, C.D. Piper, Cross-linked, water-storing polymers as aids to drought tolerance of tomatoes in growing media, J. Agron. Crop Sci. 178 (1997) 23–27. https://doi.org/10.1111/J.1439-037X.1997.TB00347.X.

[152] F. Wu, Y. Zhang, L. Liu, J. Yao, Synthesis and characterization of a novel cellulose-g-poly(acrylic acid-co-acrylamide) superabsorbent composite based on flax yarn waste,

Carbohydr. Polym. 87 (2012) 2519–2525. https://doi.org/10.1016/j.carbpol.2011.11.028.

[153] D. Feng, B. Bai, C. Ding, H. Wang, Y. Suo, Synthesis and swelling behaviors of yeast-g-poly(acrylic acid) superabsorbent co-polymer, Ind. Eng. Chem. Res. 53 (2014) 12760–12769. https://doi.org/10.1021/IE502248N.

[154] Y. Seki, A. Torgürsül, K. Yurdakoc, Preparation and characterization of poly(acrylic acid)-iron rich smectite superabsorbent composites, Polym. Adv. Technol. 18 (2007) 477–482. https://doi.org/10.1002/PAT.912.

[155] T. Wan, X. Wang, Y. Yuan, W. He, Preparation of a kaolinite-poly(acrylic acid acrylamide) water superabsorbent by photopolymerization, J. Appl. Polym. Sci. 102 (2006) 2875–2881. https://doi.org/10.1002/APP.24729.

[156] D. Gao, R.B. Heimann, J. Lerchner, J. Seidel, G. Wolf, Development of a novel moisture sensor based on superabsorbent poly(acrylamide)-montmorillonite composite hydrogels, J. Mater. Sci. 36 (2001) 4567–4571. https://doi.org/10.1023/A:1017971811942.

[157] A. Li, A. Wang, J. Chen, Studies on poly(acrylic acid)/attapulgite superabsorbent composite. I. Synthesis and characterization, J. Appl. Polym. Sci. 92 (2004) 1596–1603. https://doi.org/10.1002/APP.20104.

[158] H. Ye, J.Q. Zhao, Y.H. Zhang, Novel Degradable Superabsorbent Materials of Silicate/Acrylic-Based Polymer Hybrids, J. Appl. Polym. Sci. 91 (2004) 936–940. https://doi.org/10.1002/APP.13274.

[159] L. Wu, M.L.-C. polymers, undefined 2008, Preparation and properties of chitosan-coated NPK compound fertilizer with controlled-release and water-retention, Elsevier. (n.d.). https://www.sciencedirect.com/science/article/pii/S0144861707004110 (accessed March 18, 2023).

[160] S. Noppakundilograt, N. Pheatcharat, S. Kiatkamjornwong, Multilayer-coated NPK compound fertilizer hydrogel with controlled nutrient release and water absorbency, J. Appl. Polym. Sci. 132 (2015). https://doi.org/10.1002/APP.41249.

[161] M. Said, Y. Atassi, M. Tally, H. Khatib, Environmentally Friendly Chitosan-g-poly(acrylic acid-co-acrylamide)/Ground Basalt Superabsorbent Composite for Agricultural Applications, J. Polym. Environ. 26 (2018) 3937–3948. https://doi.org/10.1007/S10924-018-1269-5.

[162] Y. Guo, R. Guo, X. Shi, S. Lian, Q. Zhou, … Y.C.-I.J. of, undefined 2022, Synthesis of cellulose-based superabsorbent hydrogel with high salt tolerance for soil conditioning, Elsevier. (n.d.). https://www.sciencedirect.com/science/article/pii/S0141813022007371 (accessed March 18, 2023).

[163] S. Warkar, A.K.- Polymer, undefined 2019, Synthesis and assessment of carboxymethyl tamarind kernel gum based novel superabsorbent hydrogels for agricultural applications, Elsevier. (n.d.). https://www.sciencedirect.com/science/article/pii/S0032386119308298 (accessed March 18, 2023).

[164] R. Malik, S. Warkar, R.S.-M.T. Communications, undefined 2023, Carboxy-methyl tamarind kernel gum based bio-hydrogel for sustainable agronomy, Elsevier. (n.d.).

https://www.sciencedirect.com/science/article/pii/S2352492823001630 (accessed March 18, 2023).

[165] H. Agaba, L. Orikiriza, J. Obua, … J.K.-A., undefined 2011, Hydrogel amendment to sandy soil reduces irrigation frequency and improves the biomass of Agrostis stolonifera, Scirp.Org. (n.d.). https://www.scirp.org/html/8549.html (accessed April 29, 2022).

[166] C. Demitri, F. Scalera, … M.M.-I.J. of, undefined 2013, Potential of cellulose-based superabsorbent hydrogels as water reservoir in agriculture, Hindawi.Com. (n.d.). https://www.hindawi.com/journals/IJPS/2013/435073/ (accessed April 29, 2022).

[167] P. Parvathy, A.J.-J. of A.P. Science, undefined 2014, Rheological and thermal properties of saponified cassava starch-g-poly(acrylamide) superabsorbent polymers varying in grafting parameters and absorbency, Wiley Online Libr. 131 (2014) 40368. https://doi.org/10.1002/app.40368.

[168] S. Warkar, A.K.- Polymer, undefined 2019, Synthesis and assessment of carboxymethyl tamarind kernel gum based novel superabsorbent hydrogels for agricultural applications, Elsevier. (n.d.). https://www.sciencedirect.com/science/article/pii/S0032386119308298?casa_token=wGPxbqbp5j4AAAAA:ILFIjao-Sp7x0wEwxRPneIpWeCt2a7x_RAN20C3-AnjAW04wUWQIwtntF5zhKUJTTVl3YDxWK-k (accessed April 28, 2022).

[169] S. Sanyasi, A. Kumar, … C.G.-C., undefined 2014, A carboxy methyl tamarind polysaccharide matrix for adhesion and growth of osteoclast-precursor cells, Elsevier. (n.d.). https://www.sciencedirect.com/science/article/pii/S0144861713010680?casa_token=CZJjbwjF5NcAAAAA:O81AX8oz4QlYWelqMdkLo6Qrg4caVFyMJKXa21X2M-zLzCF0R3wYm5P-FkRsHqLQaZMt6CbSxbE (accessed April 28, 2022).

[170] P. Choudhury, S. Kumar, A. Singh, A. Kumar, … N.K.-C., undefined 2018, Hydroxyethyl methacrylate grafted carboxy methyl tamarind (CMT-g-HEMA) polysaccharide based matrix as a suitable scaffold for skin tissue engineering, Elsevier. (n.d.). https://www.sciencedirect.com/science/article/pii/S0144861718300973?casa_token=Cjyix2ulTG0AAAAA:T3626aroKgL6L25B9yIHwJDCs-_aH1tVTEBb-8XDWhca9HIdmCLU98Nrrv6VS9NrnmCdhYP7u-A (accessed April 28, 2022).

[171] G. Shankar Shaw, D. Biswal, I. Banerjee, K. Pramanik, A. Anis, K. Pal, Preparation, characterization and assessment of the novel gelatin–tamarind gum/carboxymethyl tamarind gum-based phase-separated films for skin tissue, Taylor Fr. 56 (2017) 141–152. https://doi.org/10.1080/03602559.2016.1185621.

[172] G. Sen, S.P.-M. symposia, undefined 2009, Polyacrylamide grafted carboxymethyl tamarind (CMT-g-PAM): development and application of a novel polymeric flocculant, Wiley Online Libr. 277 (2009) 100–111. https://doi.org/10.1002/masy.200950313.

[173] C. Niu, S. Li, F.L.-A.M. Research, undefined 2013, Adsorption of Cu2+ from Aqueous Solution by Crosslinked Carboxymethyl Tamarind, Trans Tech Publ. (n.d.). https://www.scientific.net/AMR.781-784.2100 (accessed April 28, 2022).

[174] M.G.-F. hydrocolloids, undefined 1986, Tamarind seed gum, Books.Google.Com. (n.d.).

https://books.google.com/books?hl=en&lr=&id=eV74DwAAQBAJ&oi=fnd&pg=PA223-IA10&dq=Tamarind+kernel+gum+as+a+thickener&ots=R3ZLkePYad&sig=JxgjzCTMAGsfYRRJv32pvFwObAg (accessed April 29, 2022).

[175] N.R. Gupta, A. Torris A. T, P.P. Wadgaonkar, P.R.... - Google Scholar, (n.d.). https://scholar.google.com/scholar?hl=en&as_sdt=0%2C5&q=N.R.+Gupta%2C+A.+Torris+A.+T%2C+P.P.+Wadgaonkar%2C+P.R.+Rajamohanan%2C+G.+Ducouret%2C+D.+Hourdet%2C+C.+Creton%2C+M.+V+Badiger%2C+Synthesis+and+characterization+of+PEPO+grafted+carboxymethyl+guar+and+carboxymethyl+tamarind+as+new+thermo-associating+polymers%2C+Carbohydr.+Polym.+1&btnG= (accessed April 28, 2022).

[176] L. Wang, Y. Jia, R. Nie, Y. Zhang, F. Chen, Z. Zhu, J.W.-J. of catalysis, undefined 2017, Ni-foam-supported and amine-functionalized TiO2 photocathode improved photoelectrocatalytic reduction of CO2 to methanol, Elsevier. (n.d.). https://www.sciencedirect.com/science/article/pii/S0021951717300258 (accessed May 29, 2023).

[177] K. Kailas, S. Dhawale, J.R.-M. Pharmaceutical, undefined 2017, Microemulsion based bioadhesive gel of itraconazole using tamarind gum: in-vitro and ex-vivo evaluation, Dergipark.Org.Tr. (n.d.). https://doi.org/10.12991/marupj.323593.

Chapter 2

SYNTHESIS, OPTIMIZATION, SWELLING STUDIES, AND CHARACTERIZATION OF CARBOXY METHYL TAMARIND KERNEL GUM-POLY SODIUM METHACRYLATE (CMTKG-PSMA) HYDROGEL

2.1. Introduction

Designing the synthesis of Hydrogel, a low molecular weight crosslinking agent in trace amounts is incorporated into the reaction mixture, coupled with the addition of biopolymer carboxymethyl tamarind kernel gum and sodium methacrylate. Owing to water thermodynamic compatibility, the linear polymer chains solubilize in water in the absence of crosslinking points. But, in their presence, a swelling force is generated due to the intake of water by the hydrogel, and at the same time, an elastic retractive force also originates due to the uncoiling and relaxation of the polymer. When these two opposing forces i.e., swelling force and elastic retractive force; become equal in magnitude, swelling reaches a steady state in equilibrium, that can be paralleled to the maximum swelling for that matrix [1,2]. When a hydrogel is subjected to some stimulus such as water stress/excess condition or changes in temperature and pH, the swelling degree changes resulting in swelling or shrinking of the hydrogel.

CMTKG is classified as a natural biopolymer that is non-toxic, naturally abundant, economical, bio-degradable, and easily chemically derived from Tamarind Kernel gum (TKG). Its anionic sodium salt was applied for the synthesis of “Carboxy tamarind kernel gum - poly sodium methacrylate” (CMTKG-PSMA) hydrogel. CMTKG resists biodegradation, has a high life span,

more swelling power, and high solubility in cold water, and is stable in most solvents as compared to TKG [3]. CMTKG constitutes a linear β-(1,4)-D glucose backbone with partial α-D-xylo-pyranose (C-1) substitution at the O glucopyranosyl (C-6) residues, which are further substituted at C-2 by β-D galactopyranosyl units (C-1) **(Figure. 2.1.)**.

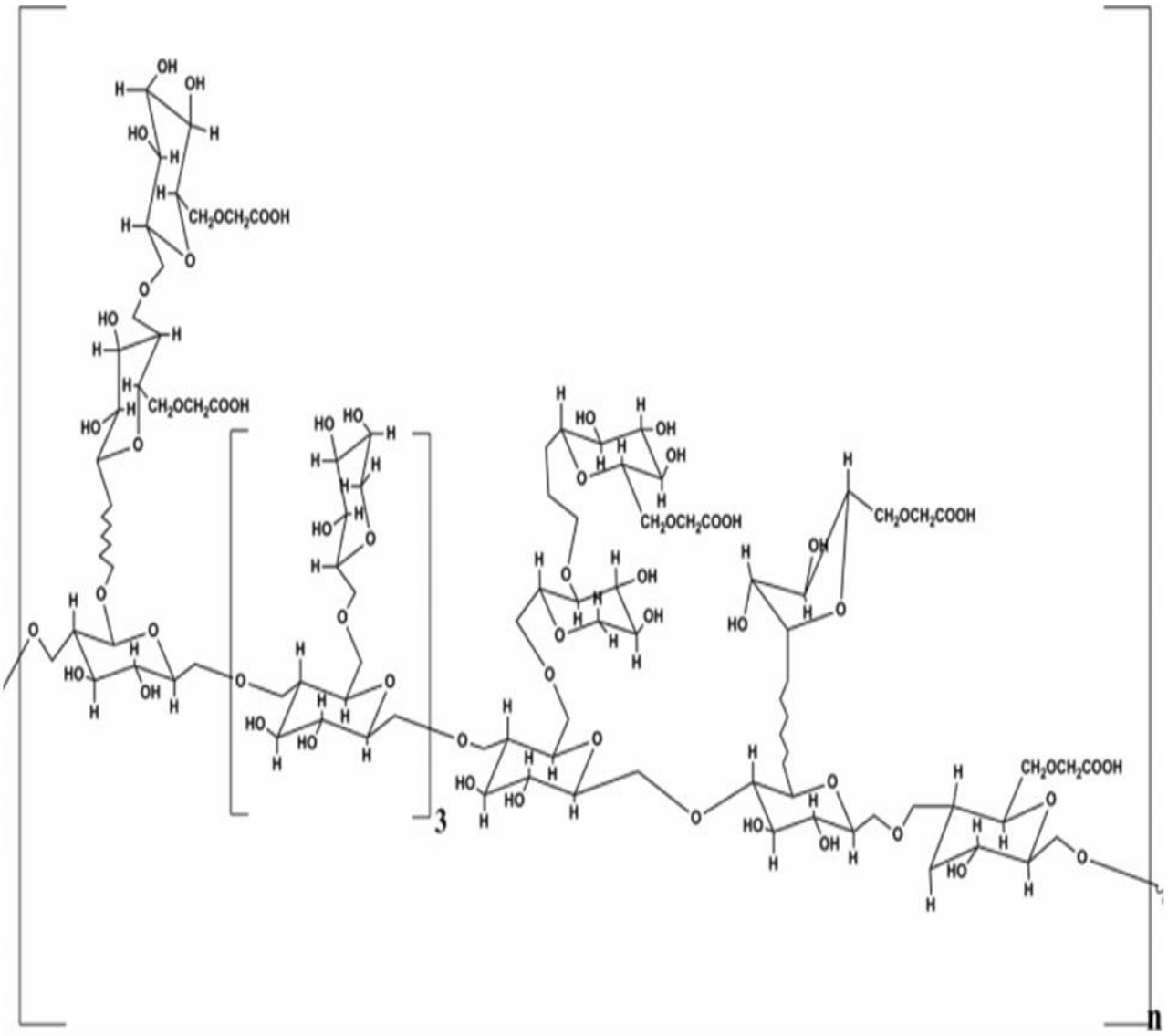

Figure. 2.1 Structure of CMTKG

2.2. Experimental Procedure

2.2.1. Materials

CMTKG possessing 0.20° of carboxymethyl substitution was amply aided by Hindustan Gum and Chemicals Limited. Haryana. Methacrylic acid, Potassium persulfate (KPS), and Sodium hydroxide (NaOH) used were of analytical reagent (AR) grade. N, N'-methylenebis(acrylamide) (MBA), was obtained from Merck, Germany. All the experimental solutions were made using distilled water and the different pH of the solutions was maintained using HCl and NaOH.

2.2.2. Synthesis of Organic CMTKG-PSMA hydrogel

The innovative organic superabsorbent hydrogel (SAH) was synthesized (Fig.1), using biopolymer CMTKG and sodium methacrylate as precursors. MBA was functional as a cross-linking agent and KPS as an initiator. A homogenous mixture of CMTKG, Sodium methacrylate, MBA, and KPS was prepared using a magnetic stirrer. CMTKG was dissolved in 10 ml of distilled water followed by the addition of sodium methacrylate, prepared by adding 8 ml of methacrylic acid to the NaOH solution. After stirring magnetically for half an hour, MBA and KPS were added. Stirring was continued for a further half an hour. Once the homogenous solution was prepared, it was allowed to stand undisturbed for 10-15 mins and then poured into test tubes, to be kept in a water bath, maintained at 65℃, for two and half hours, when the cross-linking initiated and was completed through free radical copolymerization leading to the formation of SAH. The test tubes were broken to get cylindrical-shaped hydrogel, which was cut into slices of approximately equal dimensions and immersed in distilled water for twelve hours to do away with the impurities such as unreacted monomers, initiator, or crosslinker, any acidic or basic impurity, and any side-

products owing to side-reactions. The swollen hydrogels were dried at room temperature (20℃) for few days followed by oven dehydration at a temperature of about 45℃, till weight constancy.

2.2.3. Swelling Assessment of CMTKG-PSMA hydrogel

About twenty-one Hydrogel formulations were synthesized by varying the biopolymer-CMTKG, cross-linker-MBA, and initiator-KPS, for optimization. These formulations are enlisted in Table-2.1. Based on the swelling studies at room temperature, the hydrogel with the maximum swelling ratio was selected to be applied in the research.

An experimental outline of gravimetric measurement by the continuous method was processed to study the swelling behaviours of the synthesized hydrogels.

Table 2.1. Various formulations for the synthesis of CMTKG-PSMA hydrogel with their Swelling ratios.

Hydrogel	Weight of CMTKG (g/10ml distilled water)	Volume of Methacrylic Acid (ml)	Weight of NaOH (g/ 15ml)	KPS (g)	MBA (g)	Swelling Ratio in Distilled Water [II]
HG-1	0.4	8.00	4.5	0.1	0.15	54.94
HG-2	0.4	8.00	4.5	0.1	0.1	84.05
HG-3	0.4	8.00	4.5	0.1	0.05	181.31
HG-4	0.1	8.00	4.5	0.1	0.15	66.25
HG-5	0.2	8.00	4.5	0.1	0.1	117.67
HG-6	0.3	8.00	4.5	0.1	0.05	248.88
HG-7	0.1	8.00	4.5	0.2	0.1	86.57

HG-8	0.2	8.00	4.5	0.2	0.1	87.21
HG-9	0.3	8.00	4.5	0.2	0.1	154.99
HG-10	0.1	8.00	4.5	0.05	0.1	104.09
HG-11	0.2	8.00	4.5	0.05	0.1	123.16
HG-12	0.3	8.00	4.5	0.05	0.1	117.84
HG-13	0.1	8.00	4.5	0.3	0.1	103.54
HG-14	0.2	8.00	4.5	0.3	0.1	107.04
HG-15	0.3	8.00	4.5	0.3	0.1	153.87
HG-16	0.1	8.00	4.5	0.1	0.1	100.11
HG-17	0.1	8.00	4.5	0.1	0.05	228.99
HG-18	0.2	8.00	4.5	0.1	0.15	72.14
HG-19	0.2	8.00	4.5	0.1	0.05	240.24
HG-20	0.3	8.00	4.5	0.1	0.15	89.04
HG-21	0.3	8.00	4.5	0.1	0.1	134.84

The parched dehydrated slice of hydrogel were weighed precisely and immersed in distilled water at different temperatures viz. 28℃, 38℃, 48℃, and 58℃, in various pH solutions of 2.5, 4.2, 6.35, 9, 12, and saline solutions of 0.9 % NaCl solution, 0.9% $MgCl_2$ solution and 0.9 % $AlCl_3$ solution. After a defined timeframe, the samples were taken out from the solutions, freed of excess surface water using filter paper, and weighed again. The weighing was repeated till a little decrease is observed in weight. The Equilibrium Swelling Ratio for each sample was computed using the formula **(Eq.2.1)** specified below [4]:

Equilibrium Swelling Ratio (ESR) = $\frac{(W_E - W_D)}{W_D}$ **Eq (2.1)**

Where, ESR = Equilibrium Swelling Ratio

W_E = Weight of the Hydrogel at equilibrium swelling

W_D = Weight of the dehydrated Hydrogel

The technique was repeated thrice with reproducible results.

2.2.4. Characterization of CMTKG-PSMA hydrogel

2.2.4.1. Fourier Transform Infrared (FTIR) Spectroscopy

The FTIR spectroscopic characterization technique was performed using a PerkinElmer FTIR Spectrophotometer (Model: Spectrum RX-1) in the range of 400-4000cm^{-1}.

2.2.4.2. Thermal Gravimetric Analysis (TGA)

Thermo-gravimetric analysis (TGA) was effectuated employing a Perkin Elmer TGA, having nitrogen (N_2) atmosphere and temperature ranging from 25℃ to 900℃ with 10℃ /min of uniform heating rate.

2.2.4.3. Scanning Electron Microscopy (SEM)

SEM analysis was recorded to obtain the surface morphology of the fabricated CMTKG-PSMA hydrogel using Scanning Electron Microscope (SEM) (JEOL, Japan Mode; JSM-6610LV).

2.2.5. Diffusion Studies of CMTKG-PSMA hydrogel

The rate of migration of water into the hydrogel was noted at different intervals of time for the first 15 hours and the results were applied to the Korsmeyer-Peppas diffusion equation **(Eq.2.2)** [5] to know the type of diffusion associated with the optimized hydrogel.

$$\mathbf{F = \frac{Mt}{M\infty} = kt^n} \qquad \textbf{Eq (2.2)}$$

Where, F: Type of diffusion involved; Mt: amount of water diffused in time t, and M∞ is the total amount of water diffused at equilibrium; k is the kinetic constant and n is the diffusional exponent that is dependent on the geometry of the matrix and on the physical mechanism of release.

2.3. Results and Discussions

2.3.1. Mechanism of the synthesis of CMTKG-PSMA hydrogel

The CMTKG-PSMA hydrogel was successfully synthesized using KPS as initiator and MBA as a crosslinker, via free radical polymerization of the sodium salt of methacrylic acid and CMTKG in the water bath at about 60℃ for about two hours. The monomer was incorporated into the biopolymer to enhance the hydrophilicity of the fabricated polymer network. The redox initiator KPS undergoes decomposition to persulphate radical, which abstracts hydrogen from the -OH group of the biopolymer-CMTKG and from the unsaturated double bond of SMA, to generate active radical sites leading to polymerization. MBA is a bifunctional crosslinking agent, it crosslinked biopolymer CMTKG and PSMA to form a hydrogel framework. The proposed mechanism is depicted in **Figure. 2.2**. As already discussed in Table-2.1, 21 formulations with varied concentrations of biopolymer CMTKG, initiator, and crosslinker were prepared and

researched to obtain the best hydrogel to function as a soil conditioner in agronomy. The complete procedure layout of the Synthesis of Bio-Hydrogel is depicted in the **Figure. 2.3.**

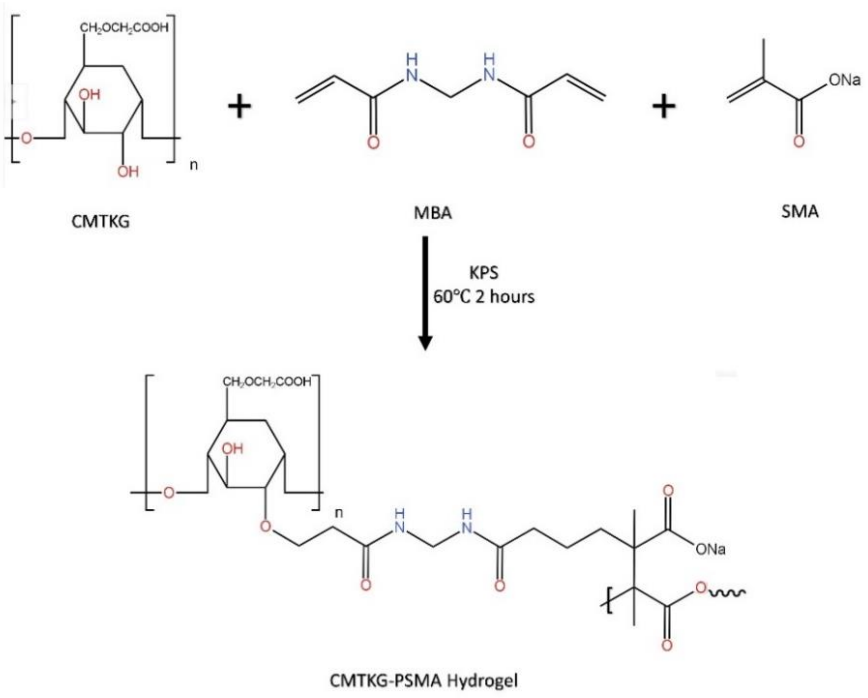

Figure. 2.2 Mechanism of synthesis of CMTKG-PSMA hydrogel

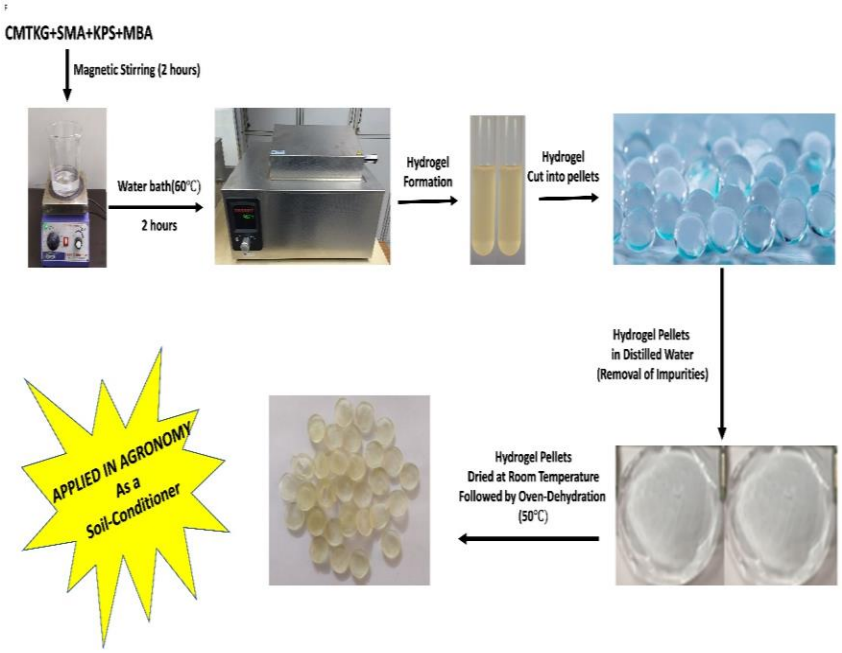

Figure. 2.3 Lay-out of Synthesis of CMTKG-PSMA Hydrogel

2.3.2. Effect of Biopolymer

The water absorption was assessed in the different formulations of hydrogels by altering the concentration of biopolymer-CMTKG and maintaining the constancy in the concentration of initiator and concentration of crosslinker. As the concentration of biopolymer is increased, the swelling ratio increases to a particular critical value followed by a further decrease as depicted in **Figure. 2.4**. The initial increase was observed as we increased the concentration of CMTKG from 0.1 to 0.3 g/10 ml of water, attributed to the increase in the number of hydrophilic groups and enhanced repulsion between them due to like charges, which create spaces allowing the water molecules to be absorbed. Further, if the concentration of CMTKG is increased to 0.4g/10 ml of distilled water, a downfall in the swelling ratio is observed [6]. This is ascribed to an increase in viscosity leading to lesser contact and non-uniform mixing of reactants, resulting in non-formation

of the desired hydrogel. Further, an attempt to prepare hydrogel with a CMTKG concentration of 0.5g/ml of distilled water was unsuccessful due to the build-up of high viscosity.

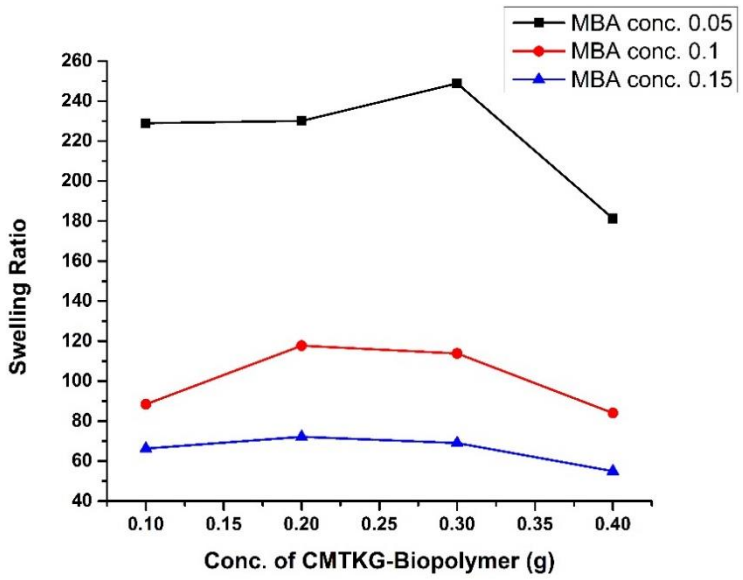

Figure.2.4. Effect of Biopolymer on Swelling

2.3.3. Effect of Cross-linking Agent

Cross-linking density is the major determinant factor for the observed swelling ratios of CMTKG-PSMA hydrogels following Flory's - Rehner theory [7, 8], as can be inferred from **Figure. 2.5.** Higher hydrodynamic 3-dimensional free volume exists at lower values of cross-linking densities as the network is loose-fitting, leading to more retention of water molecules and higher swelling. Keeping other reaction parameters constant, as the concentration of cross-linker-MBA was increased from 0.05g to 0.15g, the swelling ratios showed a substantial decrease as anticipated due to a rise in cross-linking density. The hydrogel formulation with 0.04g MBA was also tried, but only a jelly-like mass was formed, revealing that a critical lower concentration of 0.05g crosslinker is required for the successful fabrication of hydrogel to entrap water molecules.

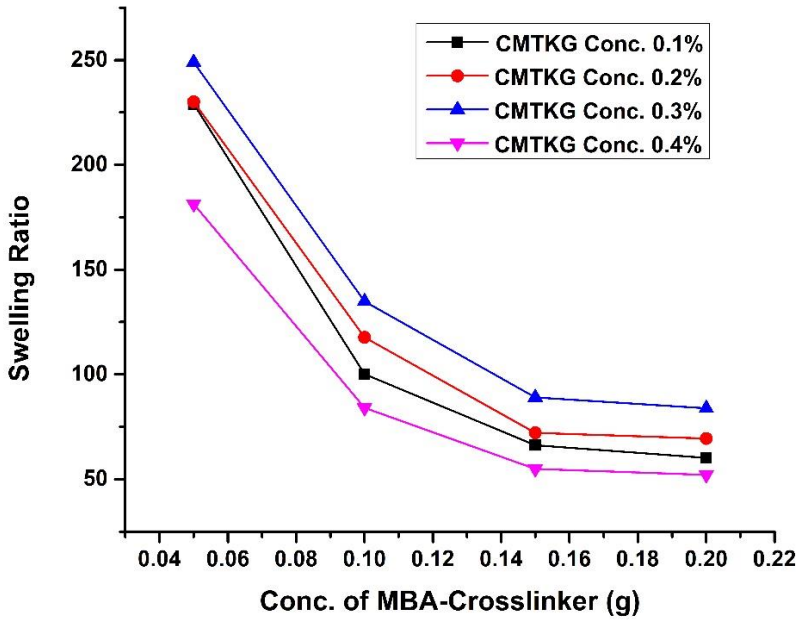

Figure. 2.5. Effect of Cross-linker on Swelling

2.3.4. Effect of Initiator

It was observed that when the concentration of initiator - potassium persulfate (KPS), was increased from 0.05g to 0.3g, maintaining the constancy of other reaction constraints, the swelling ratios revealed a linear increase [9] as inferred from **Figure. 2.6**. The highest swelling ratio (153.87) was observed for hydrogel with an initiator concentration of 0.2 g. But, with a subsequent increase in the concentration of the initiator, the swelling ratio decreases. The probable reason is that as the concentration of free radicals increases, the probability of a reaction between the free

radicals increases i.e., they act as scavengers and inhibit the formation of free radicals to initiate the reaction [10].

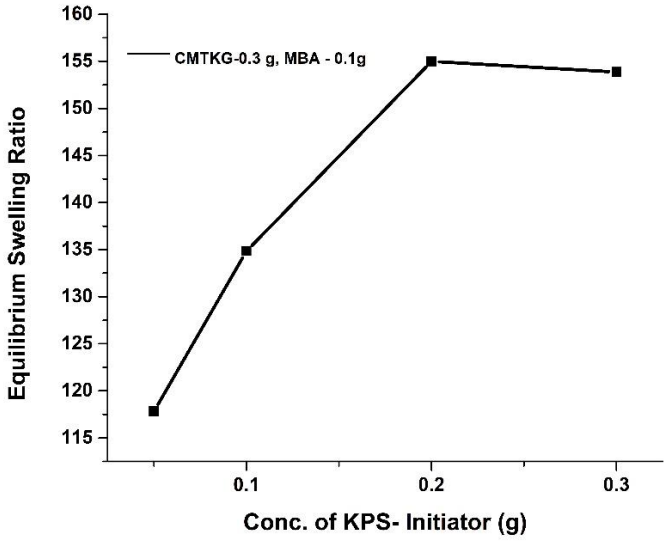

Figure. 2.6. Effect of KPS-Initiator on Swelling

2.3.5. Characterization

2.3.5.1. FTIR Spectroscopy

In the FTIR of CMTKG as shown in **Figure. 2.8**, broadband is observed at 3296 cm^{-1} due to the -OH stretch [11], which in the CMTKG-PSMA hydrogel **Figure. 2.7**, shifts to a lower frequency at 3272 cm^{-1} and is broadened due to intense hydrogen bonding. The further, symmetric, and asymmetric stretch of -COO moiety in CMTKG is observed at 1403 cm^{-1} and 1598 $cm^{-1,}$ and in CMTKG-PSMA, at 1389 cm^{-1} and 1531 cm^{-1} (**Table. 2.2).**

The intense peak at 1531 cm^{-1} in CMTKG-PSMA, can be linked to -C=O asymmetric stretching frequency, which is usually observed at 1558cm^{-1} in sodium methacrylate, verifying the decrease

in conjugation and hence, polymerization [12]. Further, the intensity of CH_2 wagging observed in sodium methacrylate at 890 cm^{-1} is less intensified and observed at 840 cm^{-1}, which is characteristic of the vinylidene group **(Table. 2.3).**

In the FTIR spectra of MBA **Figure. 2.9**, the intense peaks at 664 cm^{-1} and 1304 cm^{-1} are attributed to the O=C-N and C-N stretch. But, in CMTKG-PSMA, these peaks shift to 764 cm^{-1} and 1338 cm^{-1} respectively, confirming the loss of conjugation due to cross-linking. Further, the peak observed at 1626 cm^{-1} due to C=C stretch, is also less intensified and observed at 1656 cm^{-1}, revealing the cross-linking. The peaks at 1205 cm^{-1} and 517 cm^{-1} are characteristic of the CMTKG skeleton. N-H bending is observed at 1200 cm^{-1} **(Table. 2.3).**

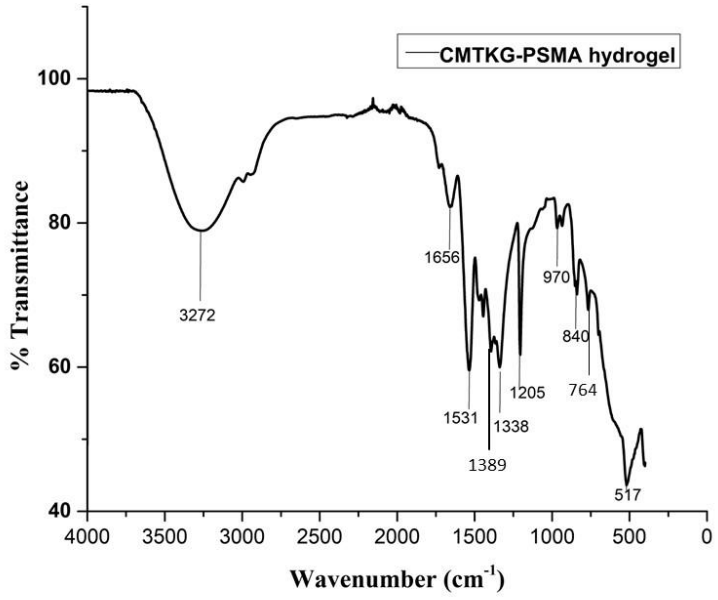

Figure. 2.7 FTIR Spectra of CMTKG-PSMA Hydrogel

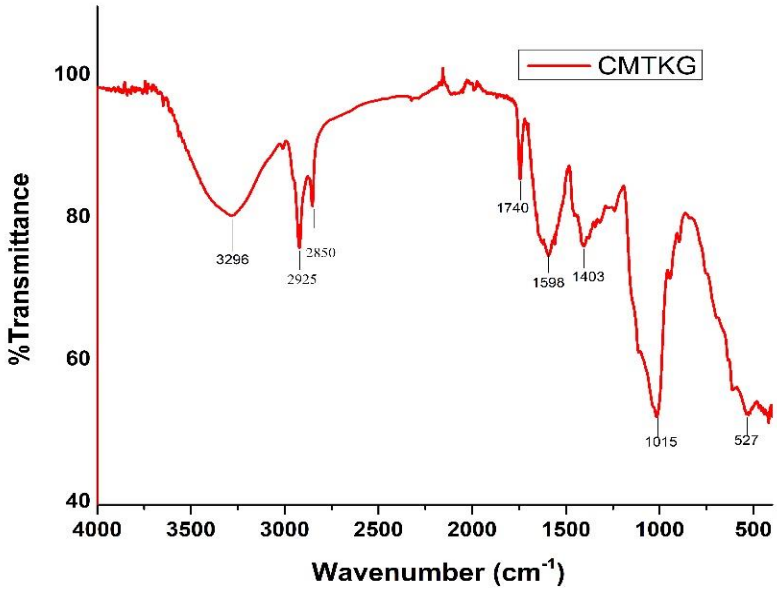

Figure. 2.8. FTIR Spectra of CMTKG

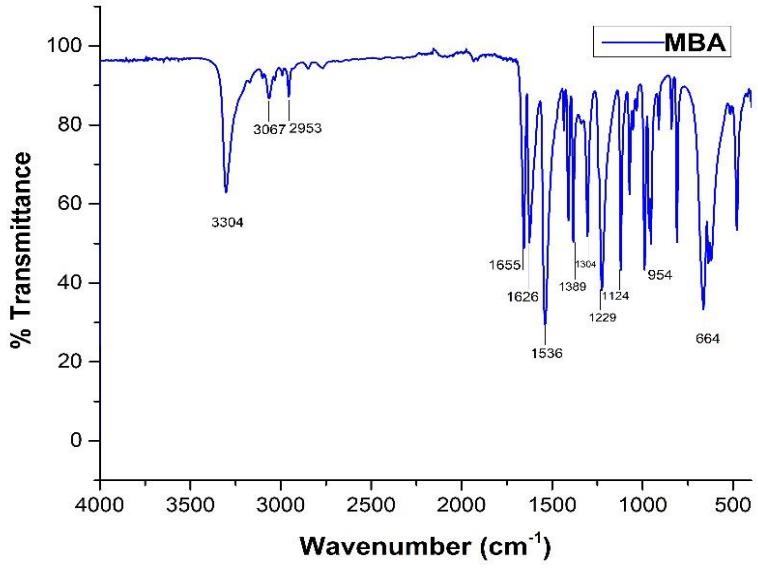

Figure. 2.9. FTIR Spectra of N, N-Methylene Bisacrylamide (MBA)

Table. 2.2. FTIR Spectra of CMTKG-PSMA Hydrogel & CMTKG

STRETCH	CMTKG-PSMA Hydrogel	CMTKG
-OH	3272 cm^{-1} Broadened	3296 cm^{-1}
>C=O	1389 cm^{-1}, 1531 cm^{-1}	1403 cm^{-1}, 1598 cm^{-1}

Table. 2.3. FTIR Spectra of CMTKG-PSMA Hydrogel & Sodium Methacrylate

STRETCH	CMTKG-PSMA Hydrogel	Sodium Methacrylate
>C=O	1531 cm^{-1} (Lower due to decreased conjugation because of polymerization)	1598 cm^{-1}
$>CH_2$ wagging (characteristic of vinylidene group)	840 cm^{-1} Less intensity	890 cm^{-1},

Table. 2.4. FTIR Spectra of CMTKG-PSMA Hydrogel & MBA

STRETCH	CMTKG-PSMA Hydrogel	MBA
O=C-N & C-N	764 cm^{-1} 1338 cm^{-1} Broadened	664 cm^{-1}, 1304 cm^{-1}
>C=O<	1656 cm^{-1}	1655 cm-1
>C=C<	_____	1626 cm^{-1}

2.3.5.2. Thermal Gravimetric Analysis (TGA)

The probable thermal stability of the CMTKG-PSMA hydrogel is supposed to be more as compared to the CMTKG and the same can be verified by the thermograms as shown in **Figure. 2.10** and **Figure.2.11.** In both thermograms, three distinct zones of weight loss are revealed. The weight loss in the first stage may be attributed to the removal of moisture; in the second stage, due to degradation of the polymeric backbone viz. degradation of -COOH and -OH moieties; and in the third stage, degradation of the remains [12].

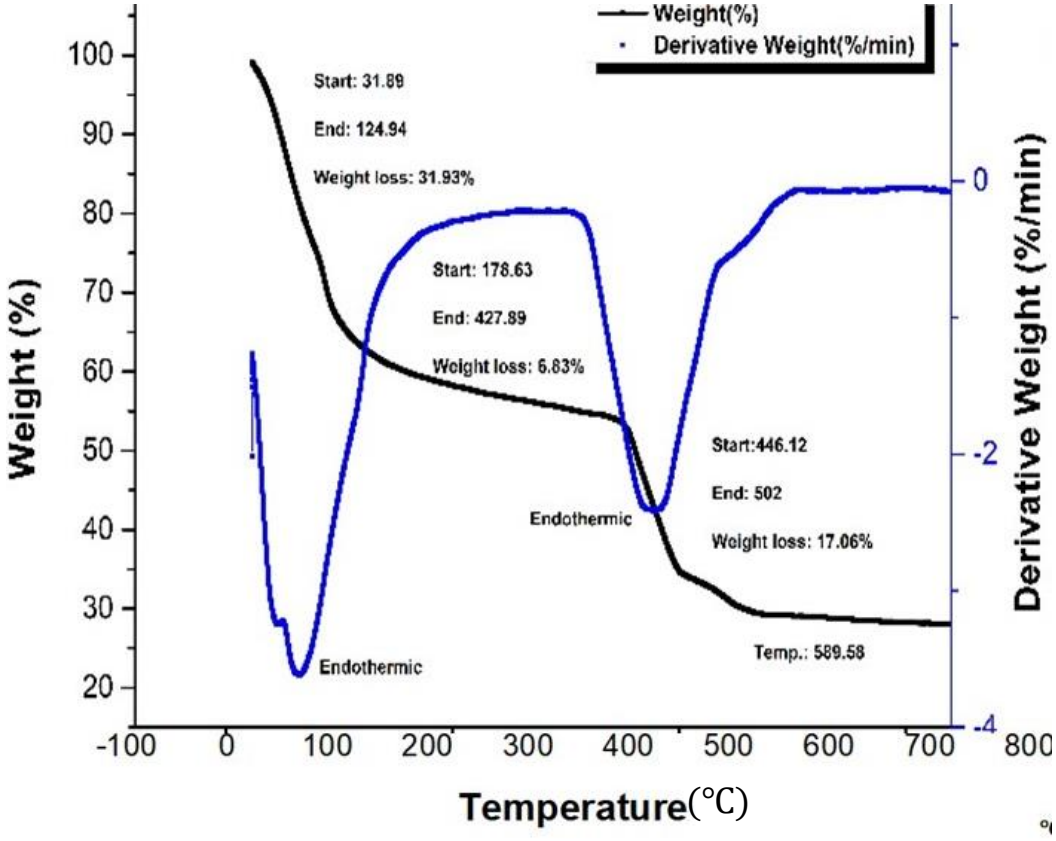

Figure 2.10. TGA curve of CMTKG-PSMA Hydrogel

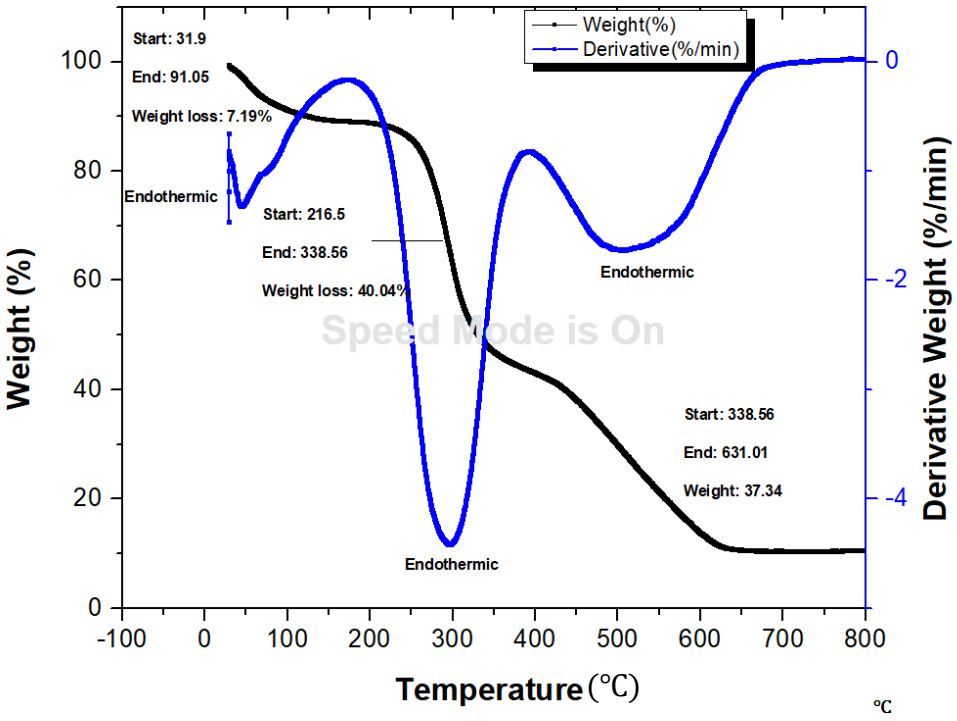

Figure 2.11. TGA Curve of CMTKG

In the TGA Curve of CMTKG-PSMA hydrogel (**Figure. 2.10.)**, more thermal stability is observed after the loss of water of crystallization from 178.63℃- 427.89℃, with negligible weight loss (6.83%), which is not observed in case of CMTKG (**Figure. 2.11)**. The derivative weight curve indicates that the whole weight loss is an endothermic process.

2.3.5.3. SEM Studies

SEM analysis revealed the morphological attributes of CMTKG-PSMA hydrogel comprising many interstitial voids as well as porous surfaces (**Figure. 2.12)**. It confirmed separate and clear boundaries in the framework. These pores account for a more swelling ratio as it allows more diffusion of the liquid into the network of polymer.

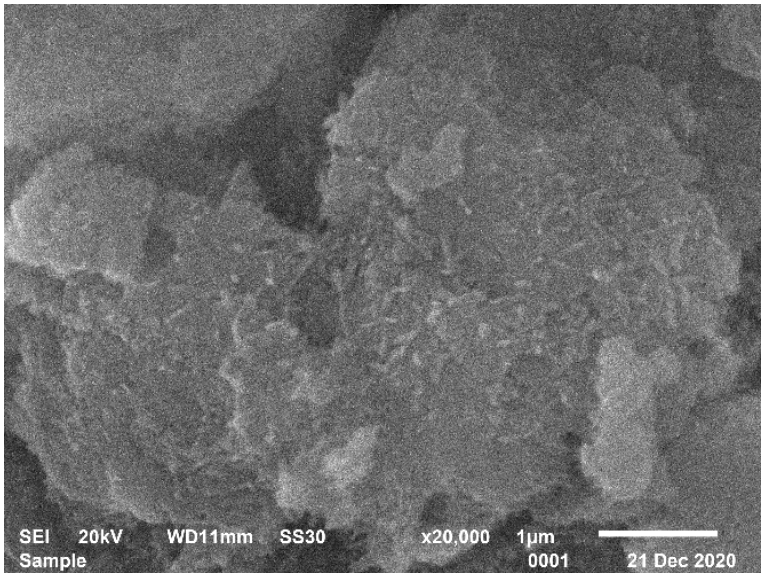

Figure.2.12.SEM studies of CMTKG-PSMA Hydrogel

2.3.6. Swelling Assessment

2.3.6.1. Effect of time

The optimized CMTKG-PSMA hydrogel exhibited a swelling ratio of 248.88 in distilled water at 18℃ as depicted in **Figure. 2.13**. It increased over time till it reaches the equilibrium state ie. when the swelling force due to the diffusion of water into the hydrogel counter balances the elastic retractive force owing to the hydrogel's uncoiling and relaxation. At the equilibrium swelling ratio, there is no net movement of water into or out of the hydrogel.

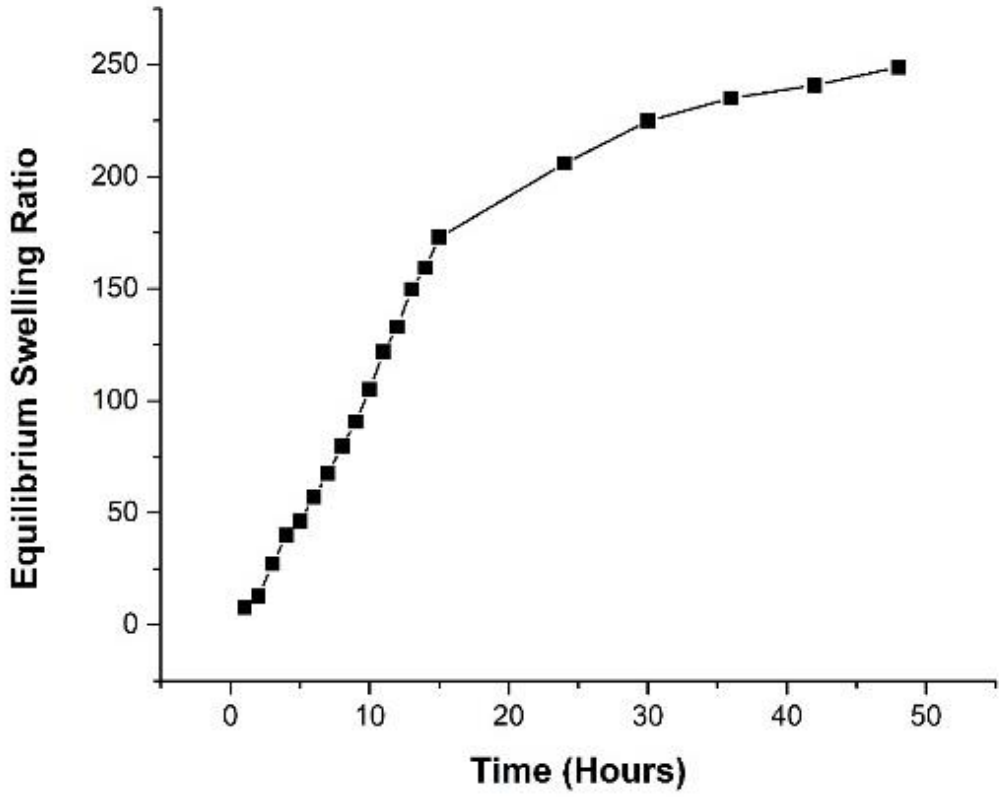

Figure.2.13 Rate of Swelling in Distilled Water with Time

2.3.6.2. Effect of pH

As the pH of the solutions was increased, -COOH moiety existed as $-COO^-$. This led to increased repulsion between them, allowing more water molecules to enter the hydrogel network. Thus, an increase in swelling ratio was observed till the pH 10 [13]. But, as the pH was further increased, the swelling ratio decreased as NaOH was added to increase the pH and more concentration of Na^+ ions decreased the charge density, thus lowering the swelling ratio of the hydrogel [14], as depicted in **Figure. 2.14**. The swelling ratio at pH 2 was noted to be 167.79, which increased to 309.9 at pH 10 and finally decreased to 230.65 at pH 12.

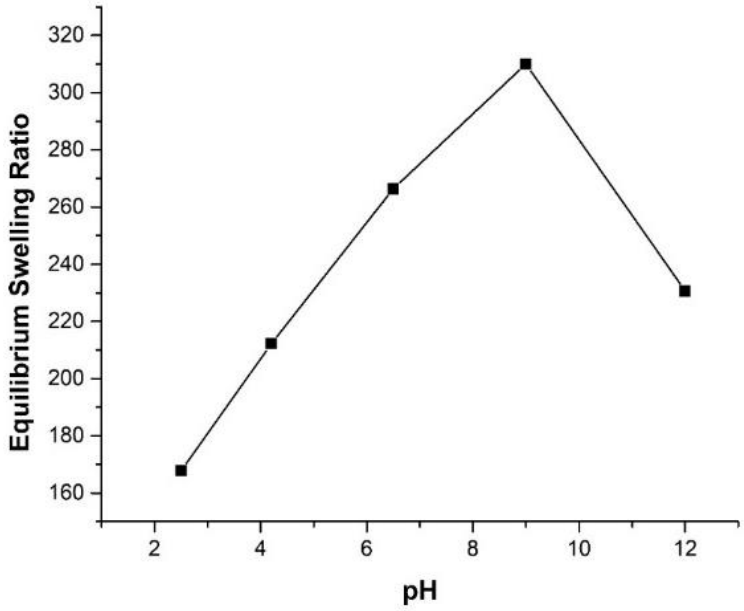

Figure.2.14. Rate of swelling at different pH

2.3.6.3. Effect of salt solutions

The rate of equilibrium swelling was assessed for NaCl and was found to be 55 as shown in **Figure. 2.15.** i.e., towards the lower side as compared to distilled water, the reason being the decrease in charge density due to surplus Na^+ cations, owing to sodium salt [15]. The higher ionic strength in the surrounding outer medium in saline solutions, reduces the osmotic pressure difference between the outer and inner medium, limiting the entry of water inside the hydrogel. Further, the lowering in the swelling ratio was also noted for $MgCl_2$ and $AlCl_3$. As the charge on the cation is increased, more $-COO^-$ chains need to be attached to it for charge neutralization, sterically hindering the water molecules to be entrapped [16]. The observed order for the swelling ratio was found to be: NaCl (55) > $MgCl_2$ (44) > $AlCl_3$ (39)

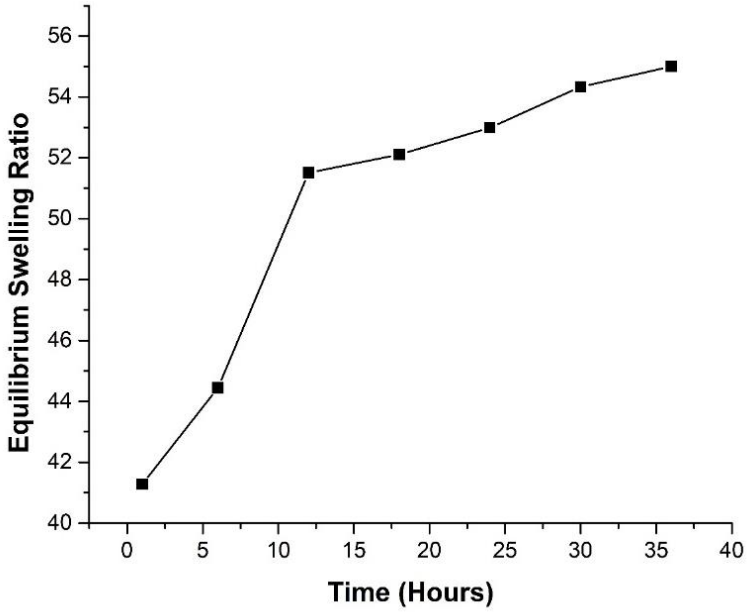

Figure.2.15. Rate of Swelling in saline solution

2.4. Diffusion Studies

The Korsmeyer-Peppas diffusion equation **(Eq.2.2)** [5] is applied to find the type of diffusion observed for the starting 15 hours, as shown in **Figure. 2.16.**

$$\mathbf{F = \frac{Mt}{M\infty} = kt^n} \qquad \textbf{Eq (2.2)}$$

As the value of n > 1, as inferred from the graph [**Figure. 2.10**], the transport mechanism is Super case II transport (involving swelling and relaxation of polymer matrix) and the release mechanism is both diffusion and relaxation.

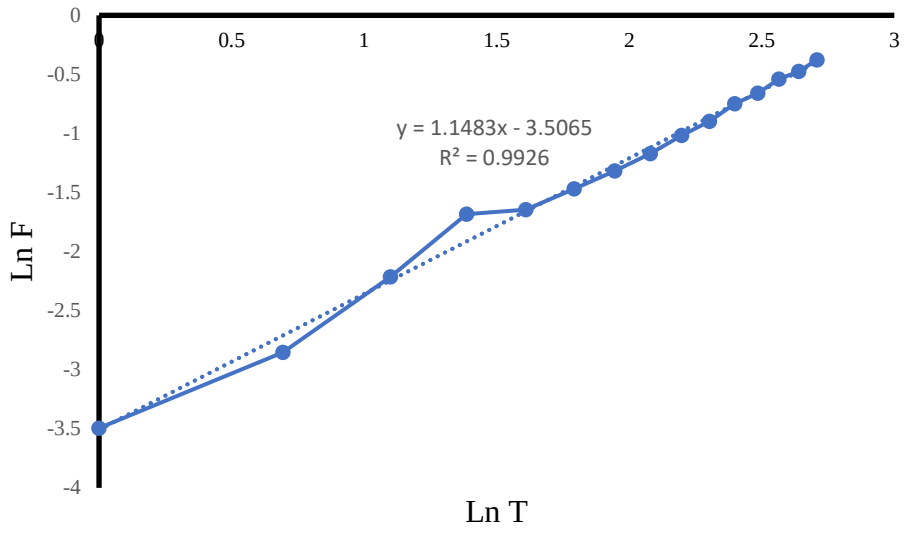

Figure. 2.16. Graph of Ln F vs. Ln T (Super case-II Diffusion)

2.5. Conclusions

The innovative superabsorbent bio-tech hydrogel was concocted by free radical polymerization of sodium-methacrylate & carboxymethyl tamarind kernel gum, for application in agronomical procedures as a soil conditioner & water harvester for sustainable agronomy. The structural morphologies of the hydrogel were characterized by techniques viz. Fourier transform infrared spectroscopy, scanning electron microscopy, and thermogravimetric analysis. The swelling behaviour of hydrogel was analysed as a function of temperature, pH, and salt solutions. Out of all the mentioned solvents, the highest swelling percentage of 24888% was noticed in distilled water. The water intake was Super case II transport (involving swelling and relaxation of polymer), following Korsmeyer-Peppas Equation. These hydrogels proffer a promising substitute as a soil conditioner in agronomy.

References

[1] A. Blanco, G. González, E. Casanova, M.E. Pirela, A. Briceño, Mathematical Modeling of Hydrogels Swelling Based on the Finite Element Method, Appl. Math. 04 (2013) 161–170. https://doi.org/10.4236/am.2013.48a022.

[2] H. van der Linden, J. Westerweel, Temperature-Sensitive Hydrogels, in: Encycl. Microfluid. Nanofluidics, Springer US, 2008: pp. 2006–2009. https://doi.org/10.1007/978-0-387-48998-8_1538.

[3] H. Prabhanjan, Studies on Modified Tamarind Kernel Powder. Part I: Preparation and Physicochemical Properties of Sodium Salt of Carboxymethyl Derivatives, Starch - Stärke. 41 (1989) 409–414. https://doi.org/10.1002/star.19890411102.

[4] Khushbu, S.G. Warkar, N. Thombare, Controlled release and release kinetics studies of boron through the functional formulation of carboxymethyl tamarind kernel gum-based superabsorbent hydrogel, Polym. Bull. (2021). https://doi.org/10.1007/S00289-021-03634-9.

[5] E. Karadag Ae, D. Saraydin, Y.C.Ë. Aldiran, O.G. Èven, Swelling Studies of Copolymeric Acrylamide/Crotonic Acid Hydrogels as Carriers for Agricultural Uses, (n.d.). https://doi.org/10.1002/(SICI)1099-1581(200002)11:2.

[6] P. Goyal, V. Kumar, P.S.-C. Polymers, undefined 2007, Carboxymethylation of tamarind kernel powder, Elsevier. (n.d.). https://www.sciencedirect.com/science/article/pii/S0144861706004772?casa_token=2yJZTHny8QoAAAAA:NLbHCbIz3Khkhr9mIFi2lXWL9YO0S7LdowGcXBXgdsQ9gmbwu8ZUR3CGtV2s5nM5iU7rQR3-3Y0 (accessed August 24, 2022).

[7] K.S. Soppimath, A.R. Kulkarni, T.M. Aminabhavi, Chemically modified polyacrylamide-g-guar gum-based crosslinked anionic microgels as pH-sensitive drug delivery systems: preparation and characterization, J. Control. Release. 75 (2001) 331–345. https://doi.org/10.1016/S0168-3659(01)00404-7.

[8] F.T. WALL, Principles of Polymer Chemistry. Paul J. Flory. Cornell Univ. Press, Ithaca, New York, 1953. 688 pp. Illus. $8.50, Science (80-.). 119 (1954) 555–556. https://doi.org/10.1126/SCIENCE.119.3095.555-A.

[9] R. Singhal, R.S. Tomar, A.K. Nagpal, Effect of cross-linker and initiator concentration on the swelling behaviour and network parameters of superabsorbent hydrogels based on acrylamide and acrylic acid, Int. J. Plast. Technol. 2009 131. 13 (2009) 22–37. https://doi.org/10.1007/S12588-009-0004-4.

[10] E.M. Ahmed, ; Magdy, A.H. Zahran, ; Fatma, S. Aggor, ; S A Abd Elhady, S.S. Nada, Synthesis and Swelling Characterization of Carboxymethyl Cellulose-g-Poly(Acrylic acid-co-Acrylamide) Hydrogel and their Application in agricultural field, (n.d.).

[11] J.H. Trivedi, Synthesis, characterization, and swelling behavior of superabsorbent hydrogel from sodium salt of partially carboxymethylated tamarind kernel powder-g-PAN, J. Appl. Polym. Sci. 129 (2013) 1992–2003. https://doi.org/10.1002/APP.38910.

[12] E.S. Rufino, E.E.C. Monteiro, Characterisation of lithium and sodium salts of

poly(methacrylic acid) by FTIR and thermal analyses, Polymer (Guildf). 41 (2000) 4213–4222. https://doi.org/10.1016/S0032-3861(99)00630-8.

[13] J. Elliott, M. Macdonald, J. Nie, C.B.- Polymer, undefined 2004, Structure and swelling of poly (acrylic acid) hydrogels: effect of pH, ionic strength, and dilution on the crosslinked polymer structure, Elsevier. (n.d.). https://www.sciencedirect.com/science/article/pii/S0032386103011911?casa_token=NKKtF944vncAAAAA:QrCTi2NQWhPtMKn0k1KfmiA8nUluEpsMwL1_IXTIWouIaowVcJakZUCtqyS7lQqmG8OTpdR0yMM (accessed August 9, 2022).

[14] P. Liu, M. Zhai, J. Li, J. Peng, J.W.-R.P. and Chemistry, undefined 2002, Radiation preparation and swelling behavior of sodium carboxymethyl cellulose hydrogels, Elsevier. (n.d.). https://www.sciencedirect.com/science/article/pii/S0969806X01006491 (accessed August 9, 2022).

[15] A. Pourjavadi, P. Eftekhar Jahromi, F. Seidi, H. Salimi, Synthesis and swelling behavior of acrylatedstarch-g-poly (acrylic acid) and acrylatedstarch-g-poly (acrylamide) hydrogels, Carbohydr. Polym. 79 (2010) 933–940. https://doi.org/10.1016/j.carbpol.2009.10.021.

[16] H. Namazi, M. Hasani, M. Yadollahi, Antibacterial oxidized starch/ZnO nanocomposite hydrogel: Synthesis and evaluation of its swelling behaviours in various pHs and salt solutions, Int. J. Biol. Macromol. 126 (2019) 578–584. https://doi.org/10.1016/j.ijbiomac.2018.12.242.

Chapter-3

AGRONOMICAL EVALUATION OF CARBOXY METHYL TAMARIND KERNEL GUM- POLY SODIUM METHACRYLATE HYDROGEL (CMTKG-PSMA), AS SOIL-WATER CONDITIONER

3.1. Introduction

Water's pivotal role and exorbitant usage in agronomical practices viz. irrigation, nutrient/ pesticide application, crop cooling, and frost control have opened a new outlook in research to develop innovative technologies for water's sustenance by effectual use with less wastage for global economic balance and food security. Henceforth, various practices are being explored that make the plants accessible to high available water content and lower the frequency of irrigation [1].

Biopolymer-based organic hydrogels are greener and more eco-friendly practices for keeping the soil moistened and nourished. Their greener attributes viz. non-toxicity, biodegradability, and higher water intake and retention capability shield the environment and natural resources and enhance plant growth and crop productivity [2]. The hydrogel amendment of the soil for agronomy is technically, socially, economically, and environmentally sustainable. These organic hydrogels contribute beneficially towards the soil morphologies, density, texture, permeability, evaporation, and infiltration rates of water through it. They boost the water holding capacity, water use efficiency, soil infiltration rate, and permeability. And, at the same time, drive down soil compaction, surface water run-off, soil erosion, leaching, evaporation of water, and seepage into the ground. They make the water content of the soil readily available to the plants, owing to their property of adhesion to the roots. To summarize, it can be inferred that these Bio-hydrogels,

unlike irrigation water, are not wasted due to percolation deep into the ground, evaporation, or due to soil erosion. But the water is entrapped by these hydrogels, acting as a water harvester, and is supplied to the plants slowly during water stress conditions. In other words, plants can survive a little longer in the water stress conditions if the soil is amended with the hydrogel. Thus, this hydrogel serves as an underground water reservoir and as artificial humus, owing to the presence of carboxylic groups, the hydrophilic moieties which allow more diffusion of water into it.

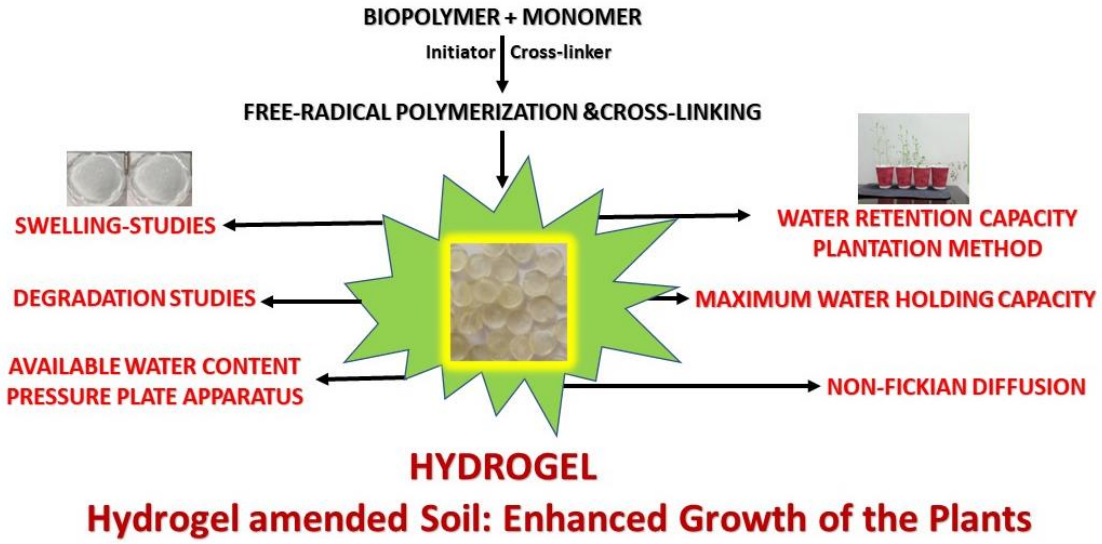

Figure. 3.1. Application of CMTKG-PSMA Hydrogel in Agronomy

To assess the synthesized CMTKG-PSMA hydrogel, the soil was amended with it and CMTKG-PSMA hydrogel was assessed for its potential to be exploited as a soil conditioner in the dynamics of agronomics via its assimilation into the soil and researching its effects on various physical soil attributes viz. water retention, available water content (AWC), maximum water holding capacity (MWHC), porosity, particle density, bulk density, employing different relevant procedures [3] **(Figure. 3.1.)**.

3.2. Experimental Procedure

3.2.1. Materials

The synthesis of CMTKG-PSMA bio-hydrogels has already been stated in chapter 2. The soil sample for experimentation was amassed from Delhi Technological University, Delhi, having a mineral portion of 87% sand and 0.8% clay and silt. The calculated particle density and bulk density were found to be 2.692 g cm^{-3} and 1.28 g cm^{-3} respectively.

3.2.2 Maximum Water Holding Capacity (MWHC)

The effect of CMTKG-PSMA hydrogel on the MWHC of the soil was investigated by preparing three samples of soil with 0.1%, 0.3%, and 0.5% hydrogel along with a control sample. The fixed weighed quantity of each of the properly dried samples was put into a plastic beaker having small holes layered up with filter paper to avoid any errors due to soil loss. All four beakers were kept in a water tub to allow maximum water absorption for about twelve hours, followed by gravitational drainage of extra water. The net weight of water engrossed by the soil was calculated by using the following formula **(Equation. 3.2):**

MWHC = [(Weight of beaker post water absorption) – (weight of the dried soil + weight of empty beaker + weight of wet filter paper**)].** **(Eq. 3.2)**

3.2.3. Soil Density and Porosity of soil

The standard method of calculating the particle density (PD) (employing the Pycnometer) and Bulk density (BD) was implied [3]. Different soil samples were prepared by adding bio-hydrogel having a size between 120 to 160 mesh in different concentrations of 0.1% 0.2% and 0.3%. A blank sample was also prepared. The samples were oven-dried (40℃), till weight constancy, filtered

through a 2mm sieve, and then applied for experimentation by standard method. The porosity [4] of the different soil samples was also calculated, using the following formula **(Eq.3.3)**:

Porosity (%) = [1 - $\frac{BD}{PD}$] X 100 **Eq (3.3)**

Where BD = Bulk density

PD = Particle density

3.2.4. Water retention capacity by Plantation method

To study the effect of CMTKG-PSMA on the growth of plants with the limited amount of water mimicking the droughts conditions, chickpea seeds (*Cicer arietinum*) were sown in three soil samples having 0.1%, 0.3%, 0.5% hydrogel concentration in addition to the control sample, taking the same amount of the soil, irrigating with the same amount of water, and maintaining the same environmental conditions. The growth in terms of the days of survival and shoot length was observed for different concentrations of the hydrogel and the procedure was repeated thrice.

3.2.5. Available water Content (AWC) using Pressure plate apparatus

Pressure plate apparatus (Model: 1600 pressure extractor, Santabarbara, CA, USA) was employed to study the effects of CMTKG-PSMA hydrogel on the water retention capacity at matric tensions of 0.33 bar and 15 bar, which correspond to the field capacity and permanent wilting point respectively. The three soil samples of 0.1%, 0.3%, and 0.5% hydrogel concentrations along with blank samples were settled one by one, in rubber rings arranged on ceramic plates. The soil was saturated with water for twelve hours. The plates were then subjected to different matric tensions in a pressure chamber, till the water flow from the soil ceases completely. The soil samples were transferred to moisture boxes and weighed accurately, followed by oven-dehydration (100℃ for

twelve hours) and reweighing after cooling. The percentage of water content (WC) was calculated using the following formula **(Eq.3.4)**:

$$\text{WC (\% w/w)} = \frac{Swet - Sdry}{Sdry} \text{ X } 100 \qquad \textbf{Eq (3.4)}$$

Where WC = Water content of the soil on a weight basis

S_{wet} = Weight of the wet soil at specific matric tension

S_{dry} = Weight of the dried soil

Available water content (AWC) is the water that can be used up by the plants for their growth and is calculated by subtracting the water content retained at 0.33 matric tension and water content retained at 15 bar matric tension corresponding to field capacity and permanent wilting point respectively, using the following formula **(Eq.3.5)**:

AWC= WC (0.33 at matric tension) – WC (15 bar matric tension) **Eq (3.5)**

3.2.6. Bio-degradation studies

Soil burial degradability test [5- 8], of CMTKG-PSMA hydrogel was performed for 60 days. The pre-weighed CMTKG-PSMA hydrogels were buried at a depth of about 5-6 cm in well-moisturized soil. After a specific time interval, and removal of soil, these hydrogels were re-weighed to obtain the degradation percentage based on the dry weight of hydrogel remnants in the soil post-degradation. SEM of the degraded hydrogel was also analysed to identify the variations in the surface morphology. The residuary dry content (RDC) percentage was calculated implying the formula **(Eq.3.1)** given below:

$$\text{RDC \%} = \frac{\text{Weight of the dry content of hydrogel X 100}}{\text{Weight of initial dry content of the hydrogel}} \qquad \textbf{Eq (3.1)}$$

3.3. Results & Discussions

3.3.1. Effect of hydrogel on Maximum Water Holding Capacity (MWHC)

An experimental determination of MWHC was conducted by saturating the different samples of the soil with water followed by gravimetric discharge of excess water without the application of any external pressure [3]. The control sample held 40.6327 g of water per 100 g of the soil, i.e., the percentage of MWHC is 40.63%. The different soil samples having 0.1%, 0.3%, and 0.5% CMTKG-PSMA hydrogel held 45.1305g, 52.2929g, and 59.5271g of water per 100g water respectively showing 11.06%, 28.68%, and 46.5% increase in MWHC percentage as compared to the control sample. The concentration of hydrogel in the soil sample and the MWHC of the soil are found to be linearly related as can be inferred from the graph shown in **Figure. 3.2.**

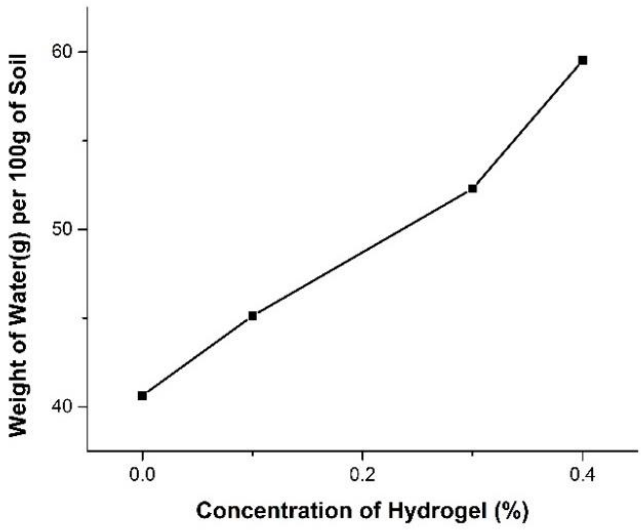

Figure. 3.2 Effect of CMTKG-PSMA hydrogel on Maximum water holding capacity (MWHC) of the soil.

3.3.2. Effect of hydrogel on Soil Density & Porosity

Particle density is significant for the approximation of porosity, air voids, and settling rates of particles in liquids. A pycnometer was employed as it can be filled with precise volume owing to excess water elimination through a capillary opening in the ground-glass stopper, leaving little scope for errors. Particle density was calculated by using the formula **(Eq.3.6)** [7]:

Particle density (PD), $\rho_p = \rho_w \frac{(W_s - W_a)}{(W_s - W_a) - (W_{sa} - W_w)}$ **Eq (3.6)**

Where W_a = Weight of oven-dried pycnometer

W_s = Weight of pycnometer plus soil sample

W_{sa} = Weight pycnometer plus soil sample plus water

W_w = Weight of pycnometer plus water at room temperature

ρ_w = Density of water at room temperature

The particle density of the soil sample was observed to be 2.692 g cm^{-3}.

Bulk density (BD) was noted for various soil samples using the standard procedure [4]. BD of the control sample was found to be 1.28 g cm^{-3} and of the soil samples containing 0.1%, 0.3%, and 0.5% CMTKG-PSMA hydrogel was found to be 1.36 g cm^{-3}, 1.44 g cm^{-3}, 1.48 g cm^{-3} respectively, revealing 6.2%, 12%, and 16% increase in relation to the control sample **(Figure. 3.3.)**.

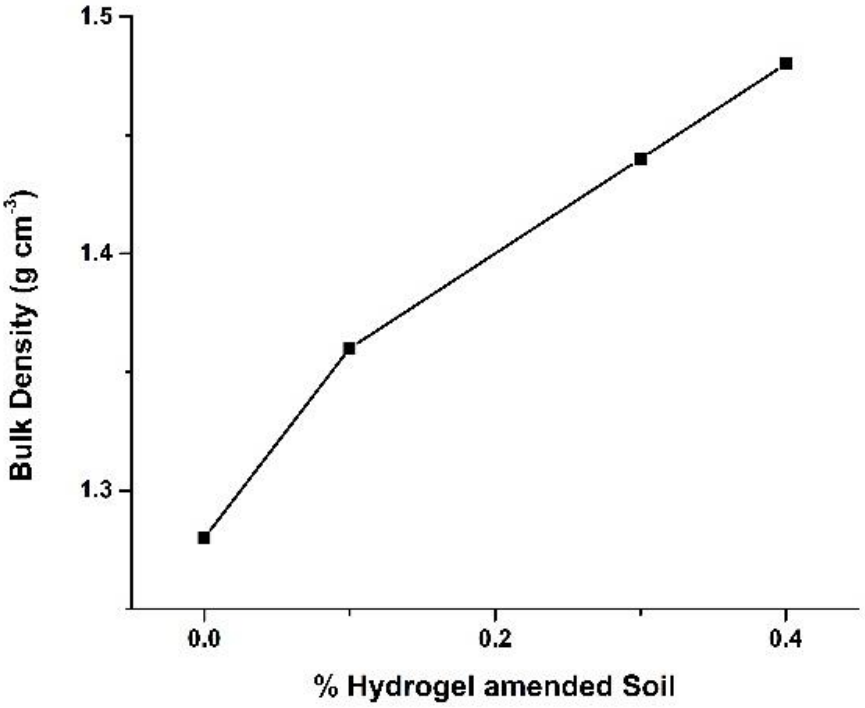

Figure. 3.3. Effect of CMTKG-PSMA hydrogel on Bulk density of the soil

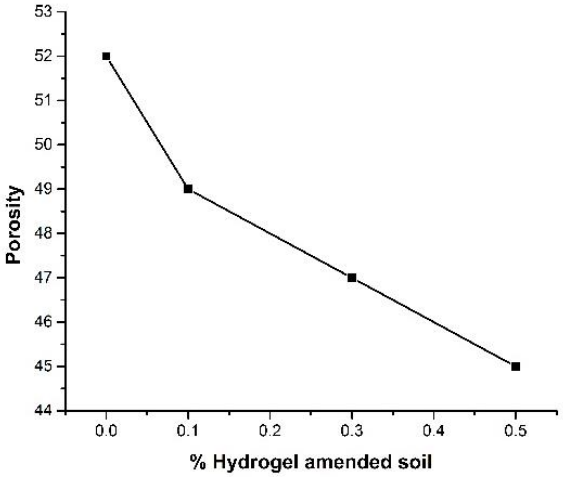

Figure. 3.4. Effect of CMTKG-PSMA hydrogel on Porosity of the soil

CMTKG-PSMA hydrogel acts as a humus due to the presence of hydrophilic groups in them, which increases the bulk density due to increase in organic content (CMTKG) [8], thereby

decreasing the porosity. Porosity decreased with the increased percentage of CMTKG-PSMA hydrogel and was revealed to be 52, 49, 47 and 45 for the control sample, and samples containing 0.1%, 0.3%, and 0.5% CMTKG-PSMA hydrogel respectively. CMTKG-PSMA hydrogel has the competency to increase the BD and decrease the porosity paving the way to more humus content which has positive effects on root functionality in plants [8]. The same can be easily inferred from the **Figure. 3.4**.

3.3.3. Effect of hydrogel on Water Retention capacity (WRC) by Plantation method

The effect of CMTKG-PSMA hydrogel on WRC was analyzed by planting chickpeas in four pots containing control soil and soil having 0.1%, 0.3%, and 0.5% CMTKG-PSMA hydrogel. All four pots were subjected to identical conditions of sunlight, water, and temperature. It was observed that post 21 days (**Figure. 3.5 a)** of the plantation, the plant grown in the controlled soil wilted followed by wilting of 0.1%, 0.3%, and 0.5% on the 33^{rd}, $40^{th,}$ and 47^{th} day of the plantation, respectively **(Figure. 3.5 b, 3.5.c, 3.5.d).** Thus, it was discovered that the plants grown in CMTKG-PSMA hydrogel-treated soil with its higher concentration, survived for a longer duration under water stress conditions. A trilogy of experiments was done for this research [9].

Further, there was enhanced growth in plants sown with a higher percentage of CMTKG-PSMA hydrogel. On the 25^{th} day of the plantation, the shoot length of plants grown in control soil and soil having 0.1%, 0.3%, and 0.5% was observed to be 14.5 cm, 16.6cm, 18.3 cm, and 20.8 cm, and a percentage increase in shoot length was found to be 14.4%, 26.2%, and 43.4% respectively as can be inferred from **Figure. 3.5 (e).**

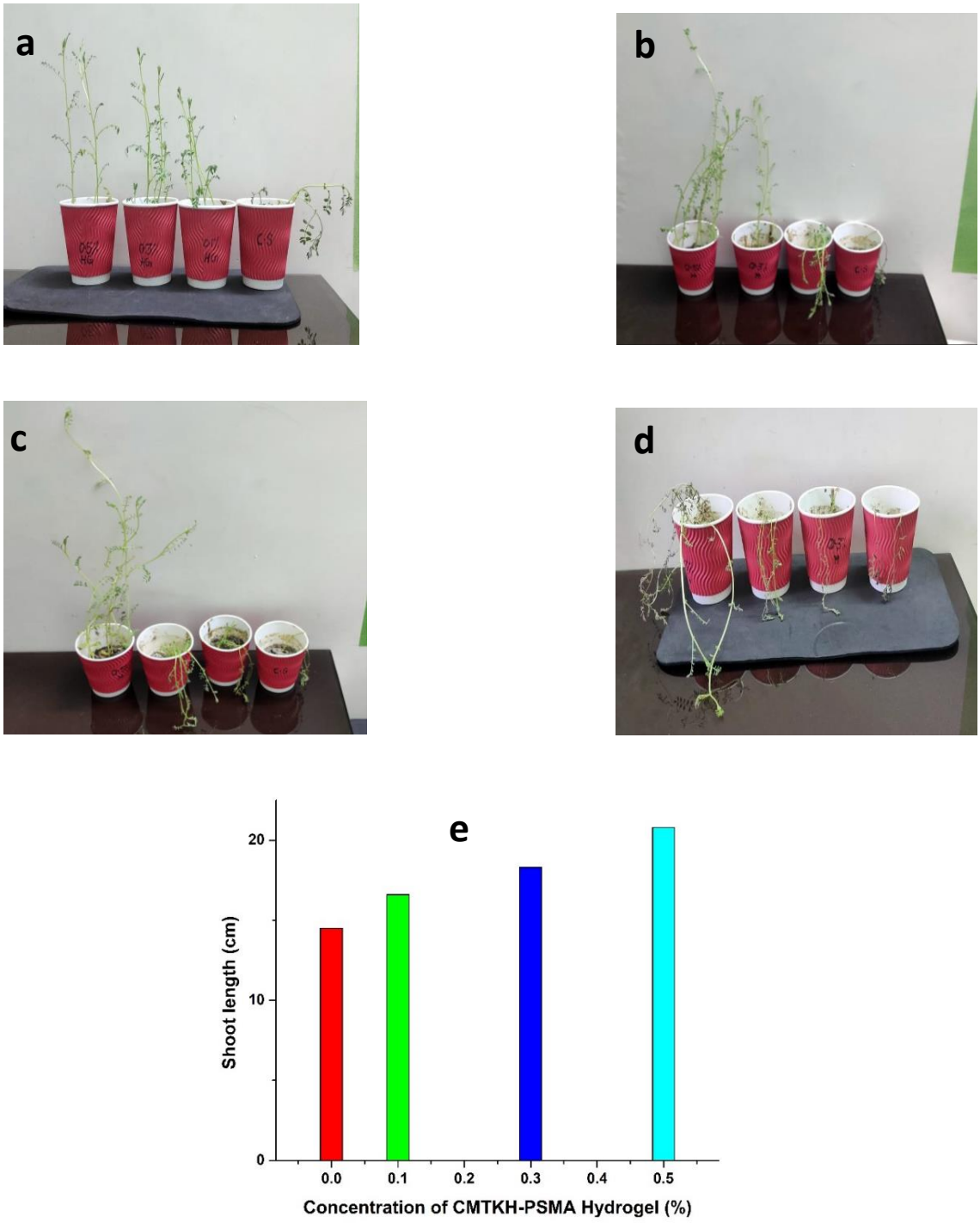

Figure. 3.5 Effect of Hydrogel on Water Retention Capacity of the Soil

a) After 21 days of plantation b) After 33 days of plantation c) After 40 days of plantation d) After 47 days of plantation e) Effect of Hydrogel on Shoot Growth

3.3.4. Effect of hydrogel on Available Water Content (AWC) by Pressure-plate apparatus

Available water content is a crucial paradigm to analyze water content in the soil profile that is readily available for the plants and, for assessing the growth of the plants [10]. As the CMTKG-PSMA hydrogel reveals a positive effect on the AWC characteristic of the soil, its usage under water stress conditions or drought is a boon for agronomy. AWC of different soil samples along with control soil was carried out employing pressure-plate apparatus, in which the different soil samples were subjected to 0.33 bar matric suction and 15 bar matric suction, which corresponds to the field capacity (amount of water retained by the soil sample upon saturation followed by excess water drainage) and permanent wilting point (water content of the soil sample below which plants wilt) respectively for each soil sample. **Figure. 3.6** depicts the effect of Hydrogel on the Available Water Content of Soil and the difference between field capacity and permanent wilting point that relates to available water content is depicted in **Figure. 3.7.** The water content of various soil samples at 0.33 Bar, 15 Bar matric suction, and AWC has been specified in the **Table. 3.1**. The percentage increase in the available water content of 0.1%, 0.3%, and 0.5% CMTKG-PSMA containing soil was found to be 21.55%, 32.64%, and 37.04% respectively.

Table.3.1 Percentage Increase in Available Water Content on Increasing the Concentration of Hydrogel

Soil Sample % CMTKG-PSMA	Water content at 0.33 Bar matric suction (Field capacity) (%)	Water content at 15 Bar matric suction (Permanent wilting point) (%)	Available water content (%)
NIL	14.111	8.079	6.032

0.1%	15.246	7.245	7.331
0.3%	17.241	8.539	8.001
0.5%	24.306	16.04	8.266

Figure. 3.6. Effect of Hydrogel on Available Water Content of Soil

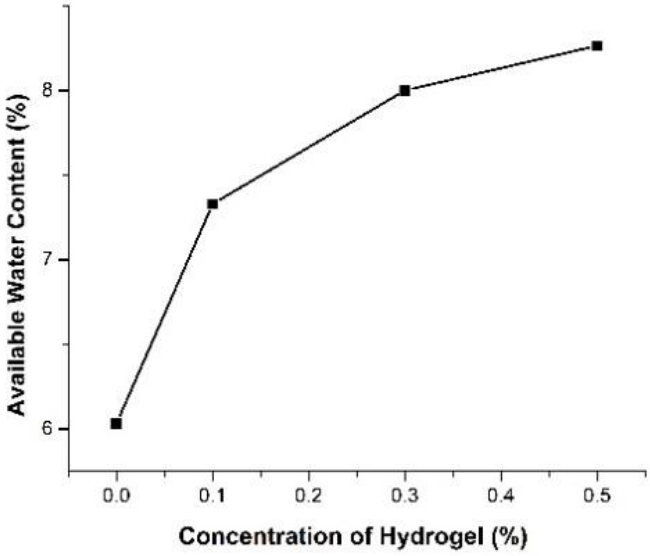

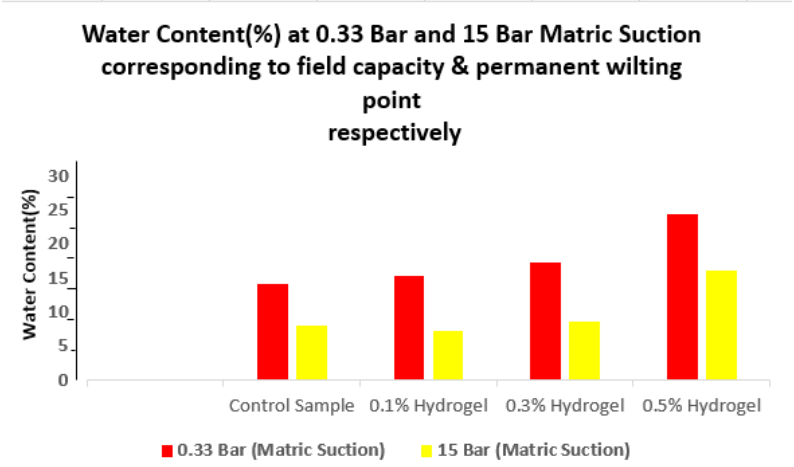

Figure. 3.7. Effect of Hydrogel on Field Capacity and Permanent Wilting Point

3.3.5. Bio-degradation Studies

In the present research, the major problem of the non-biodegradability of synthetic hydrogels was resolved comparatively by fabricating the hydrogels, using natural biopolymer- CMTKG along with sodium methacrylate. Soil burial studies were carried out, which revealed that the hydrogel synthesized can be degraded by micro-organisms existent in soil and all the factors responsible for the rapid growth of microbes such as the significant ratio of carbon and nitrogen [11], oxygen concentration, temperature, humus content, and minerals present in the soil also enhanced the process of biodegradation [12] of CMTKG-PSMA. The preliminary bio-degradation rate of the CMTKG-PSMA for the initial 30 days was high and found to be 44% followed by a slower weight loss of about 12% from the 30^{th} day to the 45^{th} day of soil burial. The initial rate of degradation was high as both the organic content (CMTKG) and oxygen present inside the hydrogel were high. But post the 45^{th} day of soil burial, the rate of degradation was observed to be slower, as the anaerobic conditions prevail causing lower microbial activity and there is lesser diffusion of oxygen into the hydrogel because of more water inflow. The hydrogels buried in soil having more microorganisms endured faster biodegradation [13]. This bio-degradation process was verified by the SEM studies (**Figure.3.8**), which revealed a comparative more eroded and more hollow-porous surface morphology of the decomposed hydrogel on the 45^{th} day as compared to decomposed hydrogel on the 60^{th} day as compared to non-degraded one, as can be easily inferred from the **Figure.3.8**.

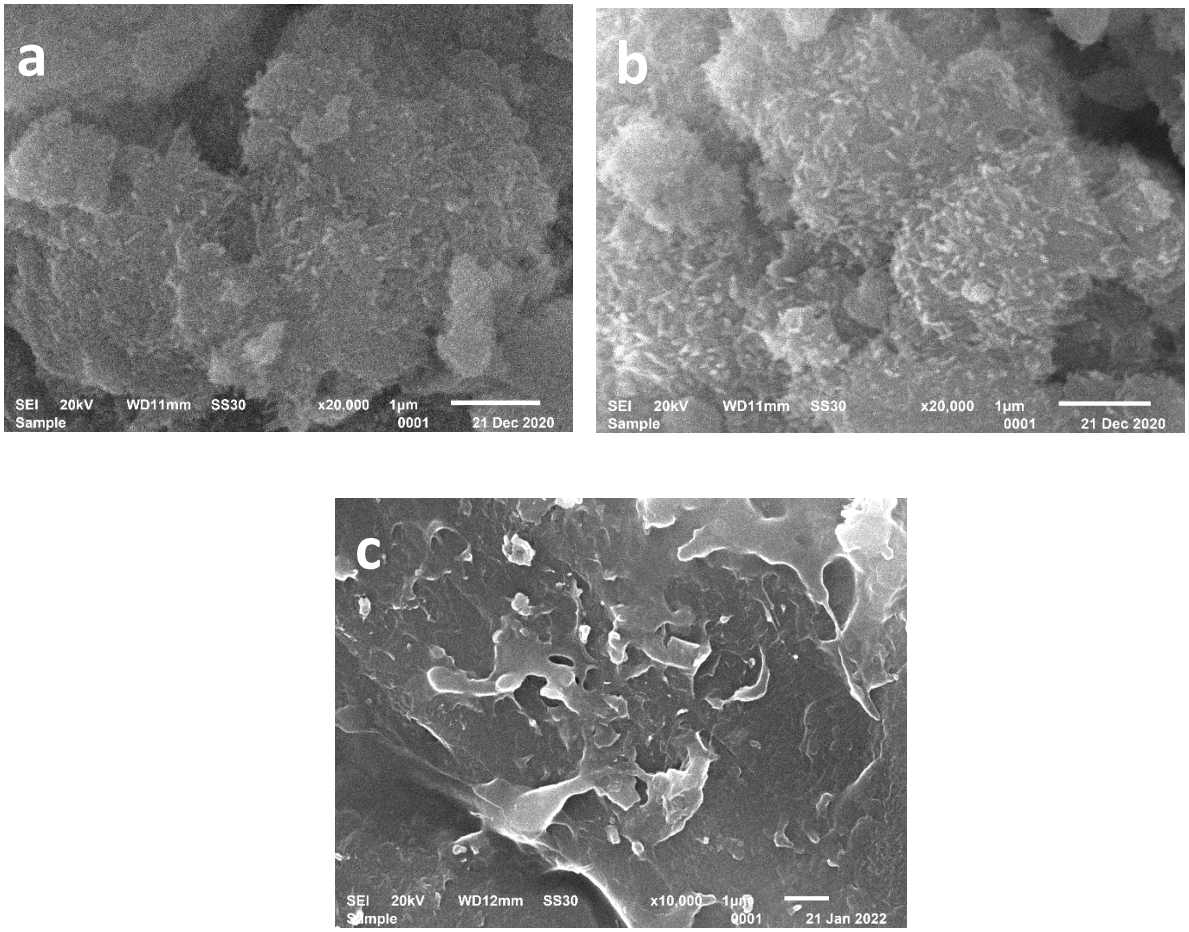

Fig.3.8. Degradation studies by SEM

a. Non-degraded CMTKG-PSMA Hydrogel

b. CMTKG-PSMA Hydrogel on the 45th Day of Decomposition

c. CMTKG-PSMA Hydrogel on the 60th Day of Decomposition

3.4. Conclusions

The formulated hydrogel, CMTKG-PSMA when treated with soil, revealed positive effects on various soil characteristics viz. 46.5% Increase in MWHC (0.5% CMTKG-PSMA Hydrogel amended soil), 37% increase in Available Water Content (0.5% CMTKG-PSMA Hydrogel amended soil, wilting on 47th day of the chickpea plant in 0.5% CMTKG-PSMA Hydrogel

amended soil as compared to wilting on 21 st day in control soil, 43.4% Increase in shoot length on 18th day of plantation of chickpea seeds, 8% increase in bulk density & 16% decrease in porosity in CMTKG-PSMA Hydrogel amended soil. All these attributes enhanced the water productivity of the plants, bestowing a conducive and safe environment for better growth of the crops in arid and semi-arid regions. This water retention CMTKG-PSMA bio-hydrogel entails lower application rates and can be applied as a proficient tool for higher water absorption for water sustenance and environment conservation in agronomics.

References

[1] Khushbu, S.G. Warkar, N. Thombare, Zinc micronutrient-loaded carboxymethyl tamarind kernel gum-based superabsorbent hydrogels: controlled release and kinetics studies for agricultural applications, Colloid Polym. Sci. 2021 2997. 299 (2021) 1103–1111. https://doi.org/10.1007/S00396-021-04831-8.

[2] Khushbu, S.G. Warkar, Potential applications and various aspects of polyfunctional macromolecule- carboxymethyl tamarind kernel gum, Eur. Polym. J. 140 (2020) 110042. https://doi.org/10.1016/j.eurpolymj.2020.110042.

[3] N. Thombare, S. Mishra, M.Z. Siddiqui, U. Jha, D. Singh, G.R. Mahajan, Design and development of guar gum based novel, superabsorbent and moisture retaining hydrogels for agricultural applications, Carbohydr. Polym. 185 (2018) 169–178. https://doi.org/10.1016/j.carbpol.2018.01.018.

[4] Manual on soil, plant and water analysis., (n.d.). https://www.cabdirect.org/cabdirect/abstract/20073118818 (accessed September 27, 2021).

[5] P. Rizzarelli, C. Puglisi, G. Montaudo, Soil burial and enzymatic degradation in solution of aliphatic co-polyesters, Polym. Degrad. Stab. 85 (2004) 855–863. https://doi.org/10.1016/J.POLYMDEGRADSTAB.2004.03.022.

[6] K. Sharma, V. Kumar, B.S. Kaith, V. Kumar, S. Som, S. Kalia, H.C. Swart, A study of the biodegradation behaviour of poly(methacrylic acid/aniline)-grafted gum ghatti by a soil burial method, RSC Adv. 4 (2014) 25637–25649. https://doi.org/10.1039/C4RA03765K.

[7] G.R. Blake, Particle density, Encycl. Earth Sci. Ser. (2008) 504–505. https://doi.org/10.1007/978-1-4020-3995-9_406.

[8] N.C. Womack, I. Piccoli, C. Camarotto, A. Squartini, G. Guerrini, S. Gross, M. Maggini, M.L. Cabrera, F. Morari, Hydrogel application for improving soil pore network in agroecosystems. Preliminary results on three different soils, CATENA. 208 (2022) 105759. https://doi.org/10.1016/J.CATENA.2021.105759.

[9] F.F. Montesano, A. Parente, P. Santamaria, A. Sannino, F. Serio, Biodegradable

Superabsorbent Hydrogel IncreasesWater Retention Properties of Growing Media and Plant Growth, Agric. Agric. Sci. Procedia. 4 (2015) 451–458. https://doi.org/10.1016/J.AASPRO.2015.03.052.

[10] Q. de Jong van Lier, E.A.R. Pinheiro, L. Inforsato, Hydrostatic Equilibrium between Soil Samples and Pressure Plates Used in Soil Water Retention Determination: Consequences of a Questionable Assumption, Rev. Bras. Ciência Do Solo. 43 (2019). https://doi.org/10.1590/18069657RBCS20190014.

[11] H. Nie, M. Liu, F. Zhan, M. Guo, Factors on the preparation of carboxymethylcellulose hydrogel and its degradation behavior in soil, Carbohydr. Polym. 58 (2004) 185–189. https://doi.org/10.1016/J.CARBPOL.2004.06.035.

[12] Khushbu, S.G. Warkar, A. Kumar, Synthesis and assessment of carboxymethyl tamarind kernel gum based novel superabsorbent hydrogels for agricultural applications, Polymer (Guildf). 182 (2019) 121823. https://doi.org/10.1016/j.polymer.2019.121823.

[13] P. Cen, L. Xia, Production of Cellulase by Solid-State Fermentation, (1999) 69–92. https://doi.org/10.1007/3-540-49194-5_4.

Chapter-4

SYNTHESIS, OPTIMIZATION, SWELLING STUDIES, AND CHARACTERIZATION OF CARBOXY METHYL TAMARIND KERNEL GUM-BASED BIO-HYDROGEL (CMTKG-PSA-PAM]

4.1. Introduction

An increased global populace necessitates sustainable and increased agronomical production, which in turn demands urgent consideration to upgrade the productivity of less productive soils viz. the sandy soil and loamy soil. These soils have a high infiltration rate due to high porosity and are not able to retain the water, lowering the amount of available water content to the plants and hence, their stagnant growth and diminished crop yields. The need for arable soils necessitates research in the development of innovative soil-conditioner alternatives with a lower rate of application and boosted water availability to the plants. Apt research in this field can lead to prodigious results paving the way for sustainable development.

Hydrogels are smart materials that can aid farmers to overcome the above challenges related to agronomical praxes of irrigation. Synthetic hydrogels have already been incorporated to overcome this challenge. But the hazards created owing to these synthetic hydrogels [1] need to be addressed by upcoming research. This research incorporates the usage of a biopolymer for the synthesis of hydrogel, to address these problems. Organic hydrogel [2] amended soil advances the hydro-physical properties of all types of soils and makes them more productive, ensuring a plant's survival in conditions of water stress. It enhances the water-holding capacity of the soil, reduces

erosion and run-off, increases soil permeability and infiltration, and reduces soil compaction[3] [4]. In other words, these hydrogels are the perfect match for the sandy soil to enhance its fertility attributes[5]. **Figure 4.1.** displays the reversible dried and swollen state of hydrogels that aids them to act as reservoirs of water, supplementing water during drought-like conditions and storing large amounts of water during its abundant availability.

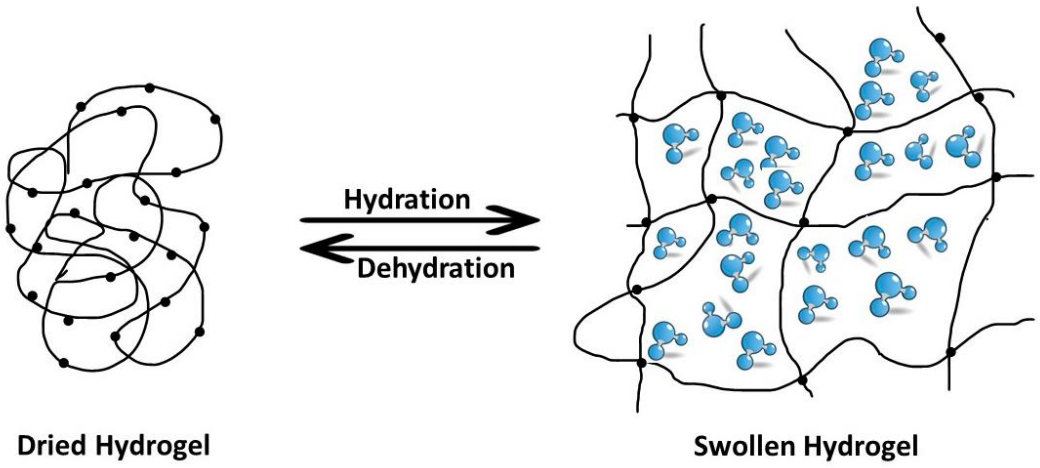

Figure. 4.1. **Dried and Swollen state of Hydrogel**

The polymerization with sodium acrylate and acrylamide incorporates the desired properties into the hydrogel with an increase in its life shell for effectual usage. The novel synthesized CMTKG-PSA-PAM hydrogel decreases the porosity of especially sandy soil, and acts as humus, thereby increasing the productivity of the soil. Different types of soil are found all over India and the world with different types of plants cultivated in them. So, to maximize the utility of hydrogel, its agricultural dynamics need to be researched on different types of soil for its precise application.

Further, as hydrogel's effect on hydro physical properties on different types of soil is rarely researched collectively, this research will be a leading edge in relating the usage of hydrogel in the agronomical industry.

4.2. Experimental Procedure

4.2.1. Materials

The Hindustan Gum and Chemicals Limited, Haryana openhandedly provided CMTKG possessing 0.20° of carboxymethyl substitution. Acrylic acid (CDH, New Delhi), Potassium persulfate (KPS), Sodium hydroxide (NaOH) (Fisher Scientific, Mumbai), and N, N'-methylenebis(acrylamide) (MBA) (Merck, Germany) were used during the synthesis. All the solutions were prepared using universal green solvent, the distilled water.

4.2.2. Synthesis of CMTKH-PSA-PAM hydrogel

The feedstock implied for the synthesis of hydrogel were CMTKG, sodium acrylate, and acrylamide, in the presence of MBA as cross-linker and KPS as initiator, using water as a solvent.. A consistent solution of CMTKG in distilled water is prepared followed by additions of sodium acrylate, acrylamide, MBA, and KPS one by one at an interval of half an hour by stirring it magnetically. The homogenous solution was kept undisturbed for about 20 minutes and was poured into test tubes to be kept in the water bath maintained at a temperature of 65℃ for about two hours for the completion of free radical polymerization. The hydrogel synthesized was taken out of the test tubes by breaking them and then cut into small pellets of an almost uniform thickness. These pellets were immersed in distilled water to do away with impurities and unreacted reactants. The swelled-up hydrogel pellets were dried at room temperature for about a fortnight followed by oven dryness at a temperature of 20 ℃ till weight constancy [6].

4.2.3. Swelling Studies of CMTKG-PSA-PAM hydrogel

About 10 variable concentrations as enlisted in **Table.4.1**., were fabricated for optimization by varying the concentrations of biopolymer, initiator, and cross-linker at room temperature. The best hydrogel based on maximum swelling capacity was chosen for the conduction of the research.

The continual Gravimetric Experimental Analysis was carried out to examine the equilibrium swelling ratios of various formulations of hydrogel for optimization.

Table-4.1 Various formulations for the synthesis of CMTKG-PSA-PAM hydrogels with their Swelling ratios.

Hydrogel	Weight of CMTKG (g)	Volume of Acrylic Acid (ml)	Weight of NaOH (g)	Weight of Acrylamide (g)	KPS (g)	MBA (g)	Swelling Ratio in Distilled Water
HG-1	0.4	8.00	4.0	0.1	0.1	0.25	98
HG-2	0.4	8.00	4.0	0.2	0.1	0.1	101
HG-3	0.4	8.00	4.0	0.4	0.1	0.1	105
HG-4	0.4	8.00	4.0	0.1	0.1	0.1	164
HG-5	0.4	8.00	4.0	0.1	0.1	0.05	189
HG-6	0.1	8.00	4.0	0.1	0.1	0.1	119
HG-7	0.2	8.00	4.0	0.1	0.1	0.1	123
HG-8	0.3	8.00	4.0	0.4	0.1	0.1	107

HG-9	0.4	8.00	4.0	0.1	0.2	0.1	171
HG-10	0.4	8.00	4.0	0.1	0.4	0.1	169

The dried CMTKG-PSA-PAM hydrogel pellets were accurately weighed and kept in distilled water at room temperature 25℃, in pH solutions of 2.5, 4.2, 6.35, 9, and 12; and in 0.9% salt solutions of NaCl, $MgCl_2$, $AlCl_3$. After a regular time, interval, the weight of the hydrogel was recorded after the removal of surface water until a little decrease in weight is noted. The equilibrium swelling ratio (ESR) was calculated by the **Equation. 4.1.** [7]:

$$\text{Equilibrium Swelling Ratio (ESR)} = \frac{W_E - W_D}{W_D} \quad \textbf{(Eq. 4.1.)}$$

Where, ESR = Equilibrium Swelling Ratio

W_E = Weight of the Hydrogel at equilibrium swelling

W_D = Weight of the dehydrated Hydrogel

The ESR was recorded thrice with concordance.

4.2.4. Characterization of CMTKG-PSA-PAM hydrogel

4.2.4.1. Fourier Transform Infrared Spectroscopy (FTIR)

The CMTKG-PSA-PAM hydrogel was characterized by the FTIR Spectroscopy characterization technique, using a PerkinElmer FTIR Spectrophotometer (Model: Spectrum RX-1) in the range of 400-4000cm^{-1}.

4.2.4.2. Thermal Gravimetric Analysis (TGA)

Thermo-gravimetric analysis (TGA) was done for the optimized hydrogel, employing a Perkin Elmer TGA, having a nitrogen (N_2) atmosphere and temperature ranging from 25℃ to 900℃ with 10℃ /min of uniform heating rate.

4.2.4.3. Scanning Electron Microscopy (SEM)

The SEM analysis was performed to understand the surface morphology of the fabricated CMTKG-PSA-PAM hydrogel (Model: JEOL JSM-6610LV).

4.3. Results and Discussions

4.3.1. Mechanism of the synthesis of CMTKG-PSA-PAM hydrogel

The CMTKG-PSA-PAM hydrogel was synthesized by way of free radical polymerization of CMTKG, sodium acrylate and acrylamide, KPS as an initiator and MBA as a crosslinker. The persulphate radical generated by the decomposition of the KPS initiator engenders active radical sites by abstracting hydrogen from the -OH group of CMTKG and from the unsaturated double bond of sodium acrylate or acrylamide to generate CMTKG macro radicals. Cross-linking leads to gel formation. The suggested mechanism is depicted in **Figure. 4.2**. and complete lay-out of the procedure is shown in **Figure. 4.3.** As earlier reported (Table-4.1), 10 different formulations of hydrogels were synthesized by varying the concentrations of biopolymer, acrylamide, and crosslinker, followed by optimization based upon the swelling assessment.

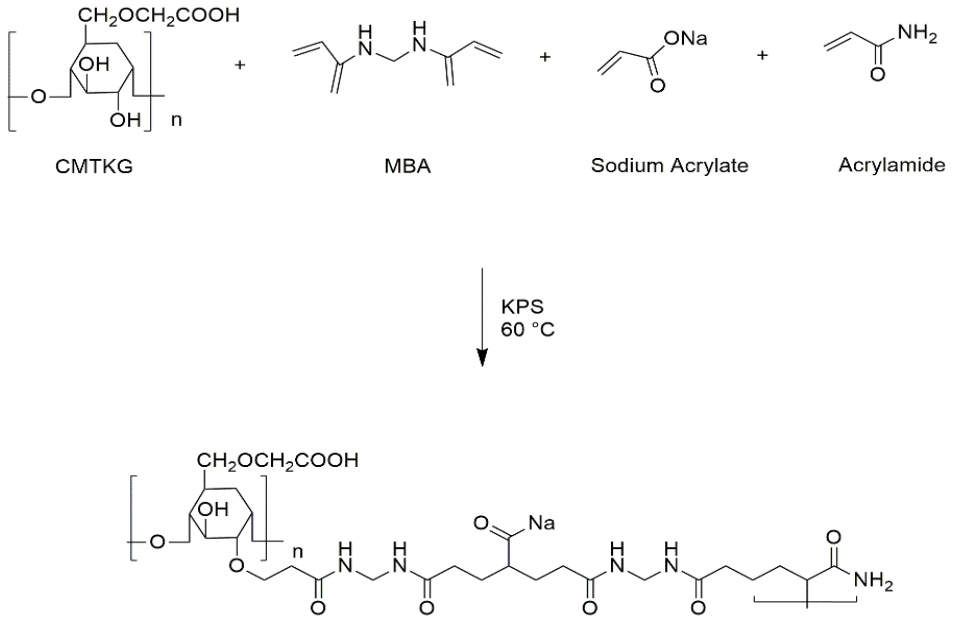

Figure 4.2. Mechanism of Synthesis of CMTKG-PSA-PAM Hydrogel

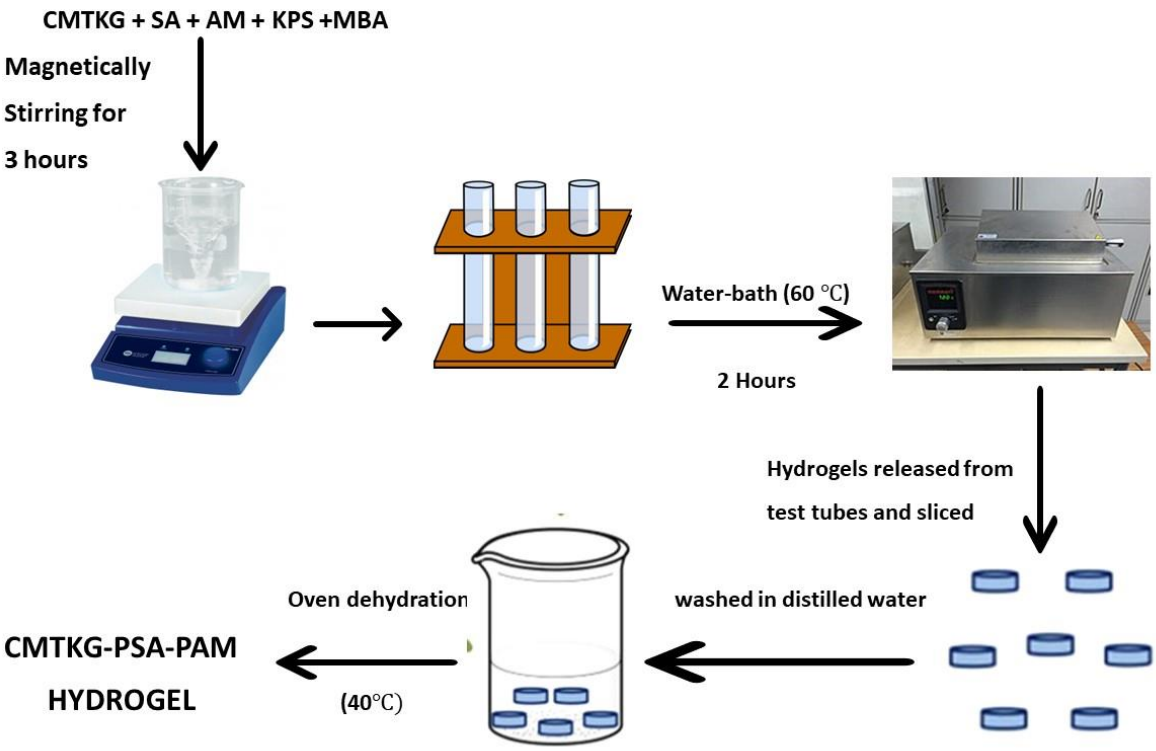

Figure. 4.3. Lay-out of Synthesis of CMTKG-PSA-PAM Hydrogel

4.3.2. Effect of Biopolymer

The swelling ratio was observed by the variance in the concentration of biopolymer and keeping all other constraints (viz. concentration of initiator and concentration of crosslinking agent etc.) constant. It was observed that when the concentration of biopolymer is increased [8], the swelling ratio also increases as can be depicted in **Figure. 4.4**. This can be explained as the concentration of biopolymer is increased from 0.1 to 0.4 g /10 ml of water, there is an increase in the number of hydrophilic groups leading to increased repulsion owing to the same charges, thereby creating more spaces for the more water molecules to be diffused inside.

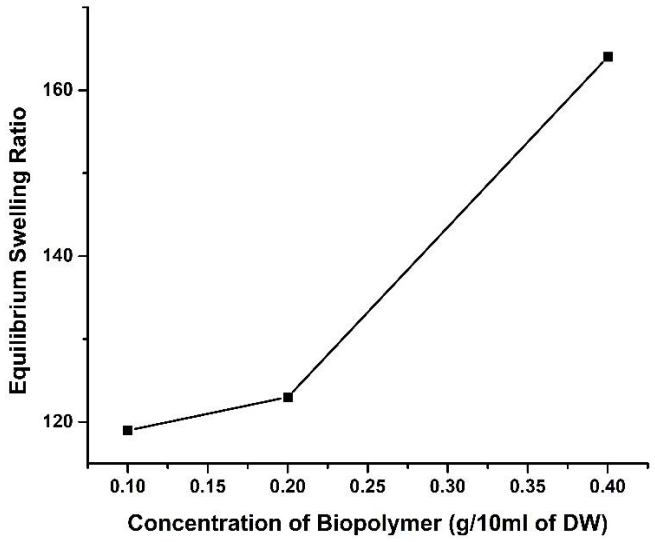

Figure. 4.4. Effect of Biopolymer on Swelling Ratio

4.3.3. Effect of cross-linking agent

Cross-linking density is a critical attribute for the observed swelling ratios of CMTKG-PSA-PAM hydrogels. It follows Flory's - Rehner theory [9][10], as can be inferred from **Figure. 4.5.** More hydrodynamic 3-dimensional free volume persists at lower cross-linking densities as the network is loose-fitting, resulting in the higher holding of water molecules and higher

swelling. Retaining other reaction parameters the same, as the concentration of cross-linker-MBA was increased from 0.05g to 0.25g, the swelling ratios showed a substantial decrease as expected due to an upsurge in cross-linking density [11, 12].

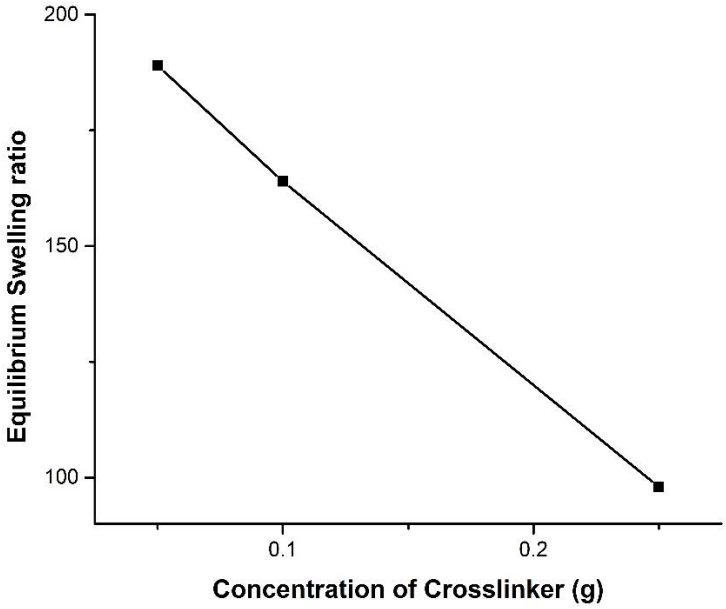

Figure. 4.5. Effect of Crosslinker on Swelling Ratio

4.3.4. Effect of Initiator

It was monitored that when the concentration of initiator - potassium persulfate (KPS), was augmented from 0.1g to 0.2g, maintaining the constancy of other reaction constraints, the swelling ratios revealed a linear increase [13] as inferred from **Figure. 4.6**. An increase in swelling ratio by 4.3 % was observed for hydrogel when the concentration of the initiator was increased from 0.1 g to 0.2 g. But, with a subsequent increase in the concentration of the initiator (0.3 g), the swelling ratio decreases. An apparent explanation is that on increasing the concentration of the initiator, the concentration of free radicals increases. This increases the

probability of a reaction between the free radicals themselves, acting as scavengers and inhibiting the formation of free radicals to initiate the reaction [14, 15].

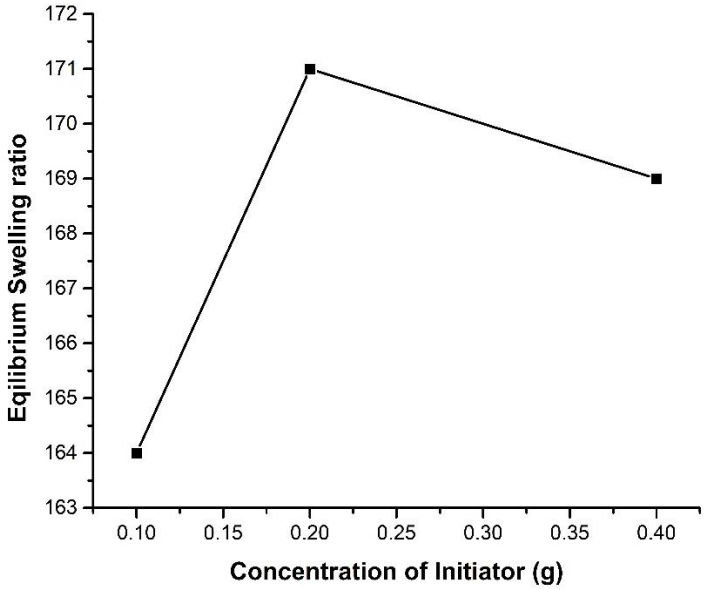

Figure 4.6. Effect of Initiator on Swelling Ratio

4.3.5. Characterization

4.3.5.1.FTIR Spectroscopy

The FTIR Spectra of CMTKG **(Figure.4.8.)** show a characteristic peak at 3296 cm^{-1} owing to -OH vibrations. The peaks at 2925 cm^{-1} and 2850 cm^{-1} are owing to -CH stretching vibrations[16, 17]. The symmetric and asymmetric stretch of $–COO^-$ moiety appears at 1403 cm^{-1} and 1598 cm^{-1} respectively. Further, the peaks at 1111 cm^{-1} and 1015 cm^{-1} are due to -C-O stretching vibrations of an alcoholic group [18]. The FTIR Spectra of CMTKG-PSA-PAM **(Figure. 4.7.),** show an intense peak at 3306 cm^{-1} for -OH vibrations because of intense hydrogen bonding in it. The peaks at 2950 cm^{-1} and 2360 cm^{-1} are assigned to -CH stretching vibrations and peaks at 1173 cm^{-1} and 1042 cm^{-1} are of -C-O stretching vibrations of the alcoholic group. The peaks at 1412 cm^{-1} and

1563 cm^{-1} are owing to the symmetric and asymmetric stretch of $-COO^-$ moiety. The peak at 1740 may be appearing because of some of the unsubstituted -COOH groups.

Further, the -NH stretch observed at 3304 cm^{-1} in MBA Spectra [19] and at 3535 cm^{-1} (asymmetric stretch), and 3416 cm^{-1} (symmetric stretch) in acrylamide Spectra[20] are observed at 3357 cm^{-1} in CMTKG-PSA-PAM. The peak at 1626 cm^{-1} in the FTIR Spectra of MBA is absent in CMTKG-PSA-PAM owing to polymerization. The same reason can also explain the absence of a peak at 992 cm^{-1} owing to the vinylic stretch of -CH=C<, in CMTKG-PSA-PAM FTIR Spectra. The intense peaks at 669 cm^{-1} and 1315 cm^{-1} are attributed to the O=C-N and C-N stretch of MBA skeleton.

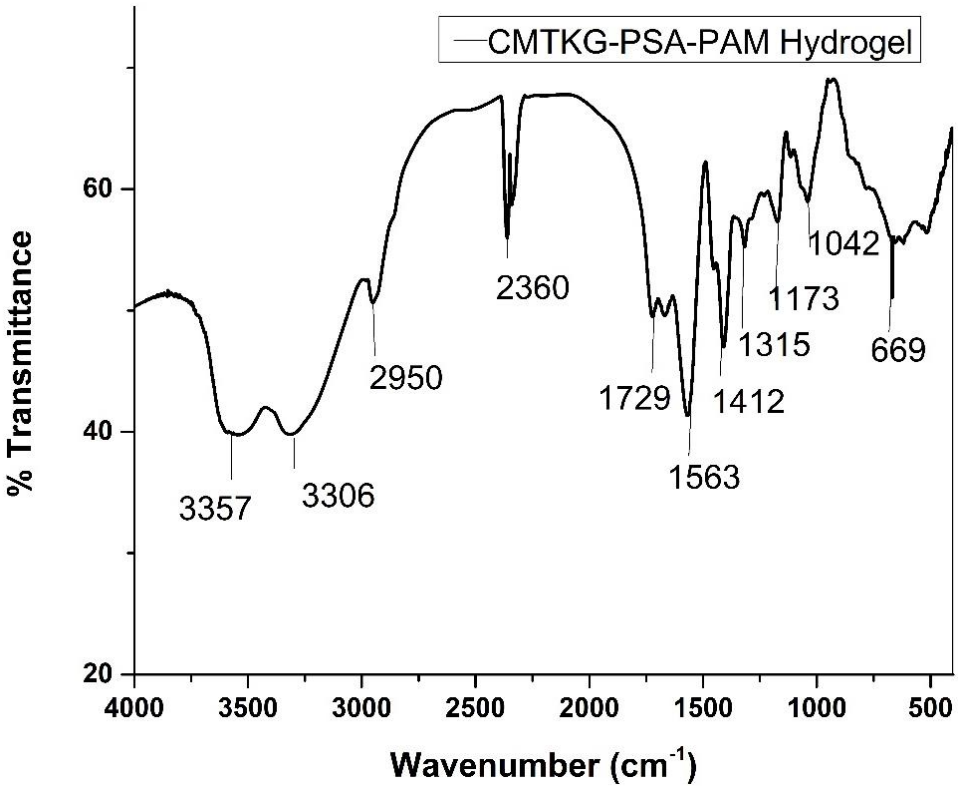

Figure 4.7. FTIR Spectra of CMTKG-PSA-PAM hydrogel

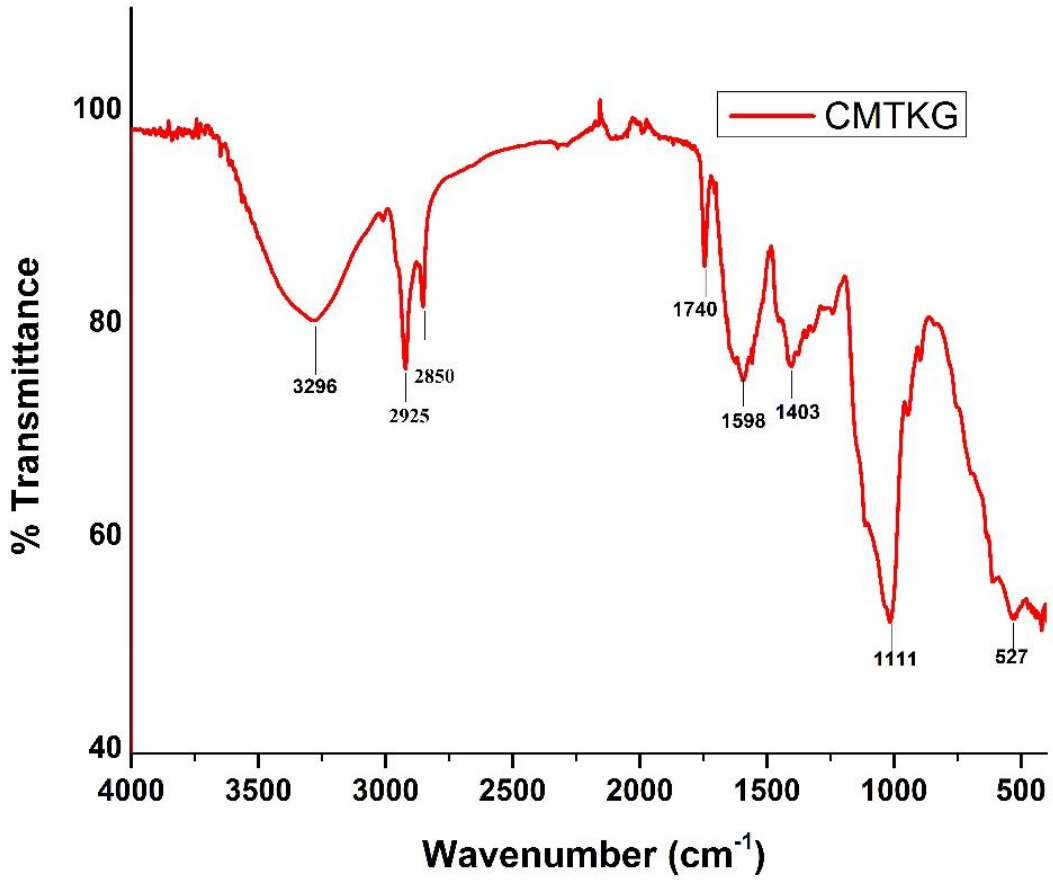

Figure 4.8. FTIR Spectra of CMTKG

4.3.5.2.Thermal Gravimetric Analysis (TGA)

The fabricated CMTKG-PSA-PAM hydrogel executed more thermal stability as compared to the starting material CMTKG. This was verified by thermal analytical studies (**Figure. 4.9. & Figure. 4.10).** As revealed, there are three different zones of weight loss. The first weight loss is attributed to the removal of water of crystallization, the second owing to the degradation of the polymeric backbone i.e., -COOH and -OH moieties, and the third due to the thermal degradation of the remains.

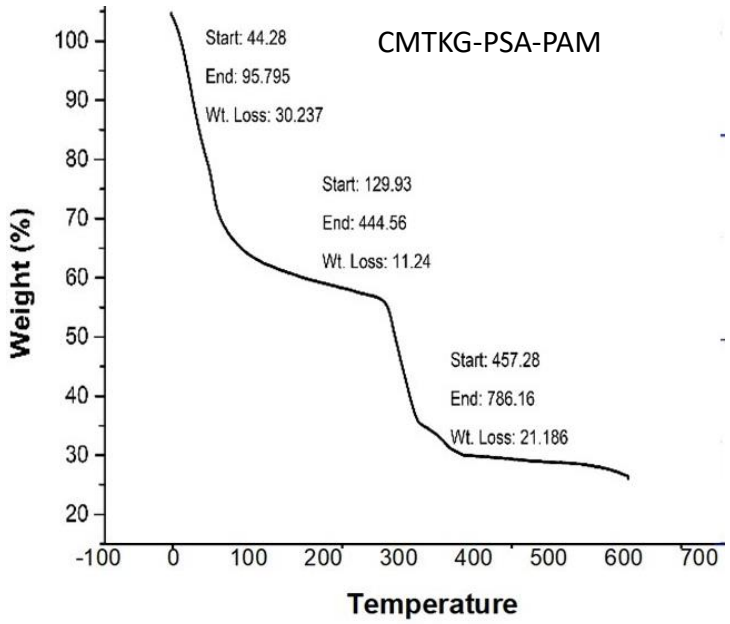

Figure 4.9. TGA curve (CMTKG-PSA-PAM)

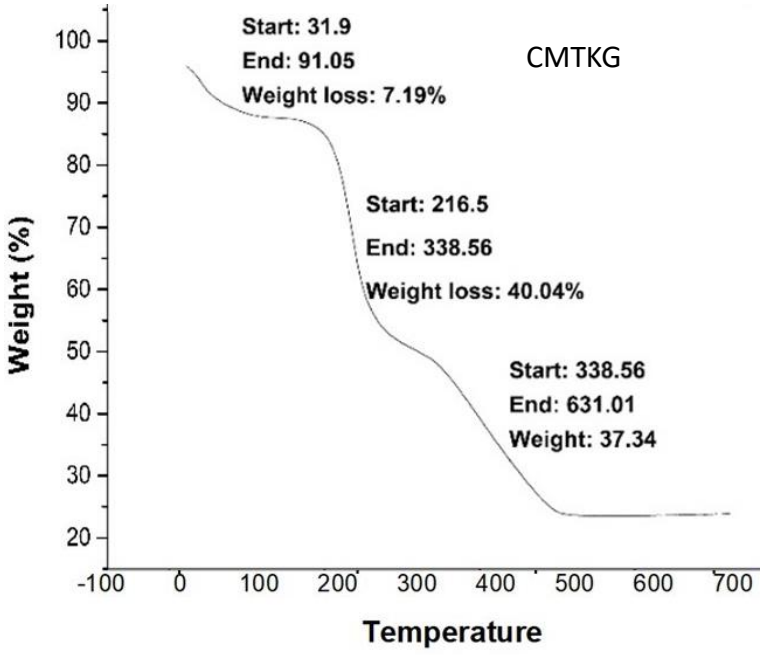

Figure 4.10. TGA curve (CMTKG)

Further in CMTKG, negligible thermal stability is maintained after the loss of water molecules while in the fabricated hydrogel thermal stability is maintained from 292.43 ℃ to 579.13 ℃ after dehydration.

4.3.5.3.**Scanning Electron Microscopy (SEM)**

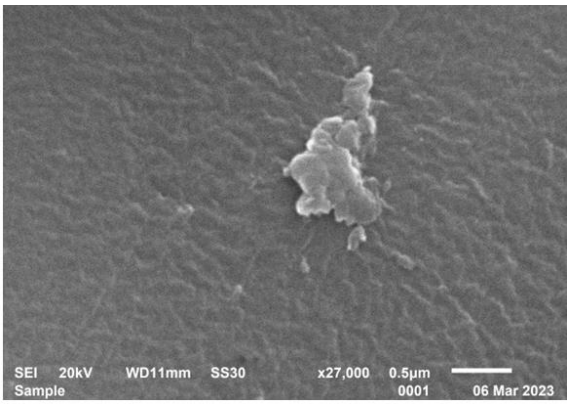

Figure 4.11. SEM studies CMTKG-PSA-PAM hydrogel

The SEM studies of CMTKG-PSA-PAM hydrogel (**Figure. 4.11.)** reveals more porous and looser framework thus accounting for more of water diffusion into the hydrogel.

4.3.6. Swelling Assessment

4.3.6.1. Effect of time

The best optimized CMTKG-PSA-PAM hydrogel showed the swelling ratio of 189 in distilled water at 23 ℃ as depicted in **Figure. 4.12.**

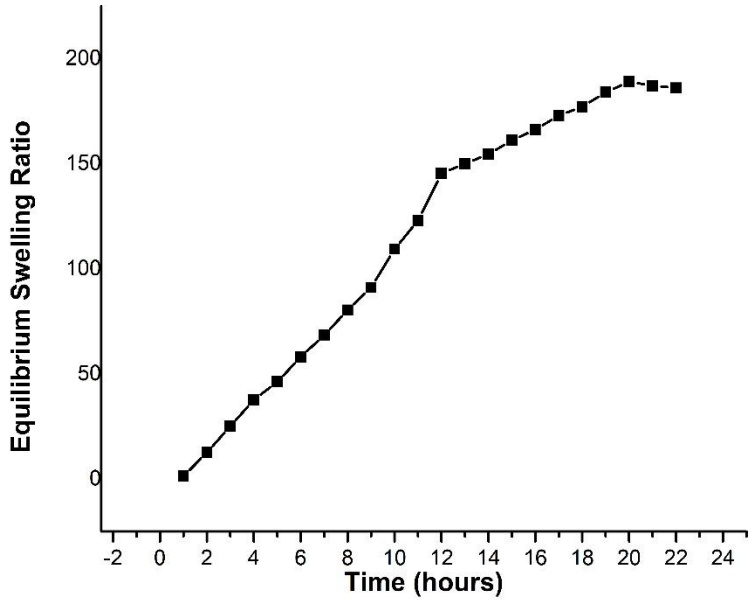

Figure. 4.12. Rate of Swelling in distilled water with time

4.3.6.2.Effect of pH

As the basicity is increased, the -COOH exists as COO^-, and more water molecules enter the hydrogel framework owing to large spaces due to repulsion between -COO^- moieties. This leads to the enhanced swelling ratio till pH 10. But, at further higher pH, the swelling ratio drops as higher Na^+ ion concentration decreased the charge density. As can be easily inferred from the graph (**Figure. 4.13**.), the observed swelling ratio is 33.29 at pH 2.5, which increased up to 249.12 at pH 9, followed by a decrease, reaching the swelling ratio of 179.61 at pH 12.

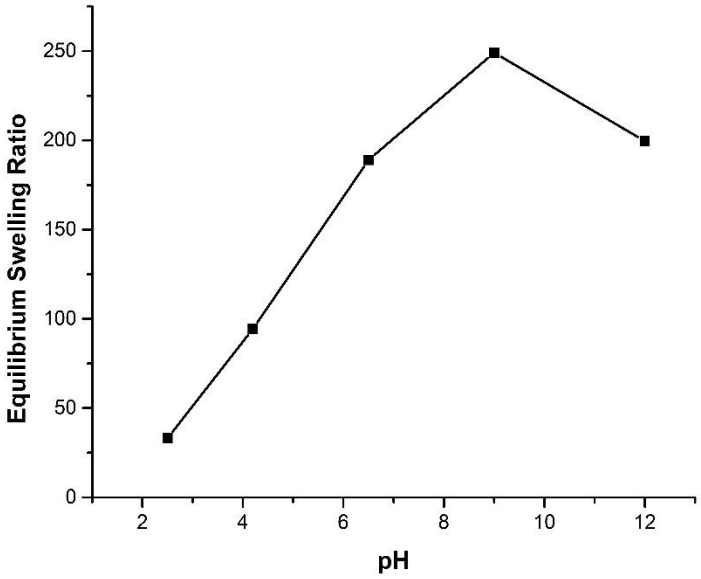

Figure 4.13. Rate of swelling at different pH

4.3.6.3.Effect of salt solutions

The swelling capacity of the CMTKG-PSA-PAM hydrogel was lower in the saline water (**Figure. 4.14.)** as compared to distilled water as expected due to the lowered charge density because of increased Na^+ ions. The water entry into the hydrogel is decreased owing to the lowering of an osmotic pressure difference between the outer saline solution and inside of hydrogel as there is more ionic concentration outside in saline solution. Further, the Swelling capacity was also observed in $MgCl_2$ and $AlCl_3$ solutions. Due to increased cationic charge, more COO^- moieties are bound, leading to steric hindrance and less mobility of water into the hydrogel. The swelling capacity order was observed to be NaCl > $MgCl_2$ > $AlCl_3$. The observed equilibrium swelling ratio of hydrogel in NaCl, $MgCl_2$ and $AlCl_3$ were 39, 36.33 and 35.86 respectively.

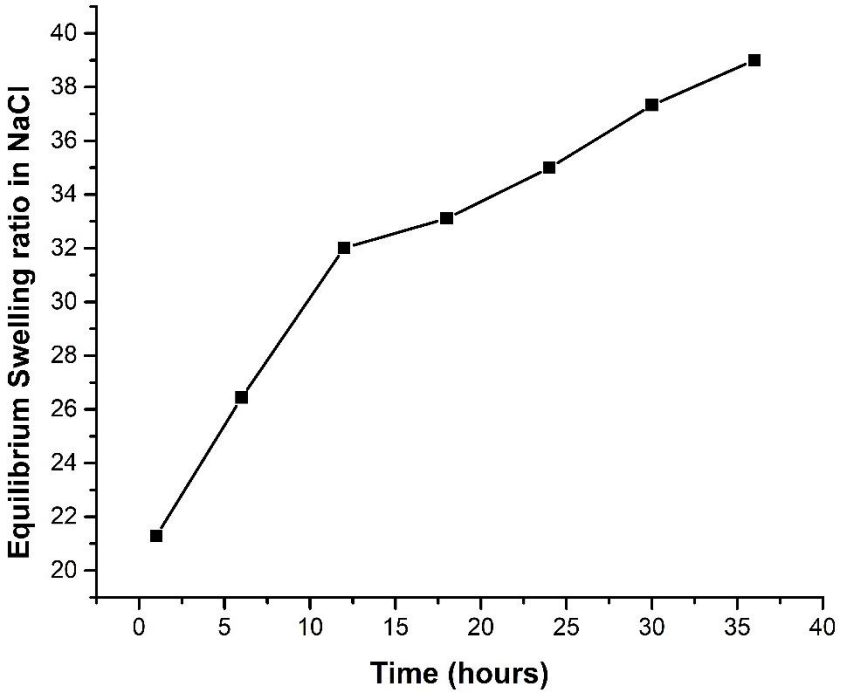

Figure. 4.14. Rate of swelling in Saline solution

4.4. Conclusions

An avant-garde organic agricultural hydrogel – CMTKG-PSA-PAM was formulated by free-radical polymerization of biopolymer: Carboxy Methyl Tamarind Kernel Gum (CMTKG) and monomers: sodium acrylate (SA) and acrylamide (AM) to explore its application to different types of soil as a soil conditioner. It was optimized based on the swelling observed in distilled water at room temperature and characterized by Fourier transforms infrared spectroscopy, scanning electron microscopy, and thermogravimetric analytical techniques. The swelling was investigated at different pH, and in different saline solutions. The formulated CMTKG-PSA-PAM hydrogel absorbed 189 ml/g of distilled water. Thus, these hydrogels based on high swelling ratio, can be successfully applied as a soil conditioner for sustainable agronomy.

References

[1] R. Malik, R. Saxena, S.W.- ChemistrySelect, undefined 2022, Biopolymer-Based Biomatrices–Organic Strategies to Combat Micronutrient Deficit for Dynamic Agronomy, Wiley Online Libr. (n.d.). https://chemistry-europe.onlinelibrary.wiley.com/doi/abs/10.1002/slct.202200006 (accessed February 11, 2023).

[2] M. Rizwan, S. Gilani, A. Durani, S.N.-J. of Advanced, undefined 2021, Materials diversity of hydrogel: Synthesis, polymerization process and soil conditioning properties in agricultural field, Elsevier. (n.d.). https://www.sciencedirect.com/science/article/pii/S2090123221000540 (accessed February 11, 2023).

[3] C. Rodrigues, Y. Oladosu, M.Y. Rafii, F. Arolu, S. Chibuike Chukwu, M. Adekunle Salisu, I. Kayode Fagbohun, T. Kolawole Muftaudeen, S. Swaray, B. Sani Haliru, Superabsorbent polymer hydrogels for sustainable agriculture: A review, Mdpi.Com. (2022). https://doi.org/10.3390/horticulturae8070605.

[4] W.A.-A.A.E.S.O. Access, undefined 2018, Impact of hydrogel polymer in agricultural sector, Epa.Hu. 1 (2030) 59–64. https://doi.org/10.30881/aaeoa.00011.

[5] J. Abedi-Koupai, F. Sohrab, G.S.-J. of plant nutrition, undefined 2008, Evaluation of hydrogel application on soil water retention characteristics, Taylor Fr. (n.d.). https://www.tandfonline.com/doi/abs/10.1080/01904160701853928 (accessed February 12, 2023).

[6] J.H. Trivedi, Synthesis, characterization, and swelling behavior of superabsorbent hydrogel from sodium salt of partially carboxymethylated tamarind kernel powder-g-PAN, J. Appl. Polym. Sci. 129 (2013) 1992–2003. https://doi.org/10.1002/APP.38910.

[7] Khushbu, S.G. Warkar, N. Thombare, Controlled release and release kinetics studies of boron through the functional formulation of carboxymethyl tamarind kernel gum-based superabsorbent hydrogel, Polym. Bull. (2021). https://doi.org/10.1007/S00289-021-03634-9.

[8] P. Goyal, V. Kumar, P.S.-C. Polymers, undefined 2007, Carboxymethylation of tamarind kernel powder, Elsevier. (n.d.). https://www.sciencedirect.com/science/article/pii/S0144861706004772 (accessed April 3, 2023).

[9] K.S. Soppimath, A.R. Kulkarni, T.M. Aminabhavi, Chemically modified polyacrylamide-g-guar gum-based crosslinked anionic microgels as pH-sensitive drug delivery systems: preparation and characterization, J. Control. Release. 75 (2001) 331–345. https://doi.org/10.1016/S0168-3659(01)00404-7.

[10] F.T. WALL, Principles of Polymer Chemistry. Paul J. Flory. Cornell Univ. Press, Ithaca, New York, 1953. 688 pp. Illus. $8.50, Science (80-.). 119 (1954) 555–556. https://doi.org/10.1126/SCIENCE.119.3095.555-A.

[11] K. Soppimath, A. Kulkarni, T.A.-J. of Controlled, undefined 2001, Chemically modified

polyacrylamide-g-guar gum-based crosslinked anionic microgels as pH-sensitive drug delivery systems: preparation and characterization, Elsevier. (n.d.). https://www.sciencedirect.com/science/article/pii/S0168365901004047 (accessed April 3, 2023).

[12] F.T. Wall, Principles of Polymer Chemistry . Paul J. Flory. Cornell Univ. Press, Ithaca, New York, 1953. 688 pp. Illus. $8.50 , Science (80-.). 119 (1954) 555–556. https://doi.org/10.1126/SCIENCE.119.3095.555.B.

[13] R. Singhal, R.S. Tomar, A.K. Nagpal, Effect of cross-linker and initiator concentration on the swelling behaviour and network parameters of superabsorbent hydrogels based on acrylamide and acrylic acid, Int. J. Plast. Technol. 2009 131. 13 (2009) 22–37. https://doi.org/10.1007/S12588-009-0004-4.

[14] E.M. Ahmed, ; Magdy, A.H. Zahran, ; Fatma, S. Aggor, ; S A Abd Elhady, S.S. Nada, Synthesis and Swelling Characterization of Carboxymethyl Cellulose-g-Poly(Acrylic acid-co-Acrylamide) Hydrogel and their Application in agricultural field, (n.d.).

[15] R. Singhal, R.S. Tomar, A.K. Nagpal, Effect of cross-linker and initiator concentration on the swelling behaviour and network parameters of superabsorbent hydrogels based on acrylamide and acrylic acid, Int. J. Plast. Technol. 13 (2009) 22–37. https://doi.org/10.1007/S12588-009-0004-4.

[16] S. Jana, R. Sharma, S. Maiti, K.S.-I. journal of biological, undefined 2016, Interpenetrating hydrogels of O-carboxymethyl Tamarind gum and alginate for monitoring delivery of acyclovir, Elsevier. (n.d.). https://www.sciencedirect.com/science/article/pii/S0141813016311461 (accessed April 2, 2023).

[17] R. V. Kulkarni, V. V. Baraskar, V. V. Alange, A.A. Naikawadi, B. Sa, Controlled Release of an Antihypertensive Drug through Interpenetrating Polymer Network Hydrogel Tablets of Tamarind Seed Polysaccharide and Sodium Alginate, J. Macromol. Sci. Part B. 52 (2013) 1636–1650. https://doi.org/10.1080/00222348.2013.789327.

[18] S. Sanyasi, A. Kumar, C. Goswami, A. Bandyopadhyay, L. Goswami, A carboxy methyl tamarind polysaccharide matrix for adhesion and growth of osteoclast-precursor cells, Elsevier. 101 (2014) 1033–1042. https://doi.org/10.1016/j.carbpol.2013.10.047.

[19] D. Handayani, P. Rahayu, M.F.-J. of P. Science, undefined 2019, Synthesis and Characterisation of Copoly-(Eugenol-N, N'-Methylene Bis (Acrylamide))., Jps.Usm.My. 30 (2019) 87–100. https://doi.org/10.21315/jps2019.30.3.6.

[20] N.J.-J. of M. Spectroscopy, undefined 1961, The infrared and Raman spectra and structure of acrylamide, Elsevier. (n.d.). https://www.sciencedirect.com/science/article/pii/0022285261902430 (accessed February 13, 2023).

Chapter-5

AGRONOMICAL EVALUATION OF CARBOXYMETHYL TAMARIND KERNEL GUM-POLY SODIUM ACRYLATE-POLY ACRYLAMIDE (CMTKG-PSA-PAM) HYDROGEL, AS SOIL-WATER CONDITIONER IN DIFFERENT TYPES OF SOILS

5.1.Introduction

Agronomy inexorably contributes an eminent role in food nutriment and the economic upswing of a country. Proper Irrigation or watering is vital for the growth, health, and higher yields of the crops. Water supplementation at a controlled rate in an economical and ecofriendly way is the major challenge an agro-researcher must deal with. The potential of scientific research entails the usage of natural, renewable, and abundant raw materials that endow a solution to the agronomical challenges of today's world. Besides being non-hazardous, CMTKG-based matrices are pertinent materials that act as a reservoir of water and are a boon for agronomy. This research explores the synthesis of CMTKG-based hydrogels to be applied as soil water conditioner in all the four types of soils viz. clay soil, silty soil, loamy soil, and sandy soil **(Figure.5.1.)** These green polymeric hydrogels augmented the maximum water holding capacity of the soil, boosted water retention by the soil and up-leveled available water content of the soil, resulting in enhanced growth, high crop yield, and sustainability.

For agronomical application as a soil-conditioner, the different hydro physical attributes of the soil were assessed by amending the different types of soil with CMTKG-PSA-PAM viz. water retention, available water content (AWC), maximum water holding capacity (MWHC), porosity, particle density, bulk density, employing different relevant procedures.[1].

Figure. 5.1. Types of Soils

5.2.**Experimental Procedure**

5.2.1. Materials

The procedure of synthesis of CMTKG-PSA-PAM hydrogel has already been discussed in Chapter 4. The different types of soils were collected from Indian Agricultural Research Institute.

5.2.2. Maximum Water Holding Capacity (MWHC)

The twelve soil samples were amended with 0.1% & 0.3% of CMTKG-PSA-PAM hydrogel along with the controlled soil sample (clay, silty, loamy and sandy soil) to analyze the effect of CMTKG-PSA-PAM hydrogel on different types of soil. Pre-weighed equal quantities of all the soil samples were put into plastic beakers and dispersed in water tubs to allow maximum diffusion of water into the CMTKG-PSA-PAM hydrogel. After 12 hours, hydrogel pellets were taken out and after gravitational drainage of extra water, were weighed again. The total water absorbed was calculated as follows [2]:

MWHC = [(Weight of beaker post water absorption) – (weight of the dried soil + weight of empty beaker + weight of wet filter paper)]

5.2.3. Soil Density and Porosity

The particle density (PD) [1] and the bulk density (BD) [3] were calculated of dried 0.3% CMTKG-PSA-PAM hydrogel amended different types of soil by employing standard methods. The soil samples were dried till weight constancy and sieved through 2 mm sieve pre-experimentation [4]. Further, the porosity was also calculated by:

Porosity (%) = [1 - $\frac{BD}{PD}$] X 100

Where BD = Bulk density

PD = Particle density

5.2.4. Water Retention Capacity (WRC) by Plantation method

Water Retention capacity was evaluated by planting the chickpea seeds in water stress conditions in 0.1% CMTKG-PSA-PAM hydrogel amended different types of soil by recording the days of survival maintaining the constancy of amount of soil, water, and environmental conditions. The experiment was repeated thrice.

5.2.5. Available water content (AWC) using Pressure plate apparatus.

Pressure plate apparatus (Model: 1600 pressure extractor, Santabarbara, CA, USA) was used to investigate the effects of CMTKG-PSA-PAM hydrogel on the water retention capacity in the four types of soils at matric tensions of 0.33 bar and 15 bar, which is parallel to the field capacity and permanent wilting point respectively. The four types of soils amended with 0.1% and 0.3% of CMTKG-PSA-PAM hydrogel along with respective blank samples were settled at a time, in rubber rings arranged on ceramic plates. The soil was saturated with water for twelve hours, followed by the application of pressure at different matric tensions in a pressure chamber, till the water flow

from the soil ended completely. The soil samples were weighed accurately, followed by oven-dryness (100℃ for twelve hours), cooled, and reweighed. The percentage of water content (WC) was calculated as follows [5]:

$$\text{WC (\% w/w)} = \frac{Swet - Sdry}{Sdry} \text{ X } 100$$

Where WC = Water content of the soil on a weight basis

S_{wet} = Weight of the wet soil at specific matric tension

S_{dry} = Weight of the dried soil

Available water content (AWC)

AWC is the water accessible to the plants for growth and is calculated, by subtracting the water content retained at 15 matric tensions from the water content retained at 0.33 bar matric tension corresponding to permanent wilting point and field capacity respectively, as follows:

AWC= WC at 0.33 at matric tension – WC at 15 bar matric tension

5.2.6. Bio-degradation Studies

The Soil burial method [6-9] was employed to know about the rate of biodegradation of CMTKG-PSA-PAM hydrogel. The studies were carried out for about 60 days. The dried and pre-weighed Hydrogel was buried 5-6 cm deep into the well-watered soils in four different pots. After intervals of 15 days, 30 days, 45 days and 60 days, the hydrogel was taken out, removed off the soil, dried and weighed again. The residual dry content (RDC) percentage was calculated using the formula:

$$\text{RDC \%} = \frac{\text{Weight of the dry content of hydrogel X 100}}{\text{Weight of initial dry content of the hydrogel}}$$

The results were verified by SEM studies which recorded the changes in surface morphology.

5.3. Results and Discussion

5.3.1. Effect of hydrogel on Maximum Water Holding Capacity (MWHC) of different types of soils

The MWHC of different soil samples were determined by saturating them with water and removing gravimetrically excess of water without applying any external pressure. The different samples having different types of soil with varied concentration of CMTKG-PSA-PAM were analyzed for MWHC. Further, the following order was observed of MWHC for different samples of soils as can be inferred from **Figure. 5.2.** to **Figure. 5.5.**, depicting the variation of MWHC of clay, silty, loamy, and sandy soil with the concentration of CMTKG-PSA-PAM hydrogel respectively:

- Control sample: Clay (38.1117 g) > Silty (33.7245 g) > Loamy (29.321 g) > Sandy (28.1231 g).
- 0.1% hydrogel amended soil: Clay (49.8417 g) > Sandy (43.0731 g) > Silty (38.1345 g) > Loamy (31.961 g).
- 0.3% hydrogel amended soil: Sandy (69.979 g) > Loamy (56.6643 g) > Silty (32.1423 g) > Clay (30.005 g).

➢ In 0.1% amended soil, increase in MWHC in Sandy soil was 43%, Clay soil: 31%, Silty soil: 29% & Loamy soil: 9%, and: increase in MWHC in 0.3% amended Clay soil was 29%, silty soil: 15%, sandy soil: 56% and loamy soil: 26%. This is illustrated with respect to the control sample **Figure. 5.6.). Table. 5.1.** depicts the % increase in MWHC of different types of soils in relation to the respective control soil.

- The MWHC increased in sandy and loamy soils as their porosity is high, resulting in availability of space for the CMTKG-PSA-PAM hydrogel to swell maximum to its capacity. So, these soils show a linear increase in MWHC with increase in concentration of hydrogel. Whereas in clay and silty soil, the MWHC first increases when the concentration is increased to 0.1%, but further decreases when the concentration is increased to 0.3%. This can be explained as the soil becomes compact due to lower porosity of these soils. So, CMTKG-PSA-PAM hydrogel does not have enough space to swell. In case, it swells, the pressure from the soil particles forces the water to exit the hydrogel, resulting in surface run-off [8]. In general, MWHC increases with amendment with CMTKG-PSA-PAM hydrogel [9]. The effect of CMTKG-PSA-PAM hydrogel on MWHC of clay, silty, loamy, and sandy soil is displayed in **Figure. 5.2., Figure. 5.3., Figure. 5.4.,** and **Figure. 5.5.**

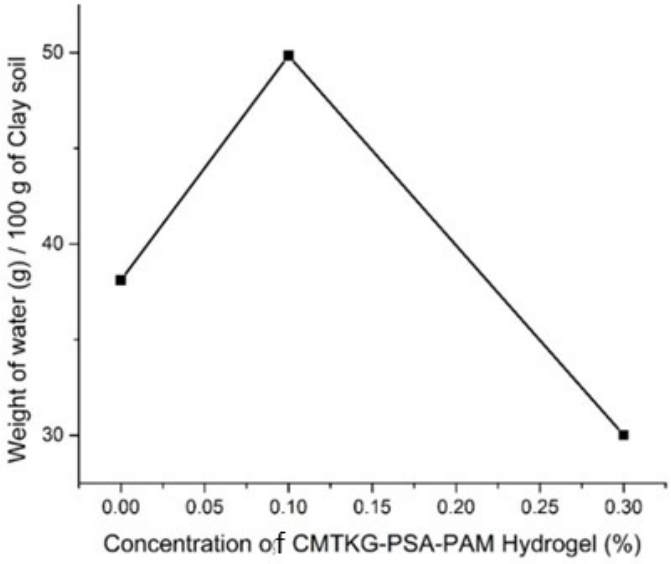

Figure 5.2. Effect of CMTKG-PSA-PAM Hydrogel on MWHC of Clay soil

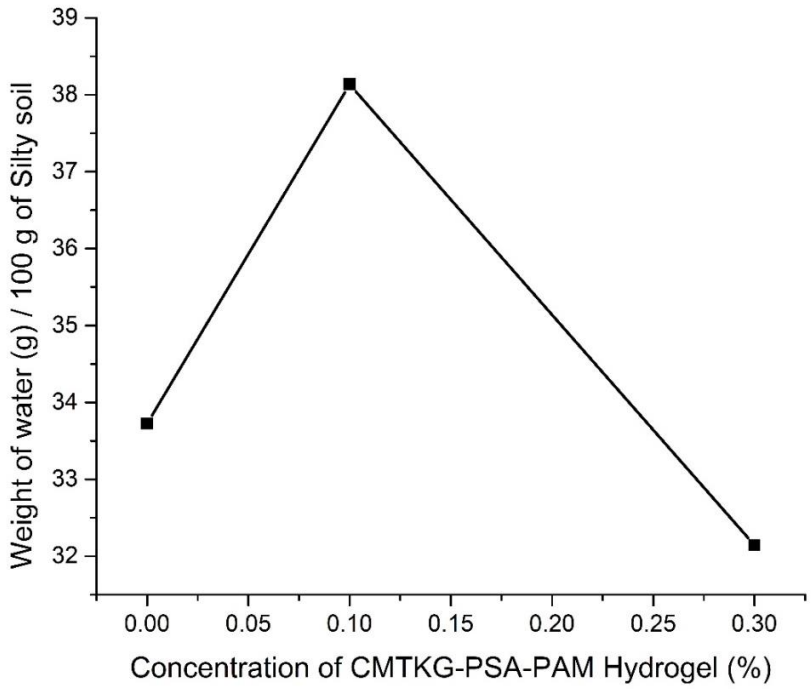

Figure 5.3. Effect of CMTKG-PSA-PAM Hydrogel on MWHC of Silty soil

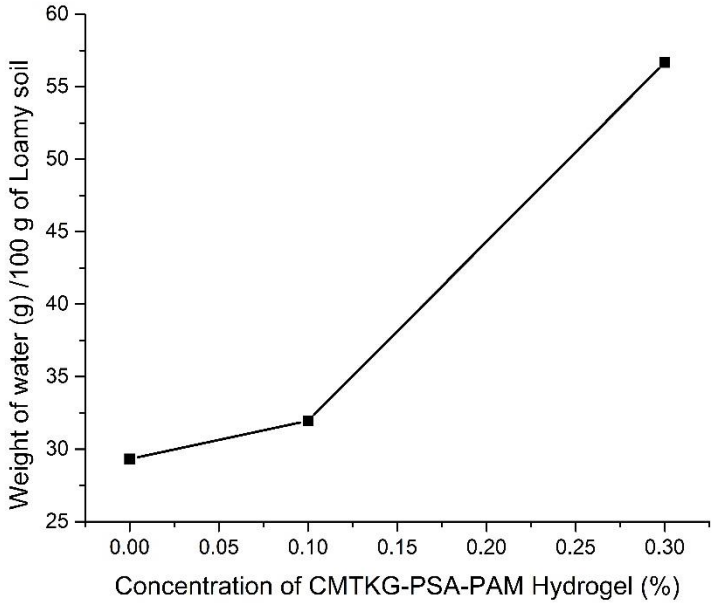

Figure 5.4. Effect of CMTKG-PSA-PAM Hydrogel on MWHC of Loamy soil

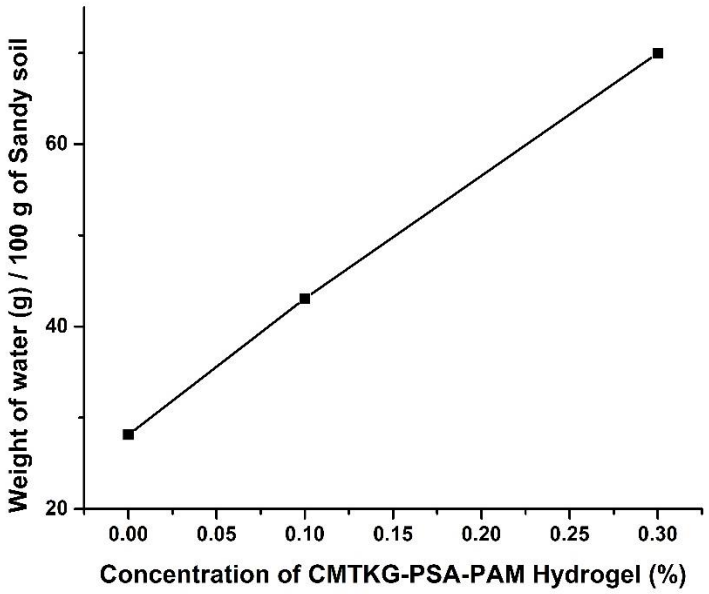

Figure 5.5. Effect of CMTKG-PSA-PAM Hydrogel on MWHC of Sandy soil

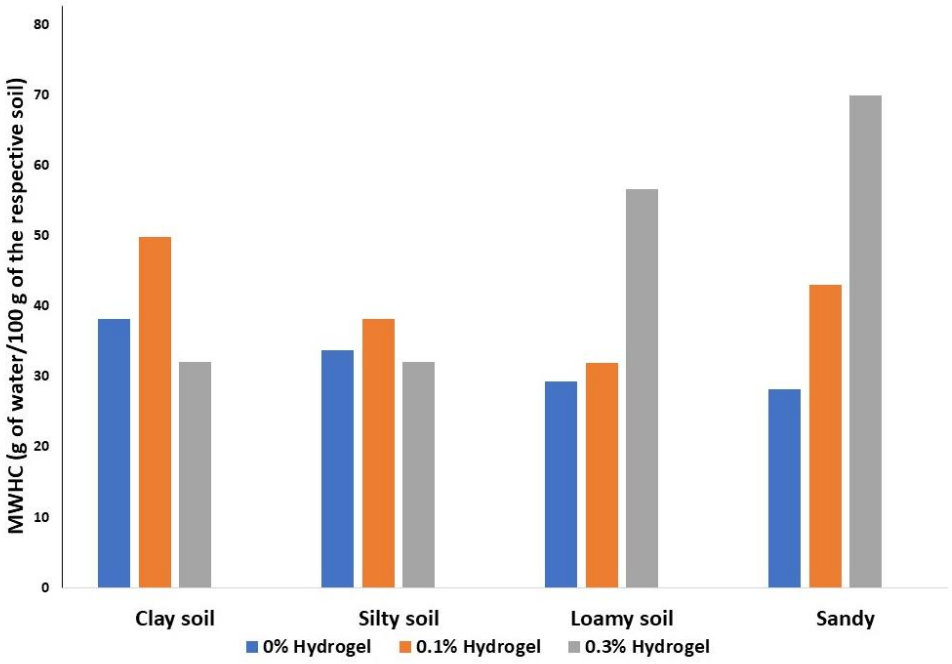

Figure 5.6. MHWC of different soil samples with different concentration of CMTKG-PSA-PAM Hydrogel

Table. 5.1. % Increase in MWHC in CMTKG-PSA-PAM hydrogel amended soils in comparison to the control soil.

Type of Soil	0.1% hydrogel	0.3% hydrogel
Clay	31%	29%
Silty	29%	15%
Loamy	9%	26%
Sandy	43%	56%

5.3.2. Effect of hydrogel Soil Density and Porosity of different types of soils

Particle density was determined by employing Pycnometer due to high accuracy achieved as excess water can be easily removed due to capillary opening in the ground glass stopper. It was calculated by applying the formula:

$$\text{Particle density (PD)}, \rho_p = \rho_w \frac{(W_s - W_a)}{(W_s - W_a) - (W_{sa} - W_w)} \quad \textbf{Eq (7)}$$

Where , ρ_p = Particle density of the soil

W_a = Weight of oven-dried Pycnometer

W_s = Weight of Pycnometer plus soil sample

W_{sa} = Weight Pycnometer plus soil sample plus water

W_w = Weight of Pycnometer plus water at room temperature

ρ_w = Density of water at room temperature

The particle density of the different soil samples was observed to be Clay soil: 2.895 g cm^{-3}, Silty: 2.791 g cm^{-3}, Loamy: 2.713 g cm^{-3}, Sandy: 2.634 g cm^{-3}.

Bulk density (BD) of various types of the soils was calculated following the standard procedure [30] and are enlisted in the **Table. 5.2**. 0.3% hydrogel amendment of clay, silty, loamy, and sandy soils revealed decrease in bulk density by 1.7%, 5.3 %, 10% and 13% respectively. [10]. The bulk density includes the density of the air, the organic content whatsoever is mixed with the soil along with the soil particle density. So, with the incorporation of CMTKG-PSA-PAM hydrogel which has hydrophilic moieties in them, acting as humus and hence organic content, increases the bulk density of the soil [11]. These observations can easily be inferred from **Table. 5.2. and Figure. 5.7.**

Table. 5.2. Bulk Density and Porosity of Different types of soils (Control Samples and Hydrogel amended soil samples)

Type of Soil	Bulk Density (g cm^{-3})		Porosity	
	Control Sample	0.3% Hydrogel amended Sample	Control Sample	0.3% Hydrogel amended Sample
Clay	1.17	1.19	62	58.9
Silty	1.33	1.40	53	49.8
Loamy	1.45	1.6	48.4	41.0
Sandy	1.68	1.9	39.3	27.9

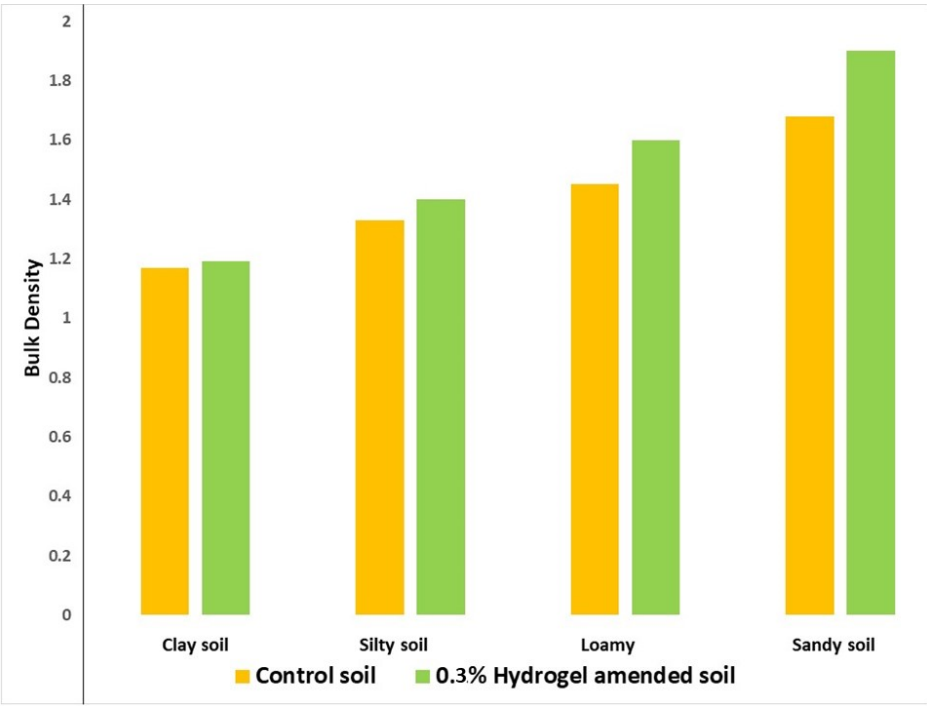

Figure. 5.7. Effect of CMTKG-PSA-PAM hydrogel on bulk density of different types of soils

Porosity on soil amendment with Hydrogel decreases as hydrogel occupies the pore spaces in between the soil particles. And the effect is more pronounced in sandy soils, following the order Sandy (29%) > Loamy (15.2%) > Silty 6 (%) > Clay (5.9 %) [12] **(Figure. 5.8.)**

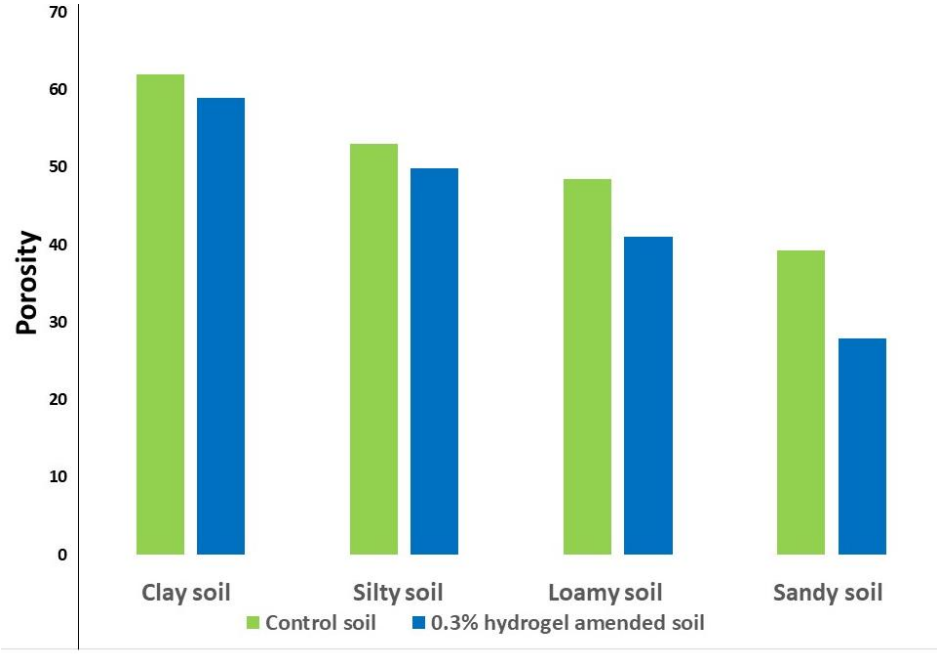

Figure. 5.8. Effect of CMTKG-PSA-PAM hydrogel on porosity of different types of soils

As the CMTKG-PSA-PAM hydrogel has been incorporated into the soils, it occupies the pores present in the soil, thus decreasing the porosity number of the soils. The same can be inferred from the results depicted in **Table. 5.2. and Figure. 5.8.**

5.3.3. Effect of hydrogel on Water Retention capacity (WRC) on different types of soils by plantation method

The effect of application of CMTKG-PSA-PAM hydrogel on water retention capacity of different types of soils was analyzed by planting fenugreek seeds in them. About nine samples of soil (2.5 kg) were prepared: Clay control sample, 0.1% amended clay soil, Silty Control sample, 0.1% amended silty soil, Loamy Control sample, 0.1% amended loamy soil, Sandy Control sample, 0.1% amended sandy soil and 0.5% amended sandy soil. With 450 ml of water, 10 healthy fenugreek seeds were planted in all the samples of the soils in the pots. All the pots were subjected to similar conditions of the environment. The day wilting occurred was noted down. It was

concluded from the studies that wilting was delayed in sandy soil for about 21 days by just applying 0.1% of the novel fabricated CMTKG-PSA-PAM hydrogel. The outcomes can be easily inferred from the **Figure. 5.9.** The water retention capacity of the different soil samples followed the order: Sandy (0.5%) > Clay (0.1%) > Silty (0.1%) > Clay (control sample) > Sandy (0.1%) > Silty (Control sample) > Loamy (0.1%) > Loamy (Control sample) > Sandy (Control sample).

The CMTKG-PSA-PAM amendment of the soil introduced hydrophilic moieties into the soil which can retain the water into them, resulting in higher water retention as compared to control soil. Further, the more porous the soil is, more space hydrogel has to swell, leading to higher retention of water. The order observed in terms of number of days the plant survived is directly related to the porosity of the soil sample and hence water retention. The **Figure. 5.9.** displays the day the sapling wilted in different types of control and CMTKG-PSA-PAM amended soils. It is clear from **Table. 5.3.** with the application of hydrogel, there is lengthening of survival period in terms of days in every type of soil. The lengthening of survival period is more pronounced in the sandy soil, following the order: sandy > clay > silty > loamy.

Figure. 5.9. Effect of CMTKG-PSA-PAM Hydrogel on water retention capacity of different types of soil sample by plantation method.

Table. 5.3. Wilting day of the sapling in different types of soil

Type of soil	Control Soil	0.1% Hydrogel amended soil	Lengthening of survival period in no. of days
Clay	29^{th}	40^{th}	11
Silty	26^{th}	40^{th}	10
Loamy	17^{th}	25^{th}	8
Sandy	27^{th}	44^{th}	14

5.3.4. Effect of hydrogel on available water content (AWC) of different types of soils by pressure-plate apparatus

Available water content is the critical attribute of the soil in deciding its agronomical applications. More available water content of the soil is reflected in enhanced growth of the crops [13]. The fabricated Hydrogel was applied to different types of the soil; Loamy, sandy loam, silty loam, clay loam and AWC was measured employing pressure-plate apparatus. The different soil samples along with the control sample were subjected to 0.33 Bar matric suction and 15 Bar matric suction, corresponding to field capacity and permanent wilting point, to assess AWC[14] .

It was observed that the order of AWC of control sample followed the order: Clay > Silty > Loamy > Sandy. It's observed that hydrogel amendment to the sandy soil yields positive and enhanced

results for plant growth [6, 7]. The results are summarized in **Table.5.4., Table. 5.5. and Figure. 5. 10.**

Table. 5.4. Percentage Increase in Available Water Content on Increasing the concentration of hydrogel in different types of soils.

Soil Sample	**Water content at 0.33 Bar matric suction (Field capacity)**	**Water content at 15 Bar matric suction (Permanent Wilting point)**	**Available Water Content (%)**
Clay Control Sample	21.304	6.788	14.516
Clay 0.1% Hydrogel	32.231	15.715	16.516
Clay 0.3% Hydrogel	58.429	48.069	10.36
Silty Control Sample	24.982	15.326	9.659
Silty 0.1% Hydrogel	38.144	22.694	15.45
Silty 0.3% Hydrogel	42.831	33.414	9.417
Loamy Control Sample	20.226	13.028	7.198
Loamy 0.1% Hydrogel	30.229	20.813	9.416
Loamy 0.3% Hydrogel	43.411	28.471	14.94
Sandy Control Sample	15.285	9.91	5.375
Sandy 0.1% Hydrogel	25.809	15.302	10.777
Sandy 0.3% Hydrogel	51.504	32.484	19.02

Table. 5.5. % Increase in AWC in comparison to control soil

TYPE OF SOIL	0.1% AMENDED SOIL	0.3% AMENDED SOIL
CLAY	17.52%	9.163
SILTY	13.45%	9.417
LAOMY	9.416	14.94
SANDY	10.575	19.02

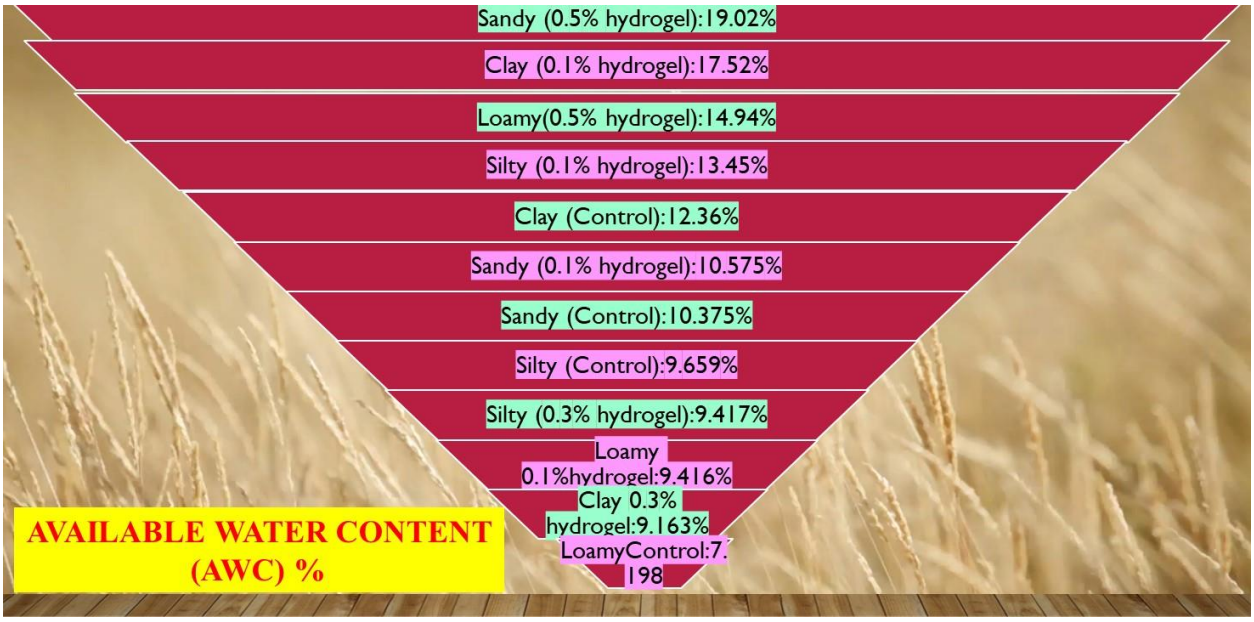

Figure. 5.10. Pyramid revealing descending order of AWC in different soil samples

5.3.5. Bio-degradation studies

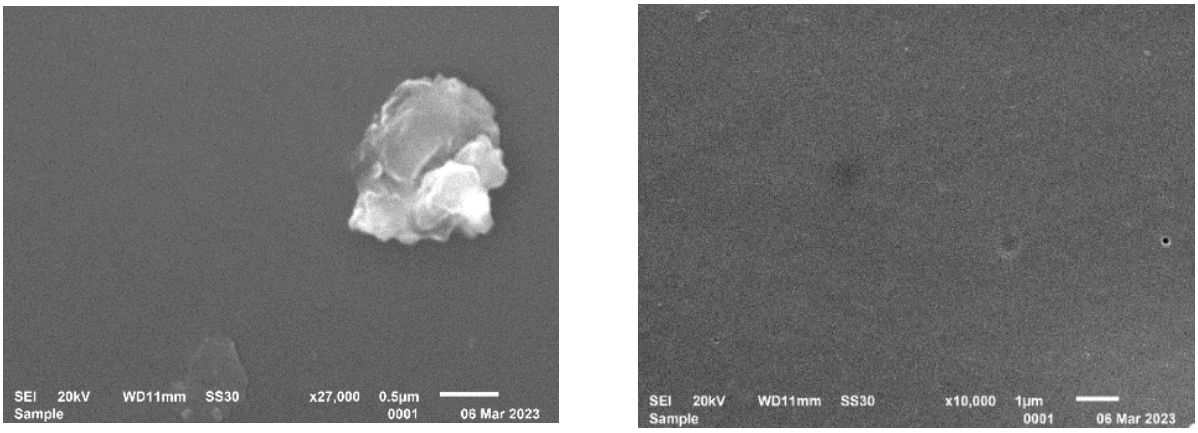

Figure 5.11. SEM Studies Non-degraded CMTKG-PSA-PAM Hydrogel

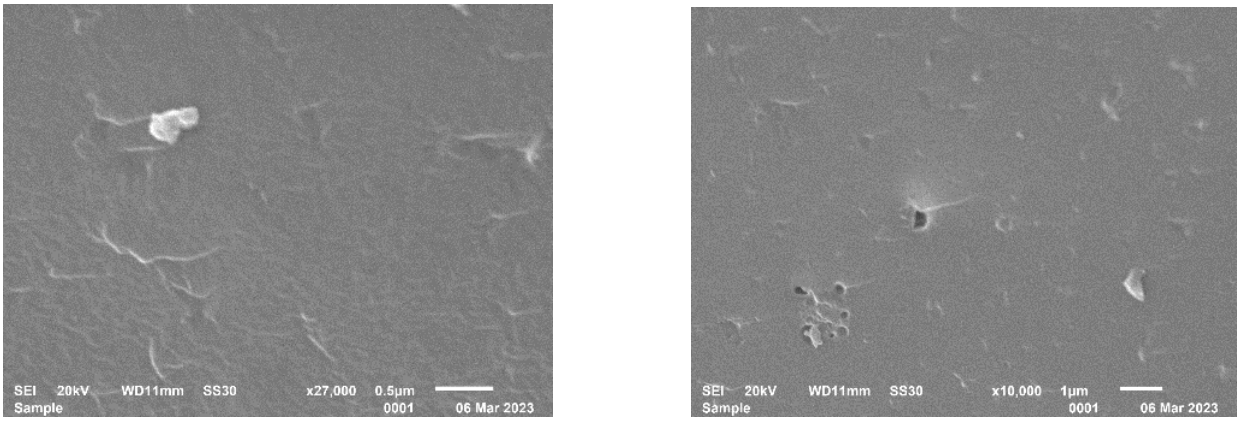

Figure 5.12. SEM Studies Biodegraded CMTKG-PSA-PAM Hydrogel (after 15 Days)

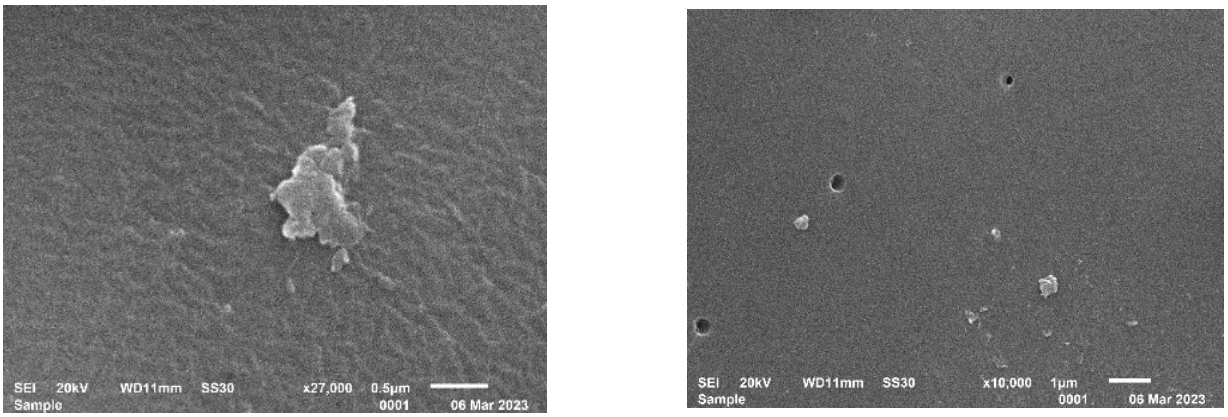

Figure 5.13. SEM Studies Biodegraded CMTKG-PSA-PAM Hydrogel (after 30 Days)

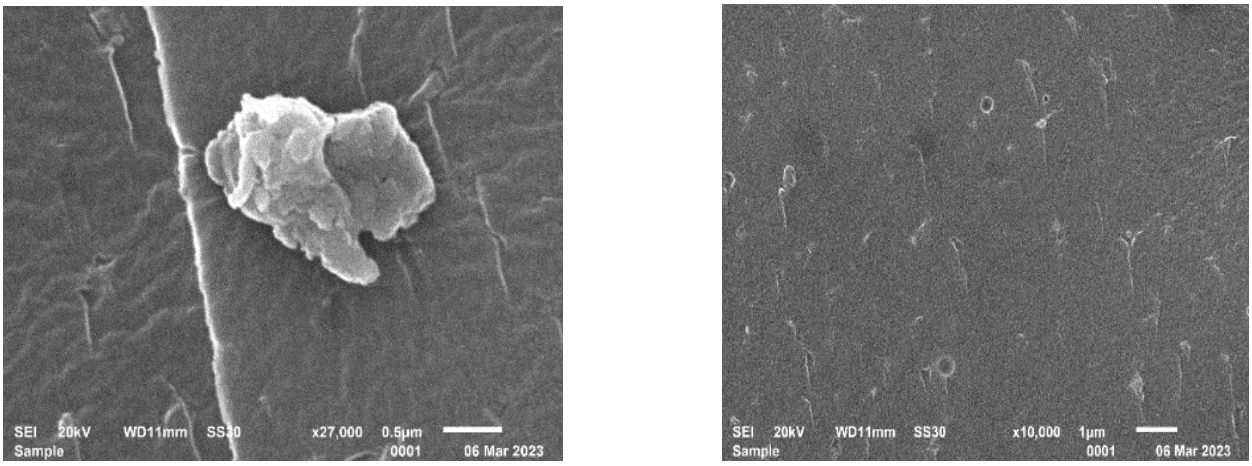

Figure 5.14. SEM Studies Biodegraded CMTKG-PSA-PAM Hydrogel (after 45 Days)

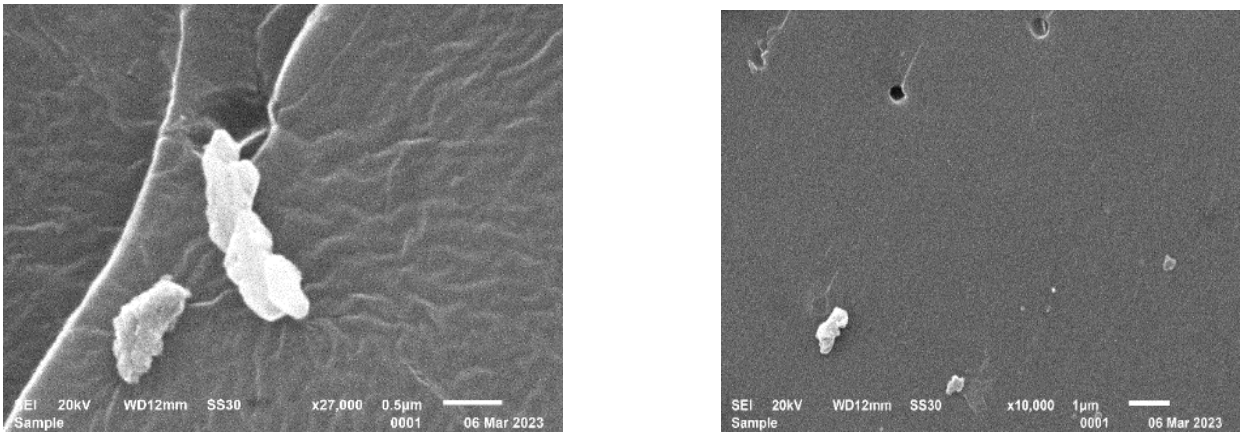

Figure 5.15. SEM Studies Biodegraded CMTKG-PSA-PAM Hydrogel (after 60 Days)

The biodegradation of the novel fabricated Hydrogel was researched via soil burial studies. The rate of biodegradation was high in the initial 15-30 days followed by a slower phase of degradation. It was found to be about 36% during the first 30 days followed by 10% in the further period of 30 days (**Figure. 5.16.)**. This was as expected as oxygen inside the hydrogel and the humus content i.e., the CMTKG concentration is high at the initial stage [17]. As time passed, anaerobic conditions developed owing to lesser oxygen [18]. Hence, less microbial decomposition is observed, leading to a slower rate of biodegradation. These results were successfully verified by the SEM Studies conducted of non-degraded hydrogel and degraded hydrogel after 15, 30, 45 and 60 days shown in **Figure. 5.11.** to **Figure. 5.15.**

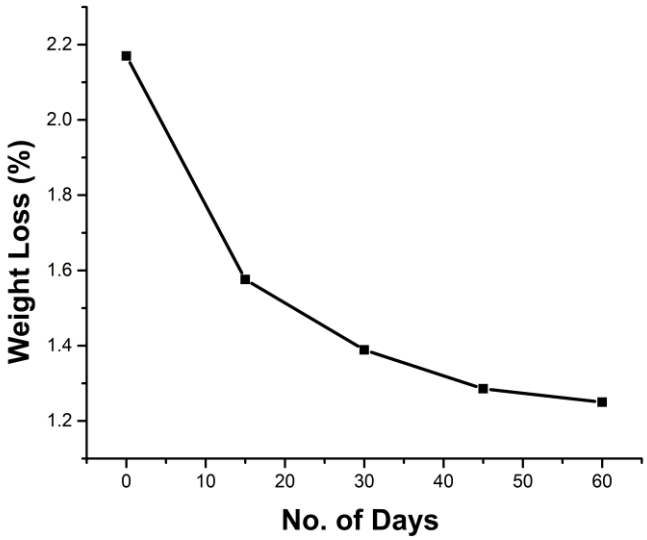

Figure. 5.16. Weight loss % vs. No. of days of biodegradation

5.4. Conclusions

Hydrogels enhance the hydro-physical and biological properties of the soil and hence enable the plants to grow even in sandy soils. It serves as soil water conditioner by reducing water loss due

to percolation, evaporation and soil erosion and providing it to the plants under dry conditions. The formulated CMTKG-PSA-PAM hydrogel absorbed 169 ml/g of distilled water and was evaluated as a soil conditioner in all the four types of soils i.e., clay, silty, loamy & sandy soil for different physical attributes of the soil viz. maximum water holding capacity (MWHC), density, porosity, water retention by plantation method and available water content (AWC). It unveiled the following order in the various attributes:

- Increase in MWHC in 0.1% amended soil: Sandy soil (43%), Clay soil (31%), Silty soil (29%) & Loamy soil (9%).
- Increase in MWHC in 0.3% amended soil: Clay soil (29%), silty soil (15%), sandy soil (56%) and loamy soil (26%)
- Decrease in porosity: Sandy (29%) > Loamy (15.2%) > Silty (6%) > Clay (5.9%),
- Increase in available water content in 0.1% hydrogel amended soil: Clay soil (17.52%), Silty (13.45%), Loamy soil (9.416%), Sandy soil (10.375%).
- Increase in available water content in 0.3% hydrogel amended soil: Clay soil (9.163%), Silty (9.147%), Loamy soil (14.94%), Sandy soil (19.02%)
- Increase in bulk density in 0.3% hydrogel amended soil: Clay (1.7%), Silty (5.3%), Loamy (10%) and Sandy (13%) as compared to the control sample.

These sequels were corroborated by analyzing the water retention capacity in chickpea plants. It was found that though the CMTKG-PSA-PAM hydrogel as a soil conditioner exhibited commendable performance on all types of soil, it is worth applying in sandy and loamy soil.

These hydrogels, being viable ecological and economical soil conditioners and serving as water sustenance techniques, pave a best way for greener agronomy.

References

[1] N. Thombare, S. Mishra, M.Z. Siddiqui, U. Jha, D. Singh, G.R. Mahajan, Design and development of guar gum based novel, superabsorbent and moisture retaining hydrogels for agricultural applications, Carbohydr. Polym. 185 (2018) 169–178. https://doi.org/10.1016/J.CARBPOL.2018.01.018.

[2] R.L. Flannery, W.J. Busscher, Use of a synthetic polymer in potting soils to improve water holding capacity, Commun. Soil Sci. Plant Anal. 13 (1982) 103–111. https://doi.org/10.1080/00103628209367249.

[3] Manual on soil, plant and water analysis., (n.d.). https://www.cabdirect.org/cabdirect/abstract/20073118818 (accessed September 27, 2021).

[4] N. Thombare, S. Mishra, M. Siddiqui, … U.J.-C., undefined 2018, Design and development of guar gum based novel, superabsorbent and moisture retaining hydrogels for agricultural applications, Elsevier. (n.d.). https://www.sciencedirect.com/science/article/pii/S0144861718300183 (accessed May 29, 2023).

[5] L. Richards, M.F.-S. Science, undefined 1943, Pressure-plate apparatus for measuring moisture sorption and transmission by soils, Journals.Lww.Com. (n.d.). https://journals.lww.com/soilsci/Citation/1943/12000/PRESSURE_PLATE_APPARATUS_FOR_MEASURING_MOISTURE.1.aspx (accessed February 12, 2023).

[6] P. Rizzarelli, C. Puglisi, G. Montaudo, Soil burial and enzymatic degradation in solution of aliphatic co-polyesters, Polym. Degrad. Stab. 85 (2004) 855–863. https://doi.org/10.1016/J.POLYMDEGRADSTAB.2004.03.022.

[7] K. Sharma, V. Kumar, B.S. Kaith, V. Kumar, S. Som, S. Kalia, H.C. Swart, A study of the biodegradation behaviour of poly(methacrylic acid/aniline)-grafted gum ghatti by a soil burial method, RSC Adv. 4 (2014) 25637–25649. https://doi.org/10.1039/C4RA03765K.

[8] H. Agaba, L.B.O.- Clean–Soil, undefined Air, undefined 2010, Effects of hydrogel amendment to different soils on plant available water and survival of trees under drought conditions, Wiley Online Libr. (n.d.). https://onlinelibrary.wiley.com/doi/abs/10.1002/clen.200900245 (accessed May 29, 2023).

[9] H. Agaba, L.J.B. Orikiriza, J.F.O. Esegu, J. Obua, J.D. Kabasa, A. Hüttermann, Effects of hydrogel amendment to different soils on plant available water and survival of trees under drought conditions, Clean - Soil, Air, Water. 38 (2010) 328–335. https://doi.org/10.1002/CLEN.200900245.

[10] H. Emami, A.A.-J. of A.S. and, undefined 2012, Effect of organic and inorganic amendments on parameters of water retention curve, bulk density and aggregate diameter of a saline-sodic soil, Jast.Modares.Ac.Ir. 14 (2012) 1625–1636.

https://jast.modares.ac.ir/browse.php?a_id=4711&sid=23&slc_lang=en (accessed May 29, 2023).

[11] R. Hussien, A. Donia, A. Atia, O.E.-S.- Catena, undefined 2012, Studying some hydro-physical properties of two soils amended with kaolinite-modified cross-linked poly-acrylamides, Elsevier. (n.d.). https://www.sciencedirect.com/science/article/pii/S0341816211002797 (accessed May 29, 2023).

[12] T.A. Adjuik, S.E. Nokes, M.D. Montross, O. Wendroth, The Impacts of Bio-Based and Synthetic Hydrogels on Soil Hydraulic Properties: A Review, Polymers (Basel). 14 (2022) 4721. https://doi.org/10.3390/POLYM14214721.

[13] J. Koupai, S. Eslamian, J.K.-E.& Hydrobiology, undefined 2008, Enhancing the available water content in unsaturated soil zone using hydrogel, to improve plant growth indices, Elsevier. (n.d.). https://www.sciencedirect.com/science/article/pii/S1642359308700983 (accessed May 29, 2023).

[14] B. Narjary, P. Aggarwal, A. Singh, D.C.- Geoderma, undefined 2012, Water availability in different soils in relation to hydrogel application, Elsevier. (n.d.). https://www.sciencedirect.com/science/article/pii/S0016706112001152 (accessed May 29, 2023).

[15] A. Bhardwaj, I. Shainberg, … D.G.-S.S.S., undefined 2007, Water retention and hydraulic conductivity of cross-linked polyacrylamides in sandy soils, Wiley Online Libr. 71 (2016) 406–412. https://doi.org/10.2136/sssaj2006.0138.

[16] B. Narjary, P. Aggarwal, A. Singh, D.C.- Geoderma, undefined 2012, Water availability in different soils in relation to hydrogel application, Elsevier. (n.d.). https://www.sciencedirect.com/science/article/pii/S0016706112001152 (accessed February 12, 2023).

[17] H. Mittal, R. Jindal, B. Kaith, A. Maity, S.R.-C. polymers, undefined 2015, Flocculation and adsorption properties of biodegradable gum-ghatti-grafted poly (acrylamide-co-methacrylic acid) hydrogels, Elsevier. (n.d.). https://www.sciencedirect.com/science/article/pii/S0144861714009230 (accessed April 3, 2023).

[18] M. Maiti, B. Kaith, R. Jindal, A.J.-P. degradation and stability, undefined 2010, Synthesis and characterization of corn starch based green composites reinforced with Saccharum spontaneum L graft copolymers prepared under micro-wave and, Elsevier. (n.d.). https://www.sciencedirect.com/science/article/pii/S0141391010002260 (accessed April 3, 2023).

Chapter-6

CONCLUSIONS AND FUTURE SCOPE OF THE WORK DONE

6.1. Summary and Conclusions

The present research thesis validates the synthesis of pioneering biopolymer CMTKG-based organic hydrogels and their applications in agronomy as a soil water conditioner. First hydrogel was designed employing natural polymer-CMTKG and synthetic monomer-sodium methacrylate while the other hydrogel employed the usage of natural polymer-CMTKG and synthetic monomers-sodium acrylate and acrylamide. These hydrogels were outcomes of the free radical mechanism, entailing KPS as an initiator and MBA as a cross-linker. The mechanism of synthesis was evidenced by instrumental methods of analysis viz. FTIR, TGA and SEM techniques. Both the hydrogels were optimized for desired attributes for maximum swelling by altering the concentrations of biopolymer-CMTKG, crosslinker, and initiator. The optimized CMTKG-PSMA hydrogel had the composition of 0.3% CMTKG, 0.1% KPS, and 0.05% MBA while the CMTKG-SMA-PAM hydrogel had the composition: 0.4% CMTKG, 0.1% KPS, and 0.25% MBA. The equilibrium swelling ratio of the optimized hydrogel was evaluated in various salt solutions, at different pH. It was also analysed in distilled water. Amongst all, for CMTKG-PSMA, the highest equilibrium swelling ratio was recorded-248.88 mg/L in distilled water at 18℃, and for CMTKG-PSA-PAM, the same was recorded-189 mg/L in distilled water at 20℃. The extensive swelling ratio of both the hydrogels allows them to be applied as a proficient tool as a soil water conditioner

for higher water absorption for water sustenance and environment conservation in praxes and procedures of agronomics.

These hydrogels were validated as biodegradable via soil burial biodegradation test. The preliminary bio-degradation rate of CMTKG-PSMA hydrogel for the initial 30 days was high and found to be 44% followed by a slower weight loss of about 12% from the 30th day to the 45th day of soil burial, while the rate of biodegradation of CMTKG-PSA-PAM hydrogel was high in the initial 15-30 days followed by a slower phase of degradation. It was found to be about 36% during the first 30 days followed by 10% in the further period of 30 days.

Amendment of the soil by little addition of any of the fabricated hydrogels, yield fruitful results regarding their application as a soil water conditioner as it led to enhanced growth of the plants owing to improved attributes of the soil. A significant upturn in the maximum water holding capacity, reduction in porosity, higher available water content, and high bulk density was observed by hydrogel application. All these factors favour plantation. These upshots were authenticated by probing water retention capacity in chickpea plants.

CMTKG-PSMA hydrogel

The CMTKG-PSMA Hydrogel was evaluated for different physical attributes of the soil viz. maximum water holding capacity (MWHC), density, porosity, water retention by plantation method and available water content (AWC). The 0.5% CMTKG-PSMA hydrogel amended soil revealed augmentation in the maximum water holding capacity by 46.5%, an increase in shoot length by 43%, uprise in available water content by 37% and decrease in bulk density by 8%. Water retention capacity was assessed by plantation method. It was observed that post 21 days of plantation, the plant grown in the controlled soil wilted followed by wilting of 0.1%, 0.3%, and

0.5% on the 33rd, 40th, and 47th day of the plantation, respectively. These upshots were validated upon chickpea plants. These hydrogels proffer a promising substitute as a soil conditioner in agronomy. Such high swelling index of synthesized CMTKG-PSMA hydrogel renders it an excellent and worthy application in the agriculture sector as a soil conditioner that further aids in water conservation.

CMTKG-PSA-PAM Hydrogel

The agronomical evaluation of CMTKG-PSA-PAM hydrogel as a soil conditioner in all the four types of soils i.e., clay, silty, loamy & sandy soil was conducted. The CMTKG-PSMA hydrogel was evaluated for different physical attributes of the soil viz. maximum water holding capacity (MWHC), density, porosity, water retention by plantation method and available water content (AWC); in all the four types of the soils. The studies unveiled the following order:

- Maximum water holding capacity
    - 0.1% amended soil: Increase in Sandy soil by 43%, Clay soil by 31%, Silty soil by 29% & Loamy soil by 9%,
    - 0.3% amended soil: Clay soil by 29%, silty soil by 15%, sandy soil by 56% and loamy soil by 26%;
- Porosity: Sandy (29%) > Loamy (15.2%) > Silty (6%) > Clay (5.9%),
- Available water content
    - 0.1% hydrogel amended soil: Clay soil: 17.52%, Silty: 13.45%, Loamy soil: 9.416%, Sandy soil: 10.375%
    - 0.3% hydrogel amended soil: Clay soil: 9.163%, Silty: 9.147%, Loamy soil: 14.94%, Sandy soil: 19.02%;

- Bulk density: 0.3% hydrogel amended soil: Clay (1.7%), Silty (5.3%), Loamy (10%) and Sandy (13%) as compared to the control sample.
- These sequels were corroborated by analysing the water retention capacity in chickpea plants.

It was found that though the CMTKG-PSA-PAM hydrogel as a soil conditioner exhibited commendable performance on all types of soil, it is worth applying in sandy and loamy soil. CMTKG-PSA-PAM hydrogel enhanced the water productivity of the plants and bestowing a conducive and safe environment for better growth of the crops in arid and semi-arid regions.

- This thesis validates that the novel designed hydrogels: CMTKG-PSMA hydrogel & CMTKG-PSA-PAA hydrogel; expertise when applied in agronomical practices as a soil water conditioner for water sustenance and a balanced environment.
- To the best of our knowledge, no biopolymer-based hydrogel has ever been reported for the agronomical evaluation as a soil water conditioner in all the four types of soils viz. clay, silty, loamy, and sandy soil.

6.2 Future Scope

The present research work reveals that the CMTKG cross-linked derivatives yield prolific results in agronomical applications. Besides being practically durable, degradable, clean, and super water-absorbent, these CMTKG-based hydrogels (CMTKG-PSMA & CMTKG-PSA-PAM) can be additionally exploited in advanced fields of pharmaceuticals, surgical gels, wound healing gels, eye lenses, baby diapers, sanitary pads, etc. Nonetheless in agronomical applications, CMTKG-based hydrogels have shown cutting-edge potential for pot experiments, but their application and assessment on a massive scale in the agricultural fields needs to be researched. Additionally, within

the field of agronomics, CMTKG-based hydrogels show great potential as soil water-retaining additives and can aid in the controlled release of pesticides, micronutrients, and fertilizers. Research efforts should focus on enhancing and incorporating the green synthesis procedures to allow for the commercial production of these materials which requires dedicated research and an innovative approach.